INFORMATION TO USERS

This manuscript has been reproduced from the microfilm master. UMI films the text directly from the original or copy submitted. Thus, some thesis and dissertation copies are in typewriter face, while others may be from any type of computer printer.

The quality of this reproduction is dependent upon the quality of the copy submitted. Broken or indistinct print, colored or poor quality illustrations and photographs, print bleedthrough, substandard margins, and improper alignment can adversely affect reproduction.

In the unlikely event that the author did not send UMI a complete manuscript and there are missing pages, these will be noted. Also, if unauthorized copyright material had to be removed, a note will indicate the deletion.

Oversize materials (e.g., maps, drawings, charts) are reproduced by sectioning the original, beginning at the upper left-hand corner and continuing from left to right in equal sections with small overlaps.

ProQuest Information and Learning
300 North Zeeb Road, Ann Arbor, MI 48106-1346 USA
800-521-0600

UMI®

EFFECT OF SURFACE CHEMISTRY AND POROSITY OF ACTIVATED CARBONS ON THE ADSORPTION OF WATER AND ORGANIC POLLUTANTS

By

ISSA I. SALAME

A dissertation submitted to the Graduate Faculty of Chemistry in partial fulfillment of the requirements for the degree of Doctor of Philosophy, The City University of New York

2002

Effect of Surface Chemistry and Porosity of Activated Carbons on the Adsorption of Water and Organic Pollutants

by

Issa I. Salame

This manuscript has been read and accepted for the Graduate Faculty in Chemistry in satisfaction of the dissertation requirement for the degree of Doctor of Philosophy.

8/1/02
Date

T. J. Bandosz
Chair of Examining Committee

8/7/02
Date

Gerald Koeppl (for)
Executive Officer

Prof. Teresa Bandosz

Prof. Ronald Birke

Prof. Richard Pizer

THE CITY UNIVERSITY OF NEW YORK

The Graduate School and University Center of
The City University of New York

Abstract

EFFECT OF SURFACE CHEMISTRY AND POROSITY OF ACTIVATED CARBONS ON THE ADSORPTION OF WATER AND ORGANIC POLLUTANTS

by

Issa I. Salame

Advisor: Professor Teresa Bandosz

Three samples were used for this study: two of wood and one of coal origin. The samples were further oxidized to study the effect of oxidation on surface chemistry and porosity. The microstructure of the carbon was studied using nitrogen adsorption isotherms. The surface chemistry was characterized using Boehm and potentiometric titrations, temperature programmed desorption (TPD), inverse gas chromatography (IGC), and diffuse reflectance FTIR. The results showed that oxidation introduces a variety of functional groups to the surface. The combination of TPD, FTIR and titration methods led to the detection of non-acidic functional groups such as nitro groups, introduced to the carbon matrix via a nitration mechanism during oxidation with HNO_3. Water and methanol adsorption isotherms were measured at various temperatures close to ambient. From these isotherms, heats of adsorption were calculated. The results showed that the

isosteric heats of adsorption are affected by surface chemical heterogeneity only at low surface coverage. The shapes of the isosteric heats indicated strong water-water interactions as a result of adsorption on secondary sites and cluster formation. The results also showed that washing the carbon with methanol significantly modifies the surface chemistry of carbon creating very easily hydrolyzed esters. This prevents a correct calculation of the heat of adsorption. Heats of methanol adsorption showed that pore size and pore volume play major roles in the adsorption process. However, surface chemistry also contributes to the process. Adsorption of diethyl ether was studied by means of inverse gas chromatography at finite concentration. Adsorption isotherms were obtained from the chromatographic peaks using the characteristic-peak elution method. The results showed that the difference in the uptake of diethyl ether depends on the porosity of the samples and their surface chemistry. Analysis of heats of adsorption indicated that ether molecules are adsorbed on the carbon surface via significant contribution of hydrogen bonding on functional groups present in narrow pores and interactions of the hydrocarbon moiety with the pore walls. Phenol adsorption from solution was studied and the results showed a strong dependence on the presence of carboxylic functional groups which act as ester formation sites and as electron withdrawing groups.

Acknowledgement

This work was completed at the City College of New York and the Graduate School and University Center of the City University of New York. I would like to express my gratitude to all those who gave me the possibility of completing this thesis.

I am deeply in debt to my supervisor and mentor Professor Teresa Bandosz whom I worked with during the last five years on this project. Professor Bandosz's help, stimulating suggestions, constant encouragement, and guidance aided me in my research and in writing this thesis. I truly have appreciated her help and working style which promotes self confidence and autonomy.

I wish to express my gratitude to Professor Richard Pizer and Professor Ronald Birke for their invaluable suggestions and their review of this thesis.

I wish to thank my laboratory colleagues: Anna Kleyman for her love and support, and Andrey Bagreev and Foad Adib for valuable scientific discussions.

I am very grateful for the love and support of my parents, my brother Samer, and my two sisters Linda and Lina.

Especially, I would like to give my sincere thanks to my wife Jennifer whose patient love enabled me to complete this work.

Table of Contents

Captions to the Tables

Captions to the Figures

1. INTRODUCTION

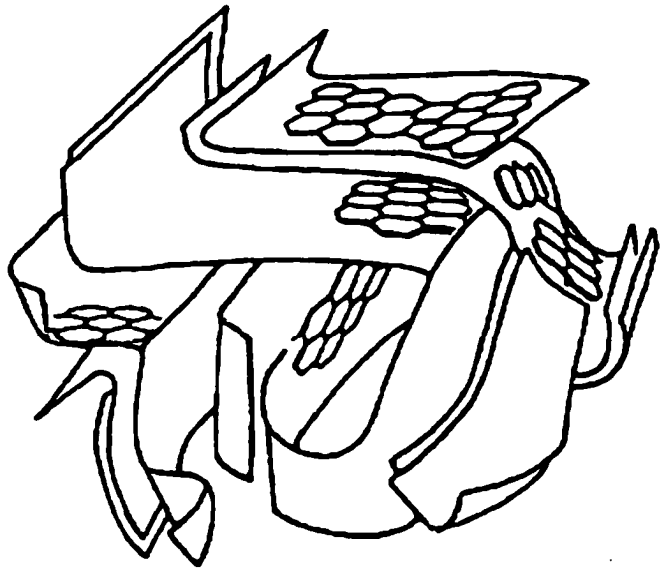

Figure 1. A schematic representation of an activated carbon [5].

Activated carbons are materials that possess a complex porous structure, high surface area, surface chemical heterogeneity, and surface hydrophobicity, which govern their applications [1 – 4]. The porous structure is the result of the presence of micropores, mesopores, and macropores. Micropores are pores that are smaller than 20 Å; mesopores are pores with the sizes of 20 Å– 500Å; macropores are pores greater in size than 500 Å. It is believed that the pores are slit-shaped [5]. The unique characteristics of activated carbons depend on the origin of the precursor and the method of activation [1]. Some of the most common precursors are bituminous coal, wood, coconut shells, peat, petroleum pitch and polymers. It is believed that highly microporous carbons with sieving properties are obtained from coal, petroleum pitch, or coconut shells, whereas mesoporous activated

carbons having low mechanical stability and low density have their origin in wood as an organic precursor [6]. Figure 1 presents a schematic structure of activated carbons [5], and Figure 2 shows a schematic representation of activated carbon granule with the micropores, mesopores, and macropores.

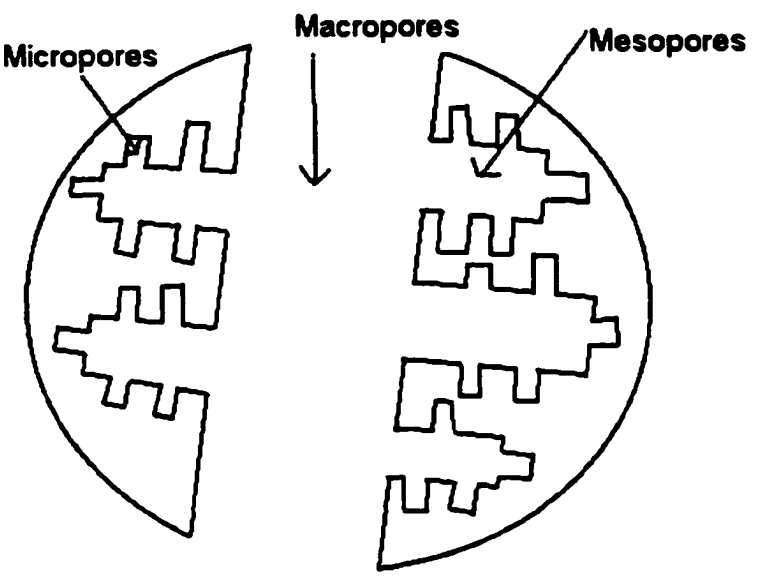

Figure 2. A schematic representation of an activated carbon granule showing micropores, mesopores and macropores.

In the process of physical activation, organic material is first carbonized at elevated temperatures and then activated with steam, carbon dioxide, or other agents to introduce porosity. Activated carbons can also be chemically activated during carbonization. In such a method, compounds such as phosphoric acid, ammonium hydrogen phosphate, or potassium hydroxide are used as activation agents at various temperatures. As a result of the different activation methods, there are a large variety of activated carbons with different structures and surface properties and, consequently,

different applications. In addition, activated carbons can be further oxidized with several oxidizing agents that will introduce a variety of different functional groups to the carbon surface.

The surface chemistry of the carbon is the result of the presence of heteroatoms such as oxygen, nitrogen, hydrogen, and phosphorus [2, 4]. Those heteroatoms are present in the form of organic functional groups at the edges of the crystallites. The content of these elements depends on the origin of the carbon and the method of activation [6]. The presence of heteroatoms such as oxygen, which can form ketones, carboxyls, phenols, ethers, and lactones; nitrogen in the form of amines and nitro groups; and phosphorus as a phosphate can determine the acidity or basicity of the activated carbon [2, 4]. Figure 3 shows the examples of the surface groups present on the carbon surface. The presence of heteroatoms has also a significant effect on the adsorption of polar species. Molecules that interact with the carbon in a specific way will be adsorbed stronger and in a greater amount when functional groups are present [7]. Moreover, heteroatoms can catalytically affect the conversion of adsorbed species as in the case of hydrogen sulfide adsorption [8, 9], or they can create obstacles for physical adsorption of non-polar molecules [10].

The experimental study of the carbon porosity and surface chemistry is not straightforward due to the complexity of the carbon structure. Some common experimental techniques include adsorption of gaseous molecules, mercury porosimetry, small angle X-ray scattering, and transmission electron microscopy [11]. However, the most commonly employed method for determining the porosity of activated carbons involves the adsorption of gases and vapors such as nitrogen or carbon dioxide [11].

Nitrogen adsorption provides valuable information about the carbon structure, surface area, and pore size distribution.

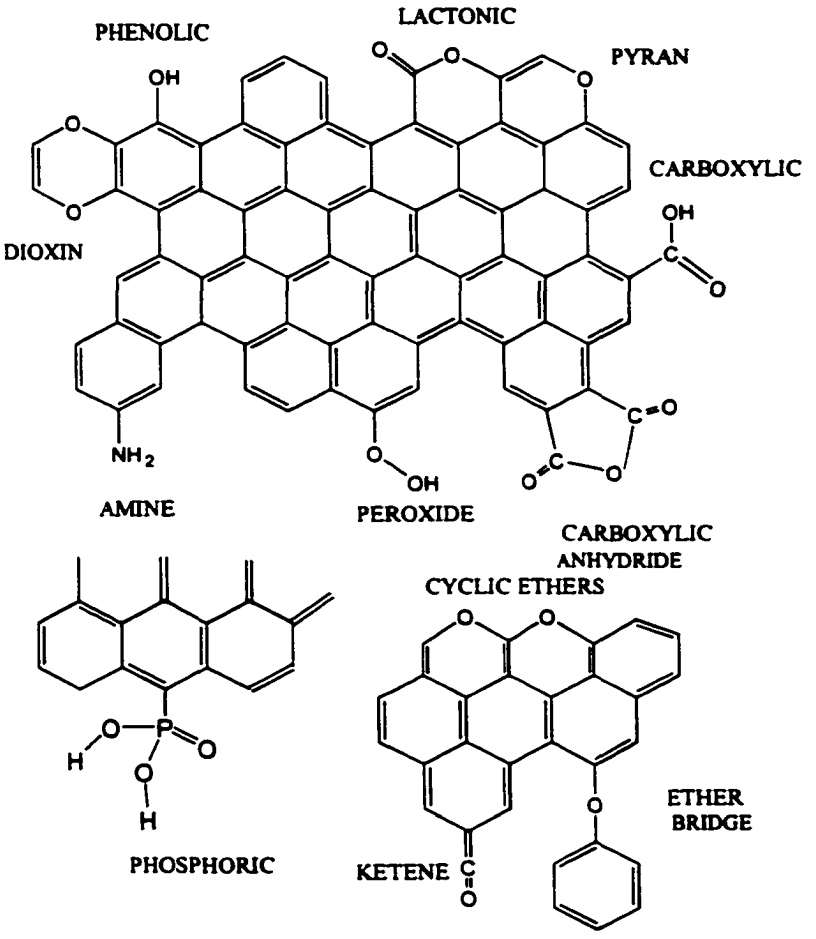

Figure 3. Some of the functional groups present on the activated carbon surface.

The surface groups of activated carbons are usually determined using "wet" and "dry" methods of analysis. The "wet" techniques involve titrations such as Boehm [2] and potentiometric titration [12-14]. "Dry" methods include diffuse reflectance FTIR (DRIFTS) [15, 16], X-ray photoelectron spectroscopy (XPS) [17, 18], thermal analysis (TA) [8], thermal programmed desorption (TPD) [19, 20], and inverse gas

chromatography (IGC) [21]. Although XPS and DRIFTS provide qualitative information about the carbon surface, the quantitative insight is not straightforward and requires special mathematical treatment with many approximations used [18]. On the other hand, Boehm and potentiometric titration methods provide qualitative and quantitative information on the carbon surface. However, the information on acidic groups is limited to such compounds as phenols, lactones, and carboxylic acids, yet neglecting other species present on the carbon surface in the form of functional groups. Temperature programmed desorption (TPD) allows one to study functional groups that decompose below 1250 K [19, 20], but it doesn't provide direct qualitative information on the carbon surface chemistry. In this method, oxygen-containing functional groups are thermally desorbed from the carbon surface in the form of oxides such as CO and CO_2.

There has been an increasing interest in the study of adsorption of organic molecules onto activated carbons. This is due to the importance of the removal of organic pollutants from water streams and the atmosphere [22]. The adsorption process depends on several factors, which include the nature of the adsorbent, adsorbate, and adsorption conditions. Adsorbent characteristics entail the surface area, pore size distribution, ash content, hydrophobicity, which is defined as the concentration of carbon atoms in the matrix, density and type of functional groups present on the surface. On the other hand, the nature of the adsorbate depends on its polarity, hydrophobicity, size of the molecule, and the acidity or basicity of the functional group present, if any. The adsorption conditions include the temperature, the polarity of the solvent, when applicable, and the presence of other competing species for the adsorption sites.

Recently, there has been an extensive study of the mechanism of water adsorption on activated carbons [23-34]. This is because very often activated carbons are used as adsorbents and separation media where moisture is present. The presence of water in the gas phase significantly affects the breakthrough curves [35], increases the uptake of methane [10], and contributes to the oxidation of hydrogen sulfide [8, 9]. Although many papers have been published on water adsorption on activated carbon [23-36], the fundamentals of the process are still poorly understood because the mechanisms of adsorption on the molecular level (at a low relative pressure) are still discussed more intuitively than empirically.

The mechanism of water adsorption was originally proposed by Dubinin and Serpinsky (DS) [37]. Their interpretation of the shape of the isotherms is based on the interactions of water molecules with either pure carbon or oxygen-containing surface species. According to the DS theory, water molecules are first adsorbed on primary adsorption centers, oxygen containing functional groups and then adsorption on secondary groups, adsorbed water molecules, occurs. Thus an increase in the water vapor pressure leads to the formation of clusters of associated water molecules via hydrogen bonding [27-29, 37]. It was proposed that below $p/p_0 = 0.3$ surface chemistry governs the adsorption process, while at higher relative pressure microporosity becomes the determining factor [23]. The number of primary adsorption centers can be calculated by fitting the experimental isotherm to the equation formulated by Dubinin and Serpinsky [37]. Many experimental results along with their interpretation have been published based on the DS approach [23, 27-29, 38, 39]. In some cases, especially for carbons with a large

number of chemical surface groups, the attempts to fit the experimental data to the proposed isotherm failed [38, 39].

Recently, Carrasco-Marin and co-workers have presented an approach linking the enthalpies of immersion to the distribution of oxygen groups [24]. The authors also demonstrated that the water adsorption isotherm maybe described as the sum of Dubinin-Astakhov isotherms of type I and V. In the study of kinetics of water adsorption, Harding et al. observed cluster formation on the basis of changes in activation energy [40]. In one study, water interactions were observed on "clean carbons" [26]. At low surface coverage, the heats of adsorption were 17-32 kJ/mol which is smaller than the heat of water condensation [26]. This indicates that the interaction energy of water with the carbon hydrophobic micropores is weaker than the water-water interaction energy. The calculated heats increased with increasing surface coverage due to water-water interaction contribution to the energy of adsorption.

A new approach to understanding of the phenomena of water adsorption on activated carbons employs Monte Carlo Grand Canonical computer simulations [25, 30]. Recent results obtained by Gubbins and co-workers showed a good agreement of molecular simulations with the experimental results [30]. Molecular simulations allow one to observe the process of cluster formation and its dependence upon the density and strength of oxygen surface groups. Moreover, the effectiveness of sorption of other gases such as methane in the presence of water can be also investigated [25].

While the water adsorption has been studied in detail, the adsorption of light aliphatic alcohols has been discussed less frequently in the scientific papers [23, 26, 39-42]. In the case of methanol sorption, the uptake is governed mainly by carbon

microporosity [23]. This is the result of the chemical nature of methanol and the significant contribution of the hydrocarbon moiety (the hydrocarbon methyl group) to dispersive sorbate-sorbent interactions. As indicated above, the dispersive interactions of the hydrocarbon moiety with slit-shaped pores are expected to predominate at low relative pressure [23]. Recently, it has been demonstrated by Naono et al. [26] that the isosteric heat of ethanol adsorption on a "clean" surface of activated carbons shows the same trend as the isosteric heat of water adsorption on the same materials. The heats reported increase with increasing surface coverage but do not reach the heat of condensation of 41 kJ/mol. According to Sun and Satyapal, the heat of methanol adsorption on activated carbons is about 55 kJ/mol [42], which is higher than the heat of condensation equal to 37 kJ/mol. The latter represents the value for the methanol-methanol interactions [43].

Diethyl ether with the chemical formula $(C_2H_5)_2O$ is a polar molecule that can interact with the carbon surface via dispersive interactions of its hydrocarbon moiety, two ethyl groups. It can also be hydrogen bonded to oxygen containing surface functional groups such as carboxylic and phenolic compounds. In addition, ether is capable of donating a pair of electrons from oxygen lone pairs and thus it interacts with the electron pair receptors on the surface as a Lewis base [44]. The heat of diethyl ether adsorption on carbon black was reported to be about 36 kJ/mol [7]. When adsorption of various ethers on amorphous nitrogenated carbons was studied, the desorption energy of diethyl ether was found to be between 50 and 60 kJ/mol [44]. On the other hand, Stanley and Guiochon reported that the energy of adsorption of ether on silica has two specific

regions one of 46 kJ/mol and the other of 57 kJ/mol which can be related to interactions with different surface sites [45].

The study of adsorption of aromatic compounds from solution has been studied extensively [46-59]. Leng and Pinto have found that the uptake of phenol is a combined effect of physisorption and surface polymerization, where physisorption is the interaction of the phenol with the basal planes [47]. They found out that the functional groups on the activated carbons plays a role in both the electrostatic and dispersive interactions. The phenol uptake increases as a result of the removal the carboxylic functional groups from the carbon surface. This is due to the increased water adsorption as a competing process, and the weakening of the interactions with the basal planes of the carbon. Radovic and co-workers have studied the effect of surface groups on the adsorption of aromatic compounds from solution [46]. They concluded that oxidation of the carbon surface decreases the π-electron density in the graphene layers and thus reduces the carbon's dispersive adsorption potential. On the other hand, the removal of the oxygen groups, the electron-withdrawing groups, causes an increase in the π-electron density and thus an increase in the adsorption potential due to dispersive interactions.

2. OBJECTIVE

1. To propose a mechanism for water, methanol, ether, and phenol adsorption based on a detailed study of surface chemistry, porosity and their relationship to the energetics of the adsorption process.
2. The following tasks must be met to satisfy our primary objective:
   A) A careful characterization of carbons
      i) Surface groups: types and density.
      ii) A comprehensive view of activated carbon surface chemistry obtained by using Boehm titration, potentiometric titration, thermal programmed desorption (TPD), and DRIFTS.
      iii) Porosity: micropores and mesopores.
   B) An understanding of how the sorption mechanism is affected by porosity and surface groups and the extent of the influence of each.

3. BACKGROUND

3.1. Water Adsorption.

A model for water adsorption on activated carbons was originally proposed by Dubinin and Serpinsky (DS) [37]. They determined that hydrogen bonding plays a dominant role in the adsorption process. They found that water adsorption is the result of the presence of oxygen functional groups on the carbon surface, which they referred to as primary adsorption centers. According to Dubinin and Serpinski (DS), water molecules are first adsorbed on the functional groups [37]. Then adsorbed water molecules, which are capable of forming hydrogen bonding with other water molecules, act as new sites for adsorption and are referred to as secondary adsorption centers. DS concluded that the isotherm for water adsorption on activated carbon obeys the following equation:

$$h = \frac{a}{c(a_0 + a)(1 - ka)} \tag{1}$$

where h = p/p_o which is the relative pressure, a_0 is the number of primary adsorption centers on the surface, a is the adsorption value at that relative pressure, c is the kinetic constant of the adsorption, and k is the adsorption parameter. The adsorption parameter is calculated by setting a as the limiting value of the water adsorption at a relative pressure equal to 1. (1 – ck) represents the decrease in the number of adsorption centers as they become occupied. Equation 1 contains three parameters, a, c and k or a at saturation pressure, which can be calculated from a single adsorption isotherm. Equation 1 can be written in the form of a quadratic equation which follows the form:

$$\frac{a}{h} = A_1 + A_2 a + A_3 a^2 \qquad (2)$$

where $A_1 = ca_0$, $A_2 = c(1 - a_0k)$, and $A_3 = ck$. This equation can be applied to study isotherms with relative pressure between 0.1 and 1. A plot of the left-hand side of equation 2 against the amount adsorbed should produce an inverted parabola. Dubinin and Serpinsky assumed that since this equation fits data in a relative pressure range between 0.1 to 1, it should be able to fit experimental data at lower relative pressures. However, studies by Barton et al. and later by Evans showed that the DS equation cannot be fitted to data at relative pressures lower than 0.1, which questions the validity of the results obtained representing the numbers of the primary adsorption sites [38, 60]. Evans argued that the reason for the inapplicability of the DS equation is that Dubinin and Sepinsky equation do not consider lower values of relative pressure and that their isotherms do not feature an initial Langmuir type region [38].

Evans proposed the use of an equation derived by D'Arcy and Watt for the analysis of water isotherms which is based on assumptions that are closely related to those proposed by DS [61]. Based on DS model, D'Arcy and Watt derived an equation which is a combination of one or more Langmuir isotherms that describe the adsorption on various energy sites. In addition to that, they added to the equation a Henry's law region which describes the adsorption on low-energy sites, and a third component of the equation that describes the adsorption on secondary adsorption centers. The equation is as follows:

$$a = \frac{KK'(p/p_0)}{1 + K(p/p_0)} + C(p/p_0) + \frac{kk'(p/p_0)}{1 - k(p/p_0)} \quad (3)$$

where K is a function of primary centers-sorbate interaction energy, K' is related to the number of primary adsorption centers, C is the Henry's law constant for adsorption on low-energy sites, k is a function of the sorbate-sorbate interaction energy, k' is related to the number of secondary adsorption centers, p/p_0 is the relative pressure, and a is the amount adsorbed. Using this method, Evans obtained a much better fit to the experimental data as compared to the fit he obtained by employing the DS approach. Work done by Bandosz et al. showed that both DS and D'Arcy and Watt approaches failed in the majority of cases [38]. The results showed that DS gives good fits only when type V isotherms were used. However, the majority of the isotherms studied were measured with samples that contain a high density of functional groups and thus the isotherms obtained were hybrids of different isotherms. Consequently, poor results were obtained for the number of primary adsorption sites using the DS approach [39].

Stoeckli and co-workers reported that water adsorption at room temperature is of type IV isotherm which can be described as the hybrid of type I and type V isotherms [62]. The first stages of the water isotherm are type I and can be described by an equation derived by Dubinin and Astakhov having the following form:

$$N = N_0 \exp[-(\frac{RT \ln(p_0/p)}{E})^n] \quad (4)$$

where N is the amount adsorbed at a given temperature and relative pressure, N_0 is the limiting capacity for the amount adsorbed, R is the universal gas constant, T is the temperature, p/p_0 is the relative pressure, n and E are characteristics of the system under study. The second part of the isotherm obeys the DS equation. Since water adsorption depends on the weak dispersive interactions with the carbon surface and the interactions with oxygen surface groups, E of the system increases with increasing oxidation, where the characteristic energy of the microporous structure is not affected [24]. Recent work by Lodewyckx and Vansant who measured the water isotherms gravimetrically in microporous activated carbon supports equation (4) [63]. Activated carbon samples were exposed to a flow of air with different relative humidity. Weighing the samples at regular intervals provided a convenient way of plotting the amount of water uptake vs. time. The results showed that equation (4), the Dubinin-Astakhov (DA) equation, underestimates the uptake of water at low relative pressure, the first region of the adsorption process. This is due to the chemisorption of water on the oxygen surface functional groups through the reaction with dangling bonds on the carbon surface. In the second region of the adsorption, which is the condensation region, water undergoes micropore filling by water-water interactions via hydrogen bonding. The DA equation was found to have an excellent fit to the experimental results when a low number of oxygen surface groups are present on the surface. As the amount of oxygen surface groups increases, the DA equation underestimates the water uptake. Also, in the third region, the DA equation underestimates the water uptake, which is the result of adsorption on the external surfaces after the pores are completely filled [63].

Recently, Do and Do proposed a model for the different shapes of water adsorption isotherms on carbonaceous materials [64]. Their model allows for the study of water adsorption on activated carbon with differernt microstructures and surface functional groups. The model assumes that the adsorption of water occurs around the surface functional groups, where clusters are formed. When the clusters have high enough concentrations, they are adsorbed into the micropores [64]. In this theory, Do and Do assume that the carbon material is made up of graphitic and amorphous carbon. The surface oxygen groups are located at the edges of the basal planes of the graphite units. In the initial stage of the adsorption, water is chemisorbed on the functional groups. Those chemisorbed water molecules act as sites for further adsorption of water molecules via hydrogen bonding. As a result of this process, a water cluster grows around the chemisorption site. When water molecules interact with one another, they form a cluster. As the size of the cluster reaches a few water molecules, they interact with the carbon surface in a dispersive way, which is in accordance with Iiyama's work [29]. The process of adsorption in the micropores will continue until the micropores reach their limiting capacity. Because the cluster of water molecules inside the micropores is made up of a few water molecules, the packing is not as effective as the packing of water in the bulk phase [64]. The consequence of this is that the volume of water molecules adsorbed in micropores is always smaller than the volume of the micropores calculated from the nitrogen adsorption isotherm. In the mesopores, the water cluster size increases until capillary condensation takes place, where the mesopores are filled with water. Do and Do derived an equation for water adsorption that has the following form:

$$C_\mu = C_{\mu s} \frac{K_\mu \sum_{n=6} x^n}{K_\mu \sum_{n=6} x^n + \sum_{n=6} x^{n-5}} + S_0 \frac{K_f \sum_{n=1} n x^n}{1 + K_f \sum_{n=1} x^n} \quad (5)$$

where C_μ is the concentration pressure, $C_{\mu s}$ is the saturation concentration in the micropores, K_μ is the micropore equilibrium constant, x is the reduced pressure of water, K_f is the chemisorption equilibrium constant, S_0 is the functional group concentration, and n is the number of water molecules. The equation also has an extended version that includes the capillary condensation in mesopores. Do and Do compared their simulated results with experimental results and found that the model is able to describe the experimental data well.

Talu and Meunier developed a theory for adsorption of water on activated carbon based on the interpretation of the nonideality of vapor and liquid phases [65]. They describe the adsorption of water on activated carbon as having three differing regions (loading ranges). In the first region, the low loading or low relative pressure, the adsorption process is dependent only on the vertical interactions between the polar water molecules and the primary adsorption centers on the carbon surface. This is closely related to the DS interpretation of the adsorption of water. In the second region, the intermediate loading, the adsorption takes place by the formation of water clusters by association via hydrogen bonding between water molecules and other adsorbed water molecules. In the third region, the high loading, the adsorption takes place as a condensation between water molecules and is controlled by the micropore volume which has to do with the finite and limited amount of space available for the water clusters to form.

Their theory of self-associating molecules in micropores is dependent on the chemical equilibrium, equation of state, and the phase equilibrium. The chemical equilibrium and the equation of state are related to the behavior of the surface phase, whereas, the phase equilibrium relates the surface phase properties to the bulk phase properties. Their isotherm equation has the following form:

$$P = \frac{H\Psi}{(1 + K\Psi)} . \exp(\frac{\Psi}{N_m}) \tag{6}$$

where P is the equilibrium pressure, H is the Henry's law constant, N_m is the measured saturation amount adsorbed of the monomer, K is the reaction constant, and Ψ is related to the measured saturation capacity, N_m, and to the amount adsorbed at a given pressure, N by:

$$\Psi(1 + K\Psi) = \frac{N_m N}{(N_m - N)} \tag{7}$$

The equation for the isotherm they obtained can reflect the behavior of isotherms of types I to V depending on the value of the reaction constant. This equation was successfully applied to experimental isotherms of water on activated carbon surfaces. The theory provided three simple yet valuable results: 1) the guest molecules interact stronger with each other than they do with the surface, however, 2) the surface does provide centers for

nucleation for adsorption, and 3) the volume available for adsorption in micorpores is finite.

Stoeckli and co-workers have shown that the constant c in the DS equation is related to the molar enthalpy of immersion of activated carbon into water [62]. Furthermore, Stoeckli et al. were able to establish an empirical formula that relates the enthalpy of immersion of water adsorption to the activated carbon surface density [66]:

$$\Delta_i H / Jg^{-1} = -25a_0 - 0.6(a_s - a_0) \tag{8}$$

where a_0 is the number of primary adsorption sites and a_s is the limiting amount of adsorption. This equation, which deals with the study of the immersion of microporous carbon into liquid, after generalization, took the following form [67]:

$$\Delta_i H / Jg^{-1} = -EN_o(1 + \alpha T)\Gamma(1 + \frac{1}{n}) \tag{9}$$

where E and n are temperature invariant parameters, E being the characteristic energy, N_0 is the limiting amount of micropores, α is the thermal expansion coefficient, and Γ is the tabulated gamma function. Further work by Carrasco-Marin and co-workers presented a good linear correlation between the enthalpies of adsorption of water and the total number of sites on the carbon surface which include carboxylic, phenolic, and lactonic groups [24]. Rodriguez-Reinoso and co-workers found that there is a parallelism between the enthalpy of immersion in water and the number of surface oxygen groups on the

carbon surface [68]. They also found that there is a small contribution of the carbon structure that adds to the immersion enthalpy of water on activated carbon.

A slightly different approach to study the adsorption of vapors on activated carbons was proposed by Barton and co-workers [41]. This approach depends on studying the free energy of immersion. Using the free energy and the enthalpy of immersion, one can easily calculate the entropy of immersion, which depends, to some extent, on the nature of the adsorbate. The entropy of immersion can provide valuable data about the degrees of freedom that a molecule loses as it becomes adsorbed.

Rodriguez-Reinoso and co-workers tried to relate the adsorption of water to the surface chemistry of the carbon and found that the water isotherms are either type V for unoxidized carbons, or the sum of type I and V for oxidized ones [23]. They reported that at low relative pressure, the water uptake increases with an increasing degree of oxidation and correlated the number of acidic groups to the water uptake. In the first stages of the adsorption, water molecules are retained by strongly binding sites such as carboxylic groups.

In studying the kinetics of water adsorption on activated carbons, Thomas, Norman and co-workers argued that the uptake of water is related to the diffusion of water into the activated carbon pores [27, 40]. Ndaji et al. has proposed an empirical description of the adsorption of gases on the activated carbon surface that follows a phenomenological model that has the following form [69]:

$$\frac{M_t}{M_e} = 1 - \exp(-kt) \tag{10}$$

where M_t is the amount adsorbed at time t, M_e is the amount adsorbed at equilibrium, k is the rate constant for the process. Plotting $\ln(1-M_t/M_e)$ versus time for water vapor adsorption gives a dependence that is close to linear for more than 90% of the total uptake. Ndaji et al. reported that the adsorption kinetics of water on activated carbons, when the pressure is changing rapidly, follow a linear driving force mass transfer. Their results indicate that rate of adsorption/desorption changes with the position on the isotherm. They found that the fastest rates are reported at low relative pressure where water is interacting with the primary adsorption centers on the carbon surface.

Another approach uses X-ray diffraction as a tool for studying water adsorption on slit-shaped carbons [29]. Iiyama and co-workers by means of X-ray diffraction successfully studied the molecular assembly structure of water that is adsorbed in carbon micropores. This direct method provided information on the state of the water molecules that are confined in the carbon micropores. The information obtained showed that the adsorbed water has a more ordered structure than in the bulk liquid. This demonstrated that water follows an ordered assembly structure when adsorbed in carbon micropores. Furthermore, adsorbed water interacts with the pore walls forming aggregates of few molecules to about 6 Å in diameter in the open hydrophobic pore space. Consequently, Iiyama and co-workers argued that water does not predominantly adsorb on activated carbons by the capillary condensation mechanism as was proposed by DS theory. On the contrary, the solid-like ordered structure is formed in the carbon micropores, as the progress of filling takes place.

Recent work by Phillips and co-workers employed microcalorimetry to study the effect of surface chemistry on the adsorption of water by high surface area carbons [70].

They were able to relate the heats of adsorption to surface chemistry. They reported the heats of adsorption on several carbons. The differential heat of adsorption decreases from a value that is greater than 50 kJ/mol at the initial stages of adsorption until it reaches a plateau of about 42 kJ/mol. In the final stage of adsorption, the heat of adsorption decreases even lower than 42 kJ/mol. The microcalorimetric studies provide information about the type of interaction that water has with the carbon surface. The first type is the chemical adsorption, which involves bond formation, characterized by heats of adsorption greater than 50 kJ/mol. The second type is the condensation, which gives heats of about 42 kJ/mol. The third type is the physical adsorption and is described by heats of adsorption smaller than 42 kJ/mol. First, the chemical adsorption takes place at the primary adsorption sites, and then it is followed by physical adsorption and condensation. They also reported that on unsaturated carbons, with dangling bonds, heats of water adsorption reach 420 kJ/mol which is due to the bond formation (chemisorption).

Aharoni proposed a model for water condensation based on the properties of the solid-liquid interface [71]. He showed that when adsorption is limited to a fraction of the pore wall surface, capillary condensation occurs at pore widths that are smaller than expected for condensation to take place. Because the number of sites capable of adsorption is limited, then the capillary condensation process takes place in the carbon micropore space.

Further work on the study of water-carbon interaction using microcalorimetry was published by Groszek and Aharoni [72]. Their flow adsorption microcalorimetry measurements showed that the heat of adsorption is high at low uptake and the rest of the

adsorption follows a condensation route where the heat is equal to the heat of condensation. The authors propose that some of the measured heat is not related to any surface-adsorbate interactions, but it is the result of changes induced in the carbon pore structure. Groszek and Aharoni argue that the sorbates exert mechanical forces on the pore walls, which results in the modification of the porous structure and this affects the adsorption properties of the adsorbent. Their research led to the following three results: first, the heats of adsorption of water at low surface coverages are very high and have values of 81 kJ/mol, which correspond to those of chemisorption between water molecules and dangling bonds on the carbon surface. However, at higher uptake the heat of adsorption reaches a constant value of 44 kJ/mol, which is close to the heat of bulk condensation. Second, oxidation results in an increase in the amount of water adsorbed but it doesn't affect the heat of adsorption. Third, water adsorption causes changes in the carbon pore structure, which is accompanied by the evolution of heat.

Molecular simulations were used by Seggra and Glandt to study the effect of the polarity of the carbon on the adsorption process of water [73]. They compared the simulation results to those of the experimental ones. The authors reported that the polar effect, the presence of oxygen groups on the carbon surface, produces the sigmoidal shape isotherm. Their work compared the experimental heats of adsorption with those calculated from the simulation. The hydrophobic nature of the carbon influences the isosteric heats of adsorption to some extent. For non-polar carbon, carbon black without oxygen surface groups, the isosteric heat of adsorption is about 6.8 kJ/mol at low surface coverages and it increases with loading until it reaches about 7.4 kJ/mol. These results indicate that the adsorption of water follows a cooperative effect, the adsorption of a

water molecule would promote the adsorption of another water molecule. Studying the isosteric heat of adsorption on polar carbons by molecular simulations showed the results are close to that of the heat of water condensation which implies that the nature of the water interactions is similar to that of the condensation of water in the bulk phase.

Studies by Gubbins and co-workers tried to further shed light on the process of water adsorption on activated carbons by applying molecular simulation methods [25], such as a grand canonical Monte Carlo approach. In this method, water is modeled as a Lennard-Jones (LJ) sphere with four square-well sites arranged in a tetrahedral geometry. Two of the sites correspond to the hydrogen bonding centers, while the other two correspond to the lone pair electrons on the oxygen atom. The active chemical sites on the carbon surface are modeled as square-well sites. The intermolecular forces including repulsion, dispersion, and hydrogen bonding are taken into account. Figure 4 is a schematic presentation of molecular simulation of water adsorption in a carbon pore as envisioned by Gubbins et al. [30]. The model shows that water is preferentially adsorbed on active sites on the carbon surface, which act as nucleation sites for the adsorption process to begin and the cluster formation to take place. The results show that water adsorption is dependent on the surface site density of groups and their distribution. Sites that are placed at appropriate distances from each other would allow for water molecules to bridge between already adsorbed water molecules. Also, clusters can form which consist of several associated water molecules. These clusters can occupy small pores even when more spaces in larger pores are still available which is consistent with the work published by Iiyama et al. [29]. Further work has shown that there is a good agreement between the experimental data and the simulation calculation [34].

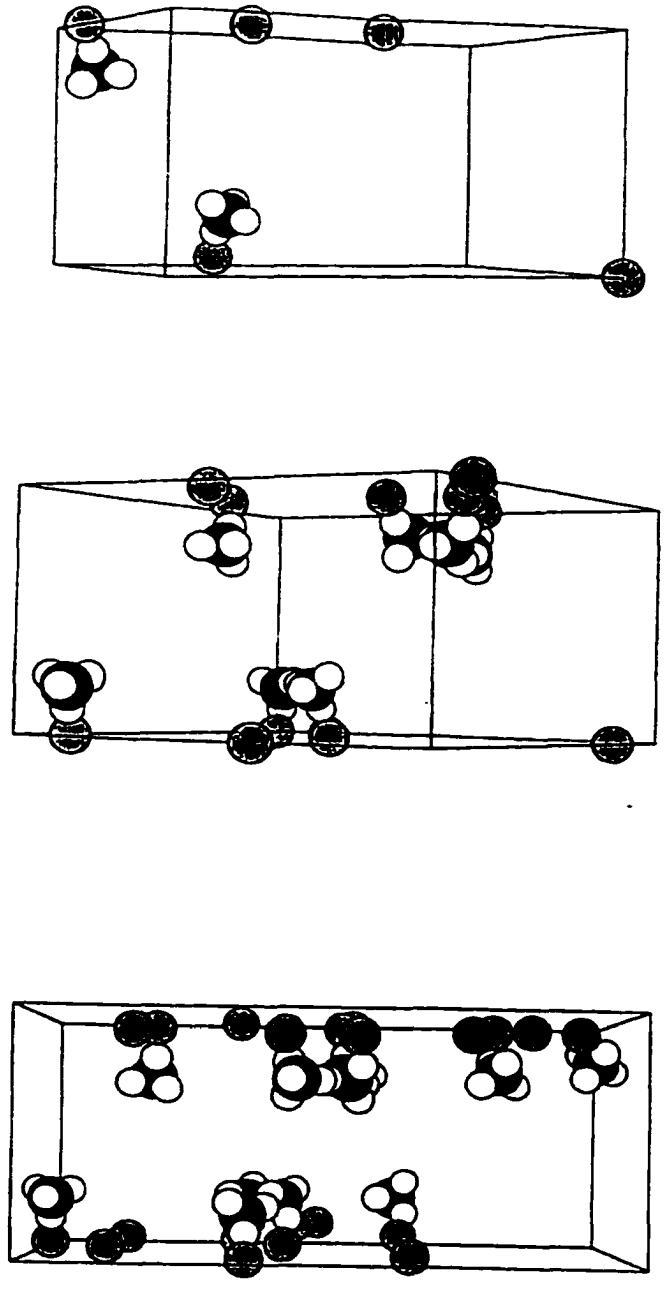

Figure 4. A schematic presentation of molecular simulation of water adsorption in a carbon pore (width of 1.69 nm) as envisioned by Gubbins et al. [30].

Sircar proposed a model for the adsorption-condensation of vapors on activated carbons [74]. According to this model, the adsorption of vapors in a microporous adsorbent can be described by a pore filling mechanism that is characterized as a Langmuir-type isotherm:

$$N_m(x) = \frac{\overline{N}_m cx}{1 + (c - x)x} \qquad 0 < x < 1 \tag{11}$$

where N_m is the amount adsorbed at a given relative pressure x, N_m is the saturation adsorption capacity at the pore filling, and c is the solid-vapor interaction parameter.

Sircar argues that this model can successfully describe types I, IV, and V isotherms as proposed by BET classifications. This model was the first model to include a quantitative description of the capillary condensation. Further work on this model by Mahle and Friday showed that this model cannot describe hysteresis [75]. The problem that faces the Sircar isotherms is that it implies that the capillary condensation takes place in pores that have a very narrow size distribution. This is not realistic for activated carbons that possess a wide range of pore size distributions. Consequently, Mahle and Friday put forward a theory that is a modification of the Sircar approach and can account for a larger pore size distribution than that proposed by Sircar [75]. Their studies showed a good correlation between the theory and the experimental part.

Work done by Bradley and co-workers showed that the microporosity of the carbons is a determining factor in the uptake of water [76]. The authors argue that the surface polarity of the carbon should play a role in the adsorption process at higher

pressures, but one has to account for the microporosity to influence the adsorption process. The pore structure would play a role in determining the shape of the isotherm.

3.2.*Methanol Adsorption.*

Unlike water, methanol has been studied to a lesser extent in the scientific literature [23, 26, 39-42]. According to Gregg and Sing, the adsorbent-adsorbate interactions in physical adsorption are dependent on both the polarity of the solid and the adsorptive [77]. Rodriguez-Reinoso and co-workers presented results which showed that both microporosity and the chemical nature of the carbon surface affect the methanol adsorption process [23]. Methanol adsorption at low relative pressures increases with increasing the degree of oxidation. This is the result of the increase in the interactions between methanol and the carbon oxygen surface groups. Studies by Bandosz and co-workers [39] showed that for methanol adsorption the presence of small pores could enhance the adsorption potential at low relative pressure. Also, their studies indicated that the presence of oxygen functional groups on the carbon surface leads to an increase in the amount adsorbed at a relative pressure of 0.3. For microporous carbon, the uptake of methanol is larger than that of water, at low relative pressure, which is the result of the stronger interactions between carbon and methanol. Bandosz and co-workers were unable to find a well-defined relationship between the uptake of methanol at low relative pressure and the amount of oxygen surface groups, which is due to the significant influence of micropores on the adsorption of methanol [39]. Although, one might expect that the dispersive interactions of methanol with the carbon walls should be weak due to the small size of the methyl group, the presence of the hydrocarbon moiety part plays a

dominant role in the adsorption process [77]. On the other hand, the presence of hydroxyl groups provides centers for hydrogen bonding with a small contribution to the adsorption energy [77].

Recently, Lopez-Ramon and co-workers used immersion calorimetry and vapor adsorption to study the specific and nonspecific interactions between methanol and activated carbons [78]. The existence of specific and nonspecific interactions between methanol and activated carbons can be seen as an increase in the enthalpy of immersion of the oxidized carbons. This shows that methanol interacts in a specific way with the carbon surface. Moreover, the specific interactions between methanol and active carbons were studied by examining the influence of oxygen groups on the affinity coefficient of a given adsorptive with respect to benzene which is taken as a reference [78].

Tamon and Okazaki studied the effect of oxidation on the uptake of methanol [79]. They found that the isotherms of methanol for oxidized carbons were located below those prior to the oxidation except at the low pressure region of the isotherms, which means lower uptake at higher relative pressures. The increase in the uptake at low surface coverage is related to the increased number of oxygen containing surface groups where methanol can hydrogen bond and be adsorbed. At higher surface coverages, the adsorption capacity decreases due to a decrease in the micropore volume as a result of the oxidation process.

An important study by Wang et al. used flow microcalorimetry to examine the adsorption of methanol from n-hexanes on coals [80]. The reported results show that the heat of adsorption measured is independent of the uptake. The methanol uptake increases until it reaches a constant value, which means that all the adsorption sites have been

occupied. The authors also suggested that the methanol adsorption occurs via strong and weak interactions. Strong adsorption involves hydrogen bonding with the carbon surface functional groups, while weak adsorption represents the physical interactions, the Van der Waals forces, between the carbon pores and the methanol molecule. The authors show that the molar heat of adsorption decreases sharply at low surface coverages and then it becomes constant when the strong adsorption sites are occupied. The decrease in the heats of adsorption indicates that methanol is adsorbed at the strongest adsorption sites at the initial stages of the adsorption. The adsorption then progresses into weaker sites which indicates that the adsorption sites for methanol on coal are energetically heterogeneous. It is noteworthy that Wang and co-workers found that the strong adsorption of methanol on coal releases molar heats between 30 and 60 kJ/mol.

Kaneko and co-workers showed that the density of ethanol molecular assemblies in very small pores is close to its solid density even at 303 K which indicates that confinement of ethanol in micopores gives rise to a solid like ordering [81]. The C_2H_5OH molecule possesses an ethyl and a hydroxyl groups and thus has a hydrophobic and a hydrophilic parts which allow it to associate with other ethanol molecules. As indicated by Kaneko and co-workers, hydrogen bonding plays an important role in the structure of ethanol molecules' assembly [81].

Naono and co-workers studied adsorption of water and ethanol on hydrophobic microporous activated carbons [26] by combining volumetric and gravimetric methods. They determined the adsorption energy of ethanol in the micropores to be 43 – 52 kJ/mol which is due to a strong interaction between the ethanol hydrocarbon part and the micropore surface. The values for the heat of ethanol adsorption obtained by Naono and

co-workers were larger than the heat of ethanol condensation (42 kJ/mol), which indicates that ethanol interacts stronger with the carbon surface than with other ethanol molecules [26].

3.2.Phenol Adsorption.

Adsorption of phenol from aqueous solution has been studied extensively. Rodriguez-Reinoso and co-workers have investigated the effect of pore structure and oxygen containing surface groups on the adsorption of substituted phenols on activated carbons [49]. They reported two important findings. First, the adsorption process is dependent on the porosity of the carbon, and this is true when the degree of activation is low. Second, phenol adsorption is affected by the chemical nature of the carbon surface. Magne and Walker reported that the chemisorption of phenol decreases as a result of the presence of acidic oxygen surface groups [50]. Vidic and Suidan found that the presence of oxygen on the carbon surface, not only decreases the capacity of phenol adsorption, but it also affects the shape of the isotherm [51]. This is related to the fact that elemental oxygen presence induces the process of polymerization of phenol and thus phenol is removed from the liquid phase but not necessarily adsorbed. The presence of elemental oxygen and its concentration affect the adsorption capacity of phenol on granular activated carbon. Since the presence of elemental oxygen in solution alters the measured isotherm, the authors recommend studying phenol adsorption in anoxic conditions, which would provide true adsorption equilibrium. Other work has shown that oxygen containing surface groups decrease the uptake of phenol by localizing the free electrons of the carbon basal planes [52]. This is because phenol adsorption on activated carbons is of

dispersive type where the π-electrons on the phenol interacts with the π-electrons on the basal planes [53]. Experimental work [52] has shown that when graphite is doped with boron, π-electrons are removed from the carbon matrix and thus the phenol uptake decreases. Studies have shown that the adsorption of phenol on activated carbon can also be the result of the formation of electron donor-acceptor complexes [54]. In those complexes, the surface oxygen functional groups act as electron donors, whereas the aromatic ring of the phenol acts as the electron acceptors [54]. Further studies by Moreno-Castilla and Rivera-Utrilla ascertained that the adsorption of phenol on activated carbon is related to the electron donor acceptor complexes formed [55]. According to them, the electron donors are the oxygen surface groups and/ or the π-electron rich region on the carbon surface and the electron acceptor is the aromatic ring on the phenol. This suggests that the adsorption affinity should increase with the basicity of the carbon surface [55].

Tessmer and co-workers have demonstrated that the presence of functional groups prevents activated carbons from adsorbing phenol when the adsorption takes place under oxic conditions, in the presence of oxygen in the solution [56]. This is the result of the reduction of the ability of activated carbon to promote adsorption via an oxidative coupling reaction. They also reported that the catalytic properties of activated carbons can be enhanced by eliminating some the acidic functional groups and introducing basic functional groups to the carbon surface. It is worth mentioning that the activated carbon surface possesses a charge density that depends on the pH of the solution. This is very important for the adsorption of phenol since it is a weak electrolyte and can be attracted or repelled by the activated carbon surface. It was found that at low pH, in acidic

solution, the amount adsorbed increases slightly with increasing pH [55]. With further increase in the pH, the phenol uptake decreases [55].

Pinto reported that the adsorption of phenol on activated carbons is the combination of physisorption and surface polymerization [47]. The polymerization process is the result of the oxidative coupling reaction that occurs on the surface of activated carbon [57]. The polymerization process results in an irreversible adsorption of phenol [57]. Although, the role of the carbon in the oxidative reaction is not clear, it is known that carbon can catalyze the oxidative reaction. However, physisorption is the dominant factor in the adsorption process and it is the result of the interactions between phenol and the basal planes [47]. The authors found an inverse relationship between the amount adsorbed and the number of carboxylic groups on the carbon surface. This was linked to the increased water adsorption on the carboxylic groups, which decreases the available sites for phenol adsorption and weakens the dispersive interaction with the carbon basal planes [47]. In addition, they reported that the presence of acidic surface groups decreases the polymerization reaction. The presence of oxygen in solution is crucial for the polymerization to take place. The results also showed that the removal of carboxylic groups from the carbon surface resulted in an increase in the process of polymerization and physisorption.

Salvador and Merchan studied the adsorption of phenol on activated carbon using liquid-phase Temperature Programmed Desorption (LPTPD) [58]. Their results showed that the thermodesorption process is complete at lower temperatures as compared to those obtained from gas phase. This is related to the ease of desorption from the liquid phase. They also reported that the desorption mechanism is a complex one that involves

diffusion control and readsorption of phenol. Furthermore, the authors were able to determine the bonding energy of adsorption which turns out to be in the range of hydrogen bonding.

The adsorption of phenol on graphite was also studied using computer simulations through the use of grand canonical Monte Carlo method [59]. In this method, the graphite surface was described as having two distinct adsorption sites, the first is located at the center of the six membered benzene ring (hexagon) and the second is located between any two carbon atoms which form what looks like a saddle. Bertoncini and co-workers reported that the two types of interactions are related to the presence or absence of oxygen containing surface groups on the carbon. Furthermore, the studies showed that there is a lateral interaction between the adsorbed phenol molecules [59].

4. EXPERIMENTAL SECTION

4.1. Choice of Carbons.

Three activated carbons were used for this study. Two are of wood origin and they are manufactured by Westvaco. The first carbon material, WVA 1100, is obtained using phosphoric acid activation at about 950 K [82]. The second material, UMC, is a developmental sorbent obtained by KOH activation of the previously mentioned activated carbon, WVA 1100, at 1300 K [83]. Those two carbons are referred to as W and U, respectively. The third type of carbon, Xtrusorb, is of coal origin, manufactured by Calgon, and is prepared by the steam activation method. This carbon is designated as C. W carbon was oxidized with ammonium persulfate [31, 32], nitric acid, and hydrogen peroxide [84]. The oxidized samples were referred to as W-APS, W-CN, and W-HP, respectively. Sample U was oxidized with ammonium persulfate and thus is referred to as U-APS. Sample C was oxidized with nitric acid and is referred to as C-CN. Samples W and W-APS were washed with methanol in a Soxhlet apparatus for 72 hours and thus are referred to as W/M and W-APS/M.

4.2. Oxidation of Carbons

To describe the oxidation conditions for nitric acid, briefly, 10 grams of the initial carbon was stirred with 100 mL of 15 M (73%) nitric acid for 24 hours at room temperature. For hydrogen peroxide oxidation, 10 grams of initial carbon was stirred with a 100 mL of 1:1 of hydrogen peroxide (30%) and sulfuric acid (1.0 M) for 24 hours at room temperature. Ammonium persulfate oxidation was carried out by using a 10 grams of the initial carbon and 100 mL of a saturated solution of ammonium persulfate in 1.0 M

sulfuric acid and allowing it to stir overnight at room temperature. Each of the oxidized carbon was then extensively washed in a Soxhlet apparatus to remove any excess of oxidizing agent and other water-soluble species.

4.3. Boehm Titration

The surface functional groups containing oxygen were determined according to Boehm titration [2, 3]. One gram of carbon sample was placed in a 50 mL of 0.1 N of the following solutions: sodium hydroxide, sodium carbonate, sodium bicarbonate, and hydrochloric acid. The vials were sealed and shaken for 24 hours and then filtered. 5 mL of the filtrate was pipetted and the excess base or acid was titrated with HCl (0.1 N) or NaOH (0.1 N), respectively. The number of acidic sites was determined under the assumption that NaOH neutralizes carboxylic, lactonic, and phenolic groups; and Na_2CO_3 neutralizes carboxylic and lactonic groups; and $NaHCO_3$ neutralizes only carboxylic groups. The number of basic sites was calculated from the amount of hydrochloric acid that reacted with the carbon.

4.4. Potentiometric Titration.

Potentiometric titration measurements were performed using a DMS Titrino 716 automatic titrator (Metrohm). The instrument was set at the mode when the equilibrium pH was collected. Subsamples of the carbons of about 0.100 g samples of carbon in 50.00 mL of 0.01 N $NaNO_3$ were placed in a container thermostatted at 298 K and allowed to equilibrate for 24 hours with the electrolyte solution. To eliminate the influence of CO_2, the suspension was continuously saturated with N_2 during the measurements. Also, the

carbon suspension was stirred throughout the measurements. Volumetric standards of 0.1 M NaOH and HCl were used as the titrants. The experiments were carried out in a pH range of 3 – 10 [12, 13, 33, 39, 85]. Each sample was titrated with both acid and base starting from the initial pH of the suspension.

The titration curves obtained were then transformed into proton binding curves, Q(pH), using the proton balance equation and the theoretical blank reference [12, 86]. The experimental window for this type of titration is limited by the buffering power of water [87]. To obtain meaningful results we confine our measurements to pH values between 3 and 10. It is assumed that the system under study consists of acidic sites that are characterized by their acidity constants, K_a. The fraction of the sites that are characterized by their individual acidity constants and are protonated at a given pH is described by the following formula:

$$q = [1 + 10^{(pH - pK)}]^{-1} \tag{12}$$

The values of the experimentally measured proton binding curve, Q, which assess the total amount of protonated sites can be related to the values of pK_a of the individual sites by using the following equation:

$$Q(pH) = \int_{-\infty}^{\infty} q(pH, pK_a) f(pK_a) dpK_a \tag{13}$$

where $f(pK_a)$ is the distribution of acidic sites in terms of their pK_a values. In order to calculate $f(pK_a)$, a method called SAIEUS was used to solve the numerical equation [88].

The SAIEUS method applies regularization combined with non-negative constraints. The choice of the degree of regularization or smoothing is based on the analysis of a measure of the effective bias that is introduced by the regularization and a measure of the uncertainty of the solution.

4.5. Sorption of Nitrogen.

Nitrogen isotherms were measured using an ASAP 2010 (Micromeritics) at 77 K. Before each experiment the samples were heated at 393 K and outgassed at this temperature under a vacuum of 10^{-5} Torr. The isotherms were then used to calculate specific surface area, S_{BET}, micropore volume (DR method), V_{mic} [89], volume in pores smaller than 10 Å, $V_{<10Å}$, and pore size distribution. All these parameters were obtained using density functional theory, DFT [90].

In order to calculate the surface area Brunauer, Emmett and Teller (BET) theory was employed. The BET method [49] is based on a theory proposed by Langmiur for the adsorption processes [91] and a multilayer structure is assumed. In this theory, the surface of the solid is regarded as an array of adsorption sites. The BET equation has the form:

$$\frac{n}{n_m} = \frac{c(p/p^o)}{(1-p/p^o)(1+(c-1)p/p^o)} \qquad (14)$$

where n_m is the monolayer capacity, and n is the amount adsorbed expressed in moles of adsorbate per gram of adsorbent, p is the pressure, p^o is the saturation vapor pressure,

and c is the BET parameter. The inflection point on the isotherm is taken to indicate the completion of the monolayer capacity, n_m, which can be used to calculate the surface area using the following equation:

$$A = L.n_m.a_m \tag{15}$$

where A is the specific surface area, L is Avogadro's number, and a_m is the average area occupied by a molecule of adsorbate (nitrogen) in the completed monolayer.

To determine pore size distribution and surface area, the density functional theory of adsorption was employed [90]. In order to study the pore size distribution, the DFT method works under the assumption that the experimental isotherm can be expressed as the sum of the convolution of a kernel function. This function represents the isotherm of an ideal homoporous adsorbent with a frequency distribution of pore sizes:

$$Q(p) = \int d\varepsilon.q(p,\varepsilon).f(\varepsilon) \tag{16}$$

where Q(p) is the experimental isotherm expressed in cm^3/g (STP), $f(\varepsilon)$ is the distribution of pore areas as a function of pore width ε, and x(p, ε) is the kernel function in terms of cm^3/m^2 (STP) which described the adsorption isotherm for an ideal homotattic surface characterized by energy ε. Since we are interested in the numerical solution of this integral, DFT allows us to calculate values for q(p, ε), however it doesn't provide an analytical form for the function and the value of $f(\varepsilon)$ is unknown. To work around this obstacle, model isotherms can be used to carry out the inversion of the summation for of

the integral equation [90]. In this method, we can study the effective adsorptive potential distribution of the adsorbent from the experimental data obtained by the isotherm. The method employed can be expressed in the following equation:

$$Q(p) = \sum_i q(p, \varepsilon_i) f(\varepsilon_i) \tag{17}$$

where Q(p) is the experimental adsorption isotherm, $q(p, \varepsilon_i)$ is the amount adsorbed per square meter [90]. The results are fitted into combinations of pre-existing isotherms until the best fit is obtained. The data obtained provide information about the surface area and micorpore volume.

4.6. FTIR.

IR spectra were collected using Nicolet Impact 410 FT-IR instrument equipped with a diffuse reflectance unit. The instrument's resolution was set at 4 cm^{-1}. Carbon powder was placed in a micro-sample holder. Before each measurement, the instrument was run to collect the background, which was then automatically subtracted from the sample spectrum.

4.7. Temperature Programmed Desorption.

Temperature programmed desorption analyses were performed using a Pulse Chemsisorb 2705 (Micromeritics). The samples were first treated by heating them to 373 K in helium gas for 18 hours. The instrument settings were as follows: heating rate, 10 K/min and helium flow rate, 17.6 mL/min. The flow rate was measured with a Veri-Flow

500 flowmeter (Humonics). The TPD is equipped with a Thermal Conductivity Detector (TCD). PeakFit v4 software was used to fit TPD curves with Gaussian peaks. There was no baseline subtraction. For the fitting of raw data, four peaks were chosen. It was done arbitrarily to ensure the presence of sufficient surface chemical heterogeneity without creating a very complicated view of surface inventory.

4.8. CHN.

CHN analysis was done in Huffman laboratory, Boulder, CO.

4.9. Inverse Gas Chromatography (IGC).

The IGC experiments were performed with a SRI 8601C gas chromatograph (SRI Instruments) equipped with a flame ionization detector. Stainless steel columns that are 25 cm in length and 2.17 mm in diameter were filled with carbon particles ranging in size from 0.2 to 0.4 mm. Helium was used as the carrier gas with a flow rate of about 20-65 mL/min. The samples were first conditioned at 473 K in the chromatographic column under helium flow for 15 hours prior to the measurement. The experiments were performed at 433-473 K with methane as the nonadsorbing species.

In IGC experiments, the amounts of injected solutes are very small, and it is assumed that the adsorption is described by Henry's law. This assumption is fulfilled when the measured net retention volume, V_N, is independent of the amount injected. The quantity V_N is calculated from the measured net retention time, t_N [92, 93]. In our case, alkanes, alkenes, and branched alkanes were used as solutes. It is well known from the

chromatographic literature [21, 92-94] that the logarithm of V_N for n-alkanes varies linearly with the number of carbon atoms.

The free energy, $\Delta G°$, is calculated using V_N,

$$\Delta G° = -RT \ln \frac{V_N}{mS} + C \tag{18}$$

where R and T are the gas constant and temperature, m and S are the mass and specific surface area of the adsorbent, and C is a constant related to the standard states of gas and adsorbed phases.

Analysis of $\Delta G°$ values obtained under the conditions of infinite dilution provides information about the interactions of probe molecules with the surface only, because the interactions between adsorbed molecules can be neglected. In the case of energetically uniform surfaces, these values are directly related to the adsorption energy, while on the energetically heterogeneous surfaces such as activated carbons, they should be considered as related to some average value of the adsorption energy. The difference in the values of $\Delta G°$ of two subsequent n-alkanes represents the free energy of adsorption of a CH_2 group. Thus, it is not related to any particular alkane molecule and, because of its incremental character, is no longer dependent on the choice of the reference state [93].

Alkanes have also been used in conjunction with unsaturated and aromatic hydrocarbons to study specific interactions of different surfaces [21, 93-98] in terms of enthalpy and free energy of adsorption. The comparison of $\Delta G°$ values of n-alkanes and n-alkenes was used to study the effect of π bond interactions with the electron acceptor

sites on the surfaces [93, 94, 98]. The specific interaction parameter ϵ_π was defined by the following equation:

$$\epsilon_\pi = \Delta G^o_{alkane} - \Delta G^o_{alkene} \quad (19)$$

Based on the well-known electronic structure of alkanes and alkenes, this parameter can be taken as a measure of the specific (electron acceptor) interaction capacity of the surface [98]. An increase in the value of ϵ_π is related to an increase in the average number and strength of acidic sites which are able to interact stronger with π bonds of alkenes.

When chromatographic measurements are performed at several temperatures, the enthalpy of adsorption at infinite dilution $\Delta H°$ is calculated by [92]

$$\Delta H° = -R\frac{\partial \ln(V_N)}{\partial(1/T)} \quad (20)$$

4.10. Sorption of Water.

Water sorption experiments were carried out at different temperatures close to ambient (283 – 303 K) using a Micromeritics ASAP 2010 equipped with a vapor sorption kit. The instrument was equipped with a homemade thermostated system instrument controlled by a Fisher Scientific Isotemp refrigerated circulator ($\Delta T < 0.1$ K). Before each measurement, samples were heated to 393 K and outgassed to 10^{-5} Torr. HPLC grade water used as an adsorbate was free of any dissolved gases. Using ASAP 2010, one

is able to measure the water uptake starting from a very low relative pressure ($p/p_0 \sim 10^{-3}$). Each point of the isotherm was recorded after an equilibrium had been reached. The measurement of one isotherm to relative pressure of about 0.3 takes a few days because of the slow equilibrium process. From the isotherms the heats of adsorption were calculated.

4.11. Sorption of Methanol.

Methanol sorption experiments were carried out at different temperatures close to ambient (283 – 303 K) using a Micromeritics ASAP 2010 equipped with a vapor sorption kit. The instrument was equipped with a homemade thermostated system instrument controlled by Fisher Scientific Isotemp refrigerated circulator ($\Delta T < 0.1$ K). Before each measurement, samples were heated to 393 K and outgassed to 10^{-5} Torr. HPLC grade methanol used as an adsorbate was free of any dissolved gases. Each point of the isotherm was recorded after an equilibrium had been reached. The measurement of one isotherm to relative pressure of about 0.3 takes a few days because of the slow equilibrium process. From the isotherms the heats of adsorption were calculated.

The carbons used for methanol sorption were first exposed to it at 303 K to ensure that any reacting groups would be esterified. Then the isotherms were measured starting from the highest temperature.

4.12. Sorption of Diethyl Ether: Inverse Gas Chromatography at Finite Concentration.

Inverse gas chromatography (IGC) at finite concentration was used to obtain adsorption isotherms for diethyl ether on the carbon samples. This method provides a useful way to determine isotherms of vapors, which are environmentally hazardous or may interfere with instruments of volumetric or gravimetric measurements [99, 100]. An important condition of measurement is the linearity of the detector's response. This condition is fulfilled by checking if several injections of different amounts of solute lead to chromatographic peaks whose tails superimpose [100]. According to this method, one single peak can be used to calculate the experimental isotherm [99-105]. Figure 5 shows the principles of the method. Quantities used for calculations are described below.

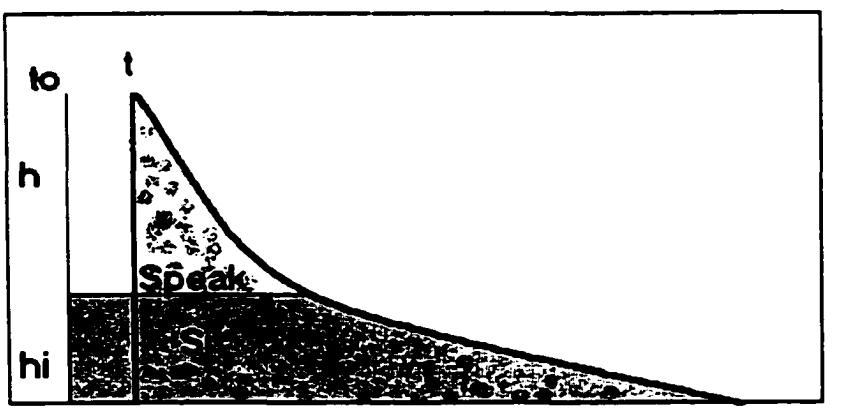

Figure 5. Principles of the finite concentration method.

In the characteristic point elution method [99-105] the total amount of solute adsorbed on the solid support is calculated from the following formula:

$$V = \frac{F_C}{m} k \int_0^h (t - t_0) dh \qquad (21)$$

where V is the amount adsorbed, F_c is the corrected flow of helium gas through the column [106], m is the weight of the adsorbent, and t and t_0 are the retention times of adsorbate and nonadsorbed species, methane, and k is a proportionality constant between the height of the peak h and the corresponding concentration at that particular height, c_i. Using this equation, one can divide the chromatographic peak into *i* slices that corresponds to *i* pressures and injected amounts [45, 96] and thus:

$$C_i = \frac{q \bullet h_i}{F_C \bullet S_{peak}} \qquad (22)$$

where q is the injected amount, and S_{peak} is the area of the chromatographic peak. To transform concentration into pressure the following expression is used:

$$P_i = C_i \bullet R \bullet T \qquad (23)$$

where R is the ideal gas constant, and T is the temperature of the column in Kelvin. The amount adsorbed at different *i*'s can be calculated from the following equation [103]:

$$V_i = \frac{q \bullet S_i}{m \bullet S_{peak}} \qquad (24)$$

where S_i indicates the adsorbate holdup contribution and is the area at h_i but it differs from S_{peak} in the respect that it includes the adsorbate holdup time.

The chromatographic experiments were carried out using a SRI 8610 gas chromatograph. Helium was used as a carrier gas. The flow rate was measured at the outlet of each column and was corrected for the pressure drop across the column [107, 108]. Before each experiment the column was conditioned by heating it to 473 K for 12 hours, under helium flow, to remove impurities form the carbon surface. The column used was 1.0 meter long and 3 mm in diameter. The amount of diethyl ether injected ranged from 1 to 5 μL. Temperatures of the measurements were between 393 K and 433 K. The areas corresponding to the chosen pressure were calculated using a software package from SRI instrument.

4.13. Sorption of Phenol.

The equilibrium adsorption isotherms for phenol from an aqueous solution on activated carbons were measured at two temperatures: 303 and 333 K. Different amounts of carbons were weighed and added into 15 bottles containing 50 mL of the organic solution with a concentration of 250 ppm. The pH of the solution was acidic in all cases (between 3.6 and 6.8). All of the solutions were prepared with deionized water. The covered bottles were then placed in a reciprocal shaking bath (Precision) and allowed to shake for 72 hours at a constant temperature, of 303 or 333 K, at 35 RPM. Afterwards, the concentration of phenol in the liquid was determined using a Shimadzu GC-MS QP5050, a gas chromatograph equipped with a mass spectrometry detector. The column used was a capillary column manufactured by Restek type XTI-5 (95% dimethyl-

5%diphenyl polysiloxane), 30 m in length and 0.25 mm in diameter. The amount adsorbed is calculated from the following formula:

$$q_e = \frac{V^l.(c^o - c_e)}{W} \tag{25}$$

where q_e is the amount adsorbed, V^l is the volume of the liquid phase, c^o is the concentration of solute in the bulk phase before it comes in contact with the adsorbent, c_e is the concentration of the solute in the bulk phase at equilibrium, and W is the amount of the adsorbent. In this method, it is assumed that the change in volume of the bulk liquid phase is negligible because the solute concentration is very small and the volume occupied by the adsorbent is also very small. The amount of phenol on the sample was calculated based on a previously determined calibration curve.

The obtained isotherms were fitted into the Freundlich single solute isotherm which has the following form [109]:

$$q_i = K_F C_i^{n_i} \tag{26}$$

where q_i is a function of C_i which is the equilibrium solution phase concentration, n (dimensionless) is an empirical parameter that represents the heterogeneity of the site energies, and K_F is related to the capacity factor.

5. RESULTS AND DISCUSSION

5.1. Pore Structure Characterization

The carbons used for this study have been prepared by different activation methods and thus differ significantly in their pore structure. Carbon C is of coal origin, whereas carbons W and U are of wood origin. Although carbons W and U were obtained from the same wood precursor, different methods of activation resulted in completely different pore structures. Nitrogen adsorption isotherms for our samples are presented in Figures 6 and 7. Their shapes indicate significant differences in the porous structure of the materials [110].

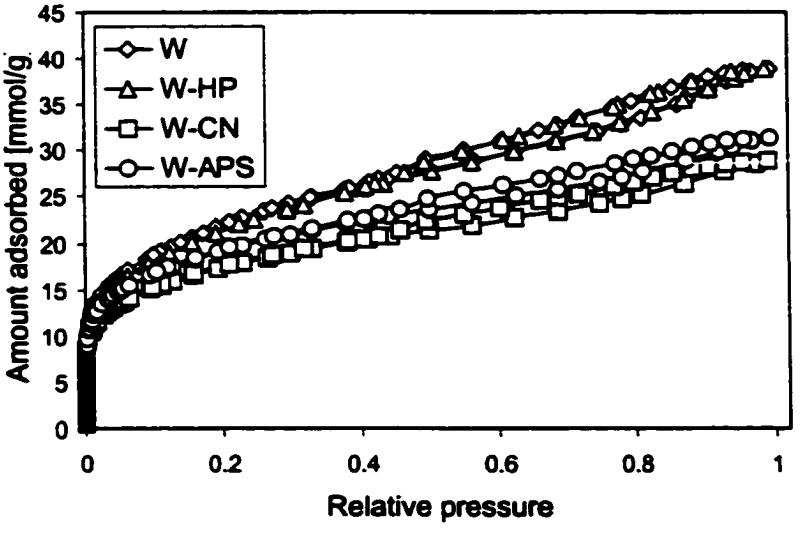

Figure 6. Nitrogen adsorption isotherms on W series of carbons.

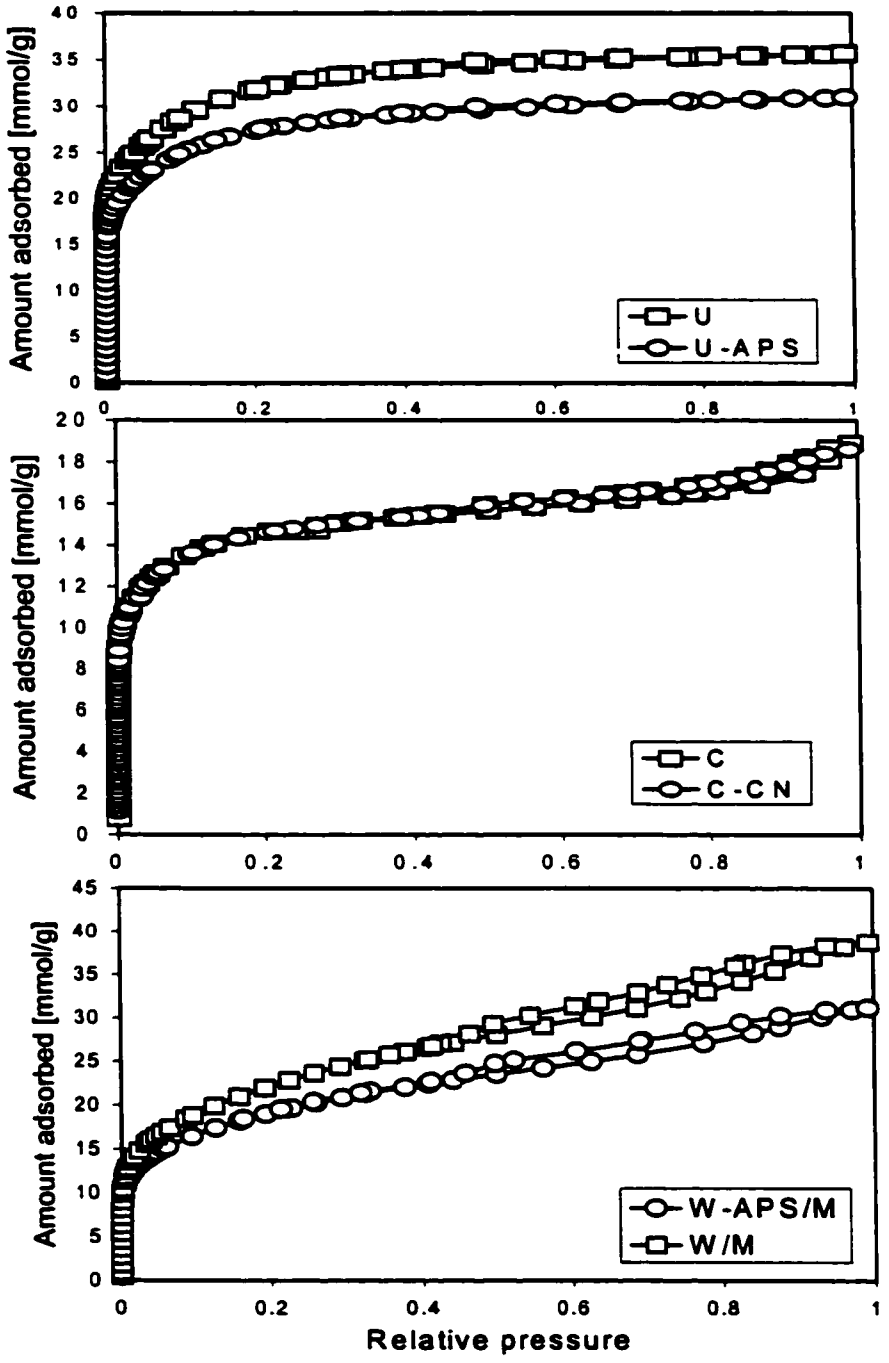

Figure 7. Nitrogen adsorption isotherms.

Although, the shapes of the isotherms are similar, a decrease in the nitrogen uptake as the samples are oxidized is noticed due to the changes in the microstructure of

the carbons [23, 24]. From the nitrogen adsorption isotherms, the structural parameters such as BET surface area, S_{BET}, micropore volume, V_{mic}, volume of pores smaller than 5Å, $V_{<5Å}$, volume of pores smaller than 10Å, $V_{<10Å}$, surface area, S_{DFT} [90], and the ratio of the micropore volume to the total volume were calculated. The results are presented in Table 1.

Table 1. Structural parameters calculated from sorption of nitrogen.

Sample	S_{BET} [m^2/g]	V_{mic} [cm^3/g]	$V_{<5Å}$ [cm^3/g]	$V_{<10Å}$ [cm^3/g]	S_{DFT} [m^2/g]	V_{mic}/V_t
W	1710	0.645	0.005	0.118	1100	0.35
W/M	1730	0.561	0.003	0.128	1157	0.36
W-APS	1472	0.541	0.008	0.134	1010	0.41
W-APS/M	1460	0.474	0.000	0.140	996	0.41
W-CN	1330	0.521	0.017	0.122	916	0.40
W-HP	1681	0.541	0.000	0.131	1102	0.33
C	1040	0.467	0.020	0.200	831	0.73
C-CN	980	0.437	0.001	0.200	825	0.76
U	2300	0.773	0.001	0.409	1790	0.76
U-APS	1970	0.719	0.000	0.353	1569	0.76

For sample C, the results show that oxidation with nitric acid did not significantly change the overall microporosity of the carbon and only the volume of very small pores decreased. This shows that carbon C is not susceptible towards oxidation and is structurally stable. The ratio of the volume of micopores to the total volume of pores increased because the population of the pores with diameter of 20 Å decreased to lesser extent as compared to the decrease in the total volume of pores after oxidation.

Oxidation of sample W with nitric acid resulted in the most pronounced changes in the carbon structure. The shapes of the isotherms for sample W indicate the presence

of mesopores, which are responsible for the hysteresis loop [110]. It is noteworthy that in the case of W carbon, the volume of very small pores increased significantly as a result of nitric acid oxidation. The observed decrease in the total volume of micropores suggests changes in the population of micropores having bigger diameters. Oxidation with hydrogen peroxide causes a slight decrease in the total volume of micropores accompanied by a disappearance of pores smaller than 5 Å. As expected, washing with methanol did not cause any significant changes in the structure of carbon samples. A slight increase in the population of small pores could be attributed to the replacement of water molecules with methanol molecules and the rearrangement of functional groups at the edges of the crystallites.

Table 1 shows that U is highly microporous with a large specific surface area close to its theoretical limit [111]. Oxidation with ammonium persulfate caused a slight decrease in volume of micropores and pores smaller than 5 Å. However, a more pronounced decrease is observed for the surface area as the result of oxidation. The observed changes in the carbon pore sizes are the effects of the destruction of some small pore walls, the removal of some of the carbon atoms from the matrix, and the formation of functional groups on the carbon surface [39]. Those functional groups can block the pore entrances thus further decreasing the carbon pore sizes and surface area. Figures 8 and 9 present the pore size distribution for our carbons. Sample U has all pores smaller than 30 Å. On the other hand, sample W has a significant contribution of mesopores. Sample C is microporous with a small contribution of mesopores. For sample U, after oxidation with ammonium persulfate the surface areas and pore volumes decreased about 15 % with the most pronounced changes in the range of mesopores. Oxidation of sample

W with nitric acid resulted in the destruction of pores on the borderline between micropores and mesopores. This led to a decrease in the surface area and the total volume of micropores and an increase in the micropore ratio and the volume of very small pores. Oxidation with hydrogen peroxide increased the volume of pores having a diameter of about 6 Å.

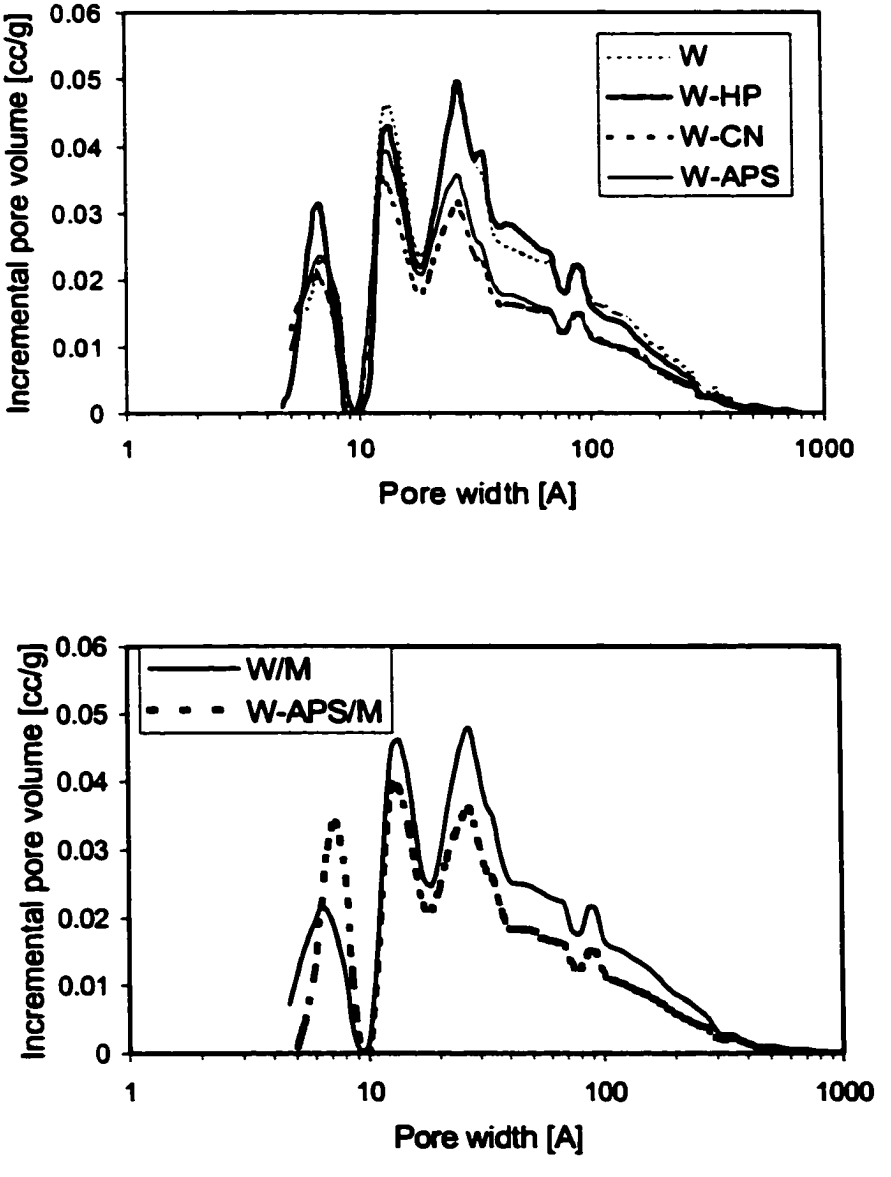

Figure 8. Pore size distribution.

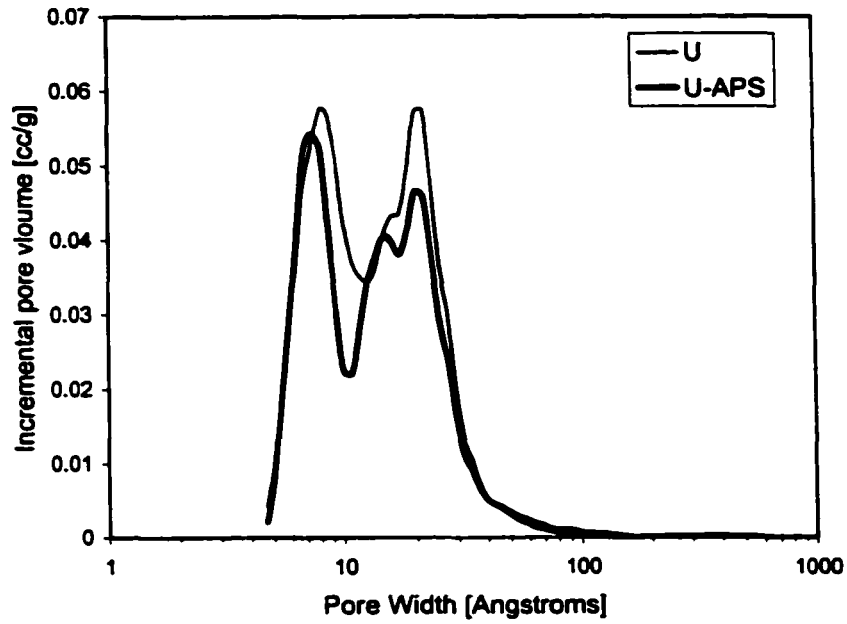

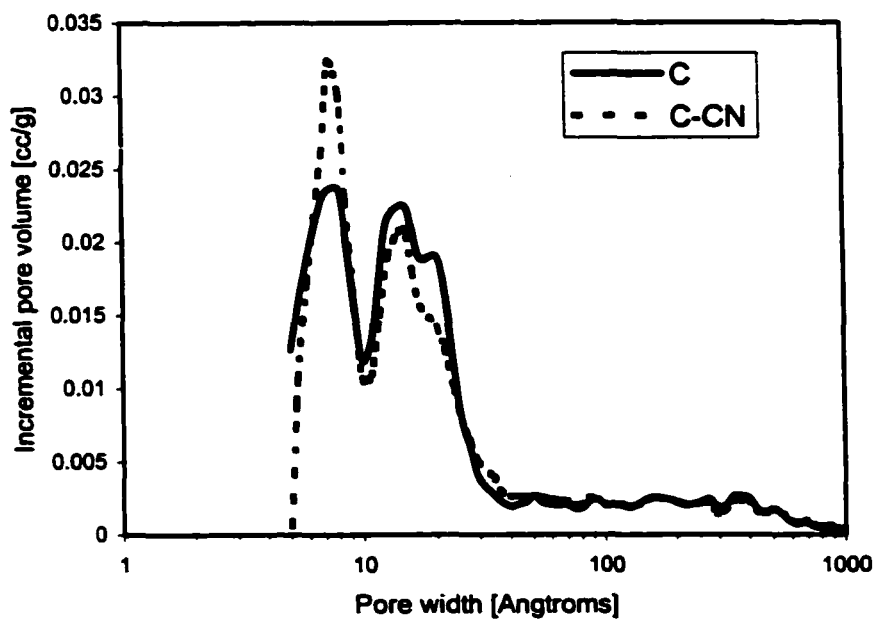

Figure 9: Pore Size Distribution.

Inverse gas chromatography (IGC) experiments revealed significant differences in the pore structure. Figure 10 presents the typical dependence of $\ln(V_N)$ upon the number of carbon atoms in the hydrocarbon molecule, which is used to calculate the parameter of dispersive interactions, ΔG_{CH2} (Table 2). This quantity is related to the pore size in the adsorbents studied [21, 93, 94]. The parameters of dispersive interactions are found bigger for carbons U and U-APS compared to W and W-APS, which indicates the more significant contribution of the surface in very small pores in the case of KOH-activated carbons compared to the H_3PO_4-activated sample [21]. The results are consistent with those obtained from nitrogen adsorption isotherms. Information about porosity can be also derived from the analysis of the enthalpies of hydrocarbon adsorption, $\Delta H°$ [112] (Table 2). They are calculated from the temperature dependence of the retention volumes (Figure 10). The enthalpies of adsorption obtained for W and U and their ammonium persulfate oxidized counterparts are similar to each other, that is related to the similar sizes of the pores in the carbons.

Table 2. Inverse Gas Chromatography results (at 473 K).

Sample	$-\Delta G_{CH2}$ [kJ/mol]	$-\Delta H_{C4}$ [kJ/mol]	$-\Delta H_{C6}$ [kJ/mol]	$\varepsilon_{\pi C4}$ [kJ/mol]
W	5.35	47.9 ± 0.1	68.9 ± 1.9	-0.437
W-APS	5.23	48.7 ± 0.8	74.2 ± 1.6	0.271
U	6.46	50.0 ± 1.5	68.1 ± 5.5	-0.894
U-APS	6.13	48.6 ± 2.9	74.3 ± 4.9	-0.647

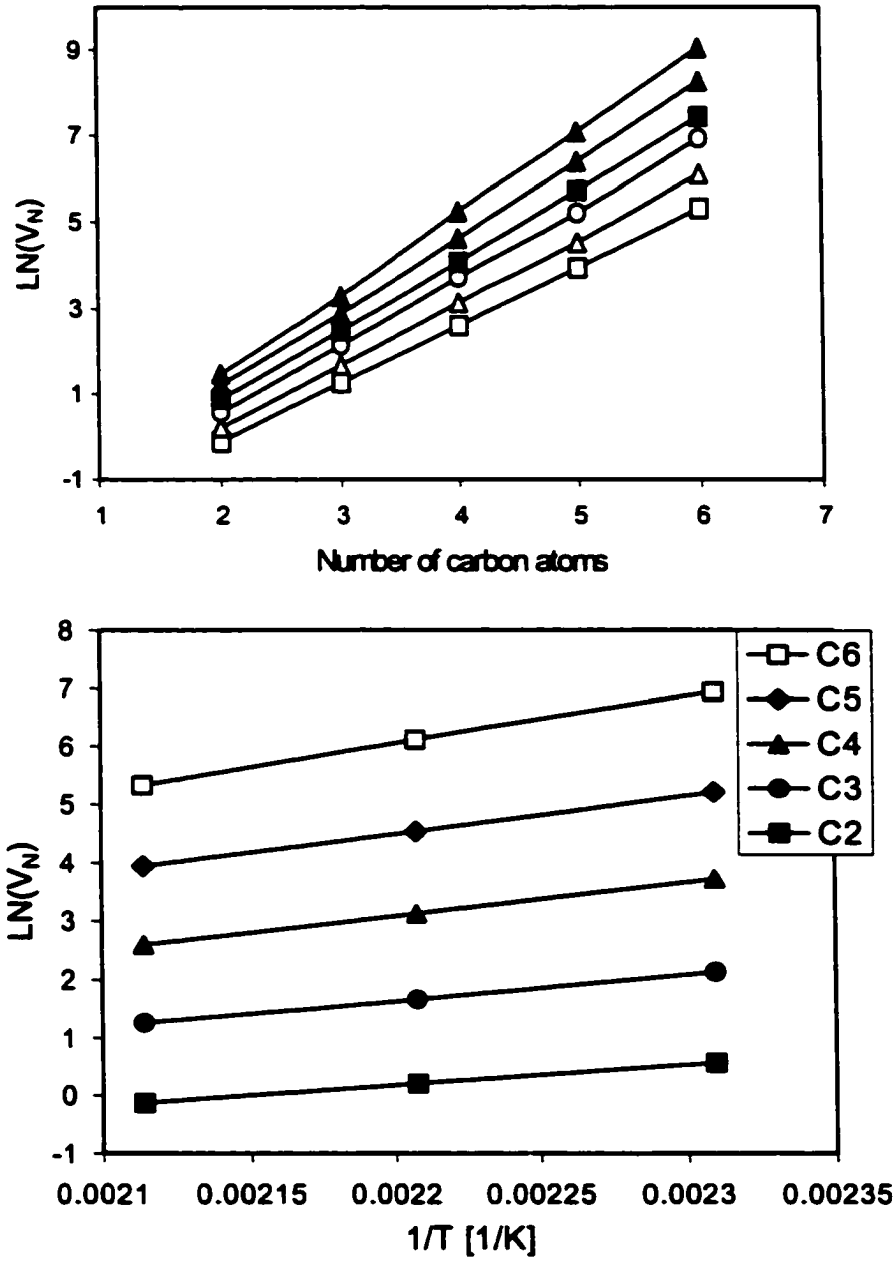

Figure: 10. Top: Dependence of $\ln(V_N)$ of alkane adsorption upon number of carbon atoms measured at 433K (squares), 453K (triangles), 473K (circles) for W (open symbols) and UMC (solid symbols).

Bottom: Dependence of $\ln(V_N)$ on 1/T for a series of alkanes from ethane to hexane.

5.2. Characterization of Surface Chemistry

The effect of oxidation on surface chemistry is more pronounced than on the pore structure. The Boehm titration method provides information about the acidic centers (Bronsted type). The results of Boehm titration in terms of the number of carboxylic acids, lactones, phenols, and bases are collected in Table 3. In order to better visualize the surface changes, the results are presented in Table 4 in terms of the density of groups (molecule per square nanometer of the surface). It was calculated by dividing the number of groups obtained from the titration experiments (in mmol/g of carbon) by the surface area of the adsorbents [31, 113]. Analysis of the data indicates that all initial samples (W, C, and U) have some groups present on the surface. The W sample has a variety of species, which are mainly acidic groups due to the origin of the carbon and the method of activation with phosphoric acid. One should be aware that sample W is likely to contain phosphorous organic functional groups in the form of phosphates which can be misidentified as phenols in Boehm titration [114].

Table 3. Results of Boehm titration [mmol/g].

Sample	Carboxylic	Lactonic	Phenolic	Basic	Acidic	All
W	0.250	0.250	0.325	0.250	0.825	1.075
W/M	0.200	0.125	0.925	0.350	1.250	1.600
W-APS	1.238	0.288	0.625	0.113	2.151	2.264
W-APS/M	0.980	0.050	1.275	0.050	2.305	2.355
W-CN	0.988	0.563	0.613	0.100	2.164	2.264
W-HP	0.755	0.438	0.838	0.000	2.051	2.051
C	0.000	0.100	0.000	0.513	0.100	0.613
C-CN	0.148	0.251	0.317	0.353	0.716	1.068
U	0.125	0.200	0.663	0.463	0.988	1.451
U-APS	1.388	0.400	0.663	0.000	2.451	2.451

As expected, nitric acid introduces the greatest number of oxygen containing-groups for sample W, while oxidation with ammonium persulfate introduces the greatest number of carboxylic groups which are strongly acidic [24, 94]. Oxidation of sample W with hydrogen peroxide results in an increase in the number of carboxylic and phenolic groups and it significantly decreases the number of basic groups. The effect of the three types of oxidation on sample W is that the total number of surface chemical species almost doubled.

Washing with methanol produced interesting results. First, the number of phenols doubled accompanied by a significant decrease in the number of lactones and a small decrease in the number of carboxylic groups. It is noteworthy that the total number of groups was not affected to a great extent by washing with methanol.

Table 4. Results of Boehm titration [molecule/nm^2].

Sample	Carboxylic	Lactonic	Phenolic	Basic	Acidic	All
W	0.137	0.246	0.219	0.123	0.602	0.739
W/M	0.104	0.065	0.482	0.182	0.651	0.833
W-APS	0.738	0.172	0.373	0.067	1.283	1.350
W-APS/M	0.593	0.030	0.771	0.030	1.394	1.424
W-CN	0.650	0.370	0.403	0.066	1.423	1.489
W-HP	0.413	0.239	0.458	0.000	1.110	1.110
C	0.000	0.072	0.000	0.372	0.072	0.444
C-CN	0.108	0.183	0.231	0.258	0.522	0.780
U	0.042	0.067	0.223	0.156	0.332	0.488
U-APS	0.532	0.153	0.254	0.000	0.940	0.940

Although initial carbons C and U contain a significant contribution of surface groups, their density is smaller than those of sample W. The overall lower acidity of

carbon U as compared to carbon W is demonstrated by its smaller number of strong acids and larger number of bases. Oxidation of U with ammonium persulfate results in significant changes in its surface chemistry and an increase in its acidity. Carbon U seems to be more susceptible to oxidation than sample W because the number of strong acids increased significantly, and the number of bases was reduced to zero. For sample C, Boehm titration results show an increase of about sevenfold in the total number of acidic groups. However, the total number of groups in this sample less than doubled due to a decrease in the number of basic groups.

The surface chemistry of the initial carbon samples and the changes in the surface chemistry as a result of oxidation and methanol washing were also studied using potentiometric titration. The proton binding curves obtained for the initial and oxidized carbons are presented in Figures 11 and 12. The solid lines represent the goodness of the fit of equation 13 to the experimental points. The shape of the binding curves changes as a result of oxidation which indicates the existence of different degrees of surface heterogeneity. The effect of oxidation is seen on calculated pK_a distributions presented in Figures 12 and 13 for the initial carbons and their oxidized counterparts.

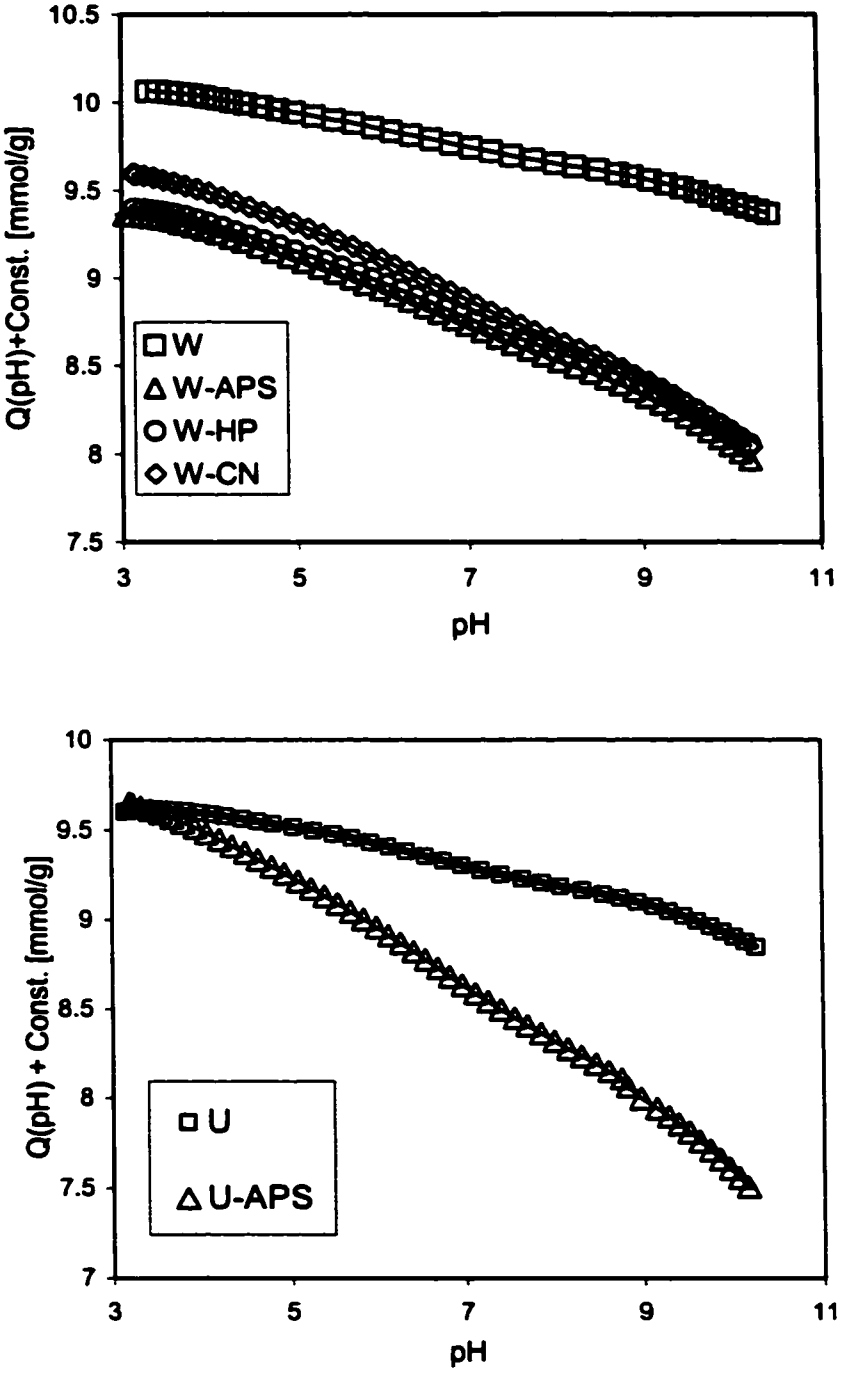

Figure 11. Proton Binding curves.

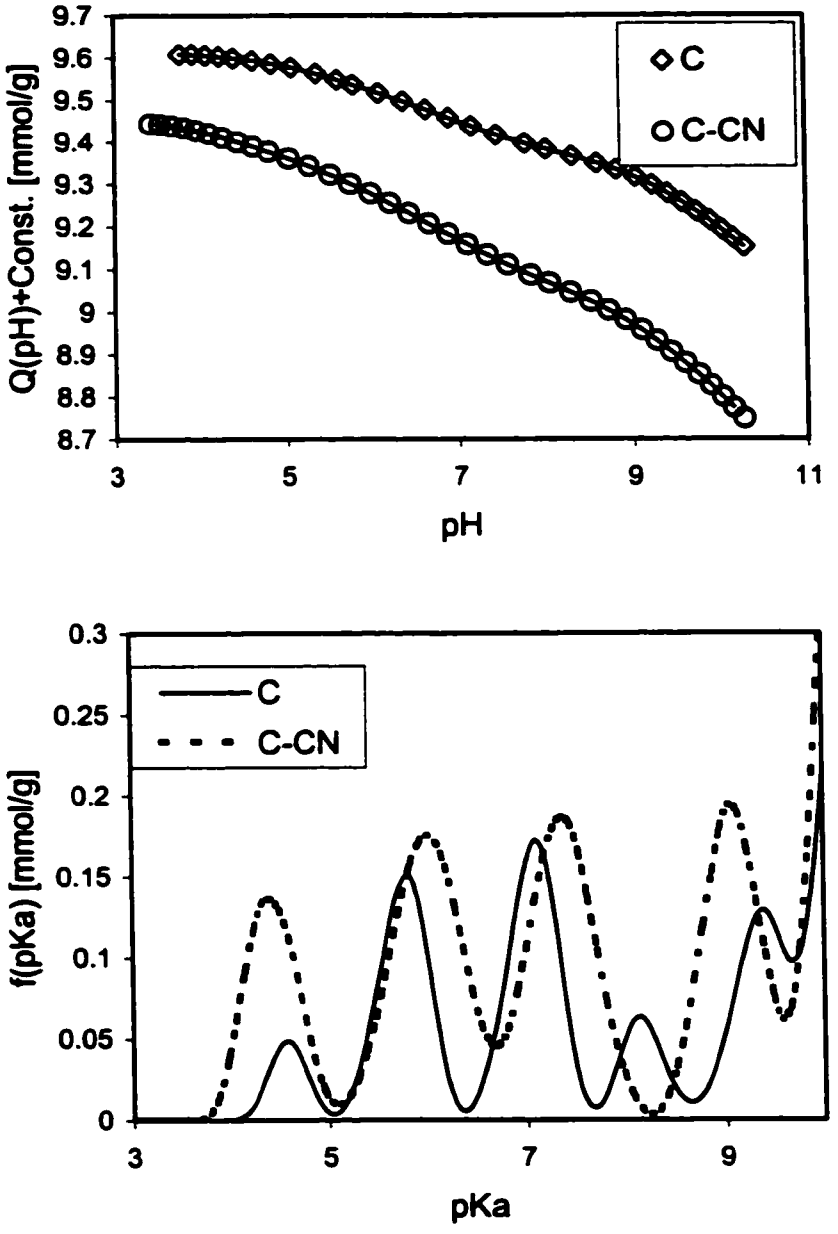

Figure 12. Proton Binding curves and pK_a distributions.

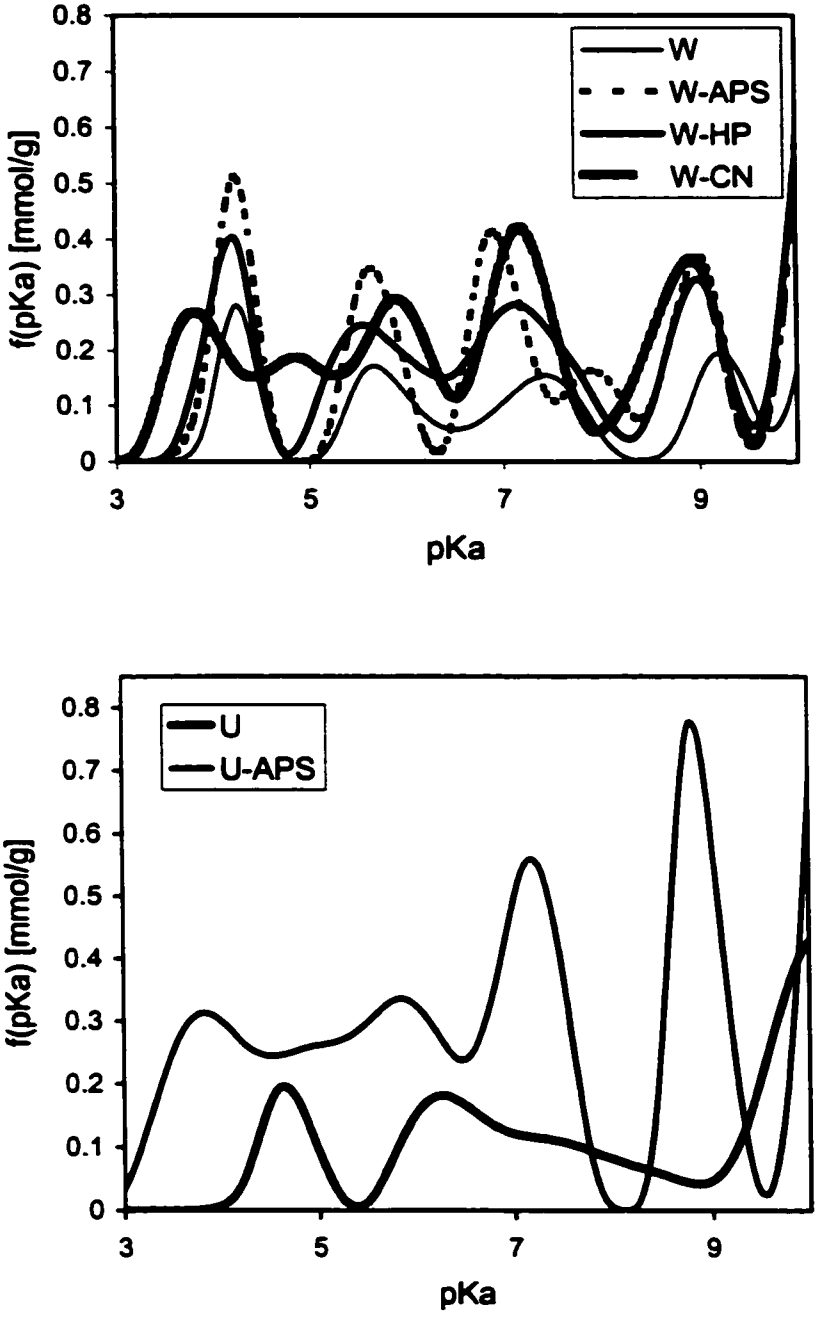

Figure 13. pK_a distributions for initial carbons and their oxidized counterparts.

The position of the peaks and the number of groups are presented in Table 5. The results indicate that the surfaces of Westvaco carbons, W and U, are much more heterogeneous than the surface of C carbon.

Table 5. Results of potentiometric titration: Peak position and the number of groups (in parentheses; molecule/nm^2).

Sample	pK_a 3-5	PK_a 5-6	PK_a 6-7	PK_a 7-8	PK_a 8-9	pK_a 9-11*	All
W	4.23 (0.076)	5.80 (0.0800)		7.31 (0.092)	9.23 (0.077)	10.30 (0.125)	0.450
W/M	4.41 (0.059)	5.91 (0.067)		7.33 (0.072)	9.09 (0.062)	10.35 (0.178)	0.438
W-APS	4.21 (0.162)	5.67 (0.137)	6.95 (0.166)	7.89 (0.065)	8.94 (0.155)	10.25 (0.362)	1.047
W-APS/M	4.06 (0.175)	5.69 (0.219)		7.21 (0.199)	8.85 (0.181)	10.25 (0.415)	1.189
W-CN	3.99, 4.9 (0.276)	5.95 (0.151)		7.17 (0.237)	8.80 (0.214)	10.25 (0.421)	1.299
W-HP	3.8,4.98 (0.227)		6.42 (0.151)	7.96 (0.214)		10.35 (0.190)	0.782
C	4.57 (0.017)	5.76 (0.069)		7.07 (0.076)	8.20 (0.025)	9.3,10.3 (0.419)	0.606
C-CN	4.41 (0.068)		6.01 (0.120)	7.37 (0.107)		9.1,10.2 (0.348)	0.643
U	4.75 (0.046)		6.75 (0.100)		8.46 (0.023)	10.00 (0.149)	0.318
U-APS	4.11 (0.190)	5.75 (0.173)		7.13 (0.191)	8.86 (0.186)	10.27 (0.310)	1.050

The results also show that sample U is slightly more heterogeneous than sample W. This is demonstrated on the distribution obtained for W carbon by the absence of well-defined peaks representing strong acids [85]. The results obtained from potentiometric titration are in agreement with the results of Boehm titration where the number of acidic groups almost doubled for the all of the three carbons after oxidation.

For sample W, after nitric acid and ammonium persulfate oxidation, the number of functional groups more than doubled with a significant increase in the variety and population of carboxylic acids [13, 33, 39, 114]. On the other hand, hydrogen peroxide oxidation, besides introducing new carboxylic species, results in a relatively large increase in the population of phenols, which corresponds to that reported by Boehm titration. Washing the samples with methanol results in a small change in the number of groups. Although, it is noteworthy that a small decrease in the population of strong carboxylic acids ($pK_a < 8$) occurs which is accompanied by an increase in the number of phenols ($pK_a > 8$) [114]. This observation is supported by the results obtained from Boehm titration.

The number of acidic groups increased only slightly as a result of the oxidation with nitric acid for sample C, which indicates that sample C is not as susceptible to oxidation as sample W. Sample U showed the greatest susceptibility towards oxidation which is demonstrated by the threefold increase of acidic sites after oxidation. After washing with methanol, the total number of acidic groups is not changed significantly; however, a small decrease in the population of strong acids ($pK_a < 8$) is noted accompanied by an increase in the number of phenols on the carbon surface ($pK_a > 8$). These results are similar to those obtained by Boehm titration.

The similarity of potentiometric titration to Boehm titration results is expected based on the chemistry of the acid-base titrations and the pK_a values of the bases used in the method proposed by Boehm [2, 3]. Figure 14 shows the correlation between the total number of groups detected using both titration methods. The fact that the slope differs from 1 (0.99) and the correlation coefficient is only 0.76 is related to slightly different

conditions of experiments and limitations of potentiometric titration which detects, within acceptable certainty, groups having pK_a smaller than 11 due to the buffering effect of water [85]. As reported elsewhere, we classify species having $pK_a < 8$ as carboxylic acids and those having $pK_a > 8$ as phenols and quinones [12,13]. The advantage of potentiometric titration is clear distribution of species having pK_a in the range between 3 and 11 [13]. In this method, contrary to the method proposed by Boehm, the precise assignment of pK_a to a certain group of organic acid is not done due to the heterogeneity of carbon surfaces. It is possible that there are species on the surface which contain heteroatoms different than oxygen and whose pK_a corresponds to pK_a of carboxylic acid. Examples here can be ammonium ions with pK_a about 5 [114].

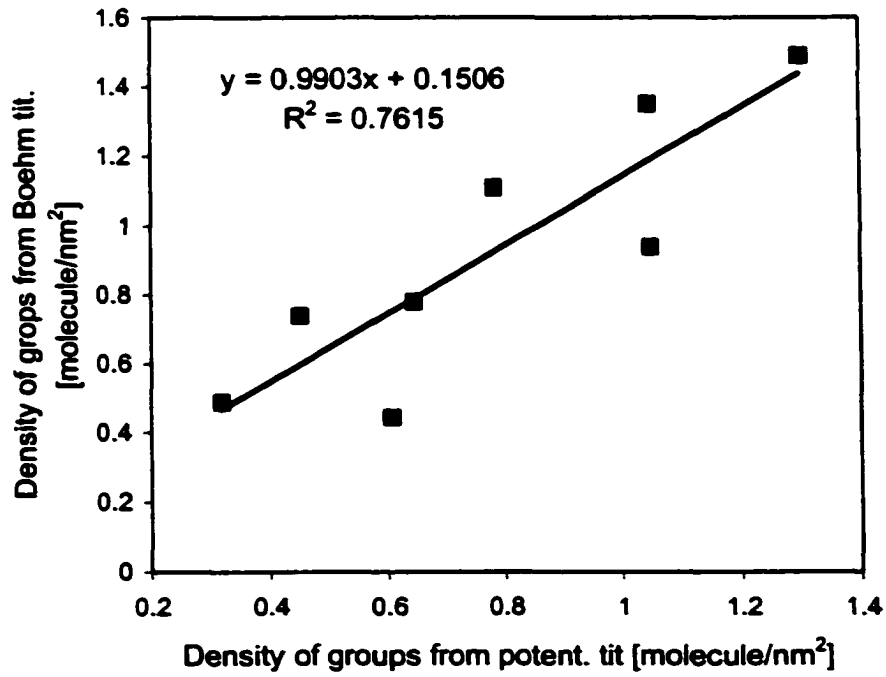

Figure 14. Number of acidic groups from Boehm titration vs. number of groups determined using potentiometric titration.

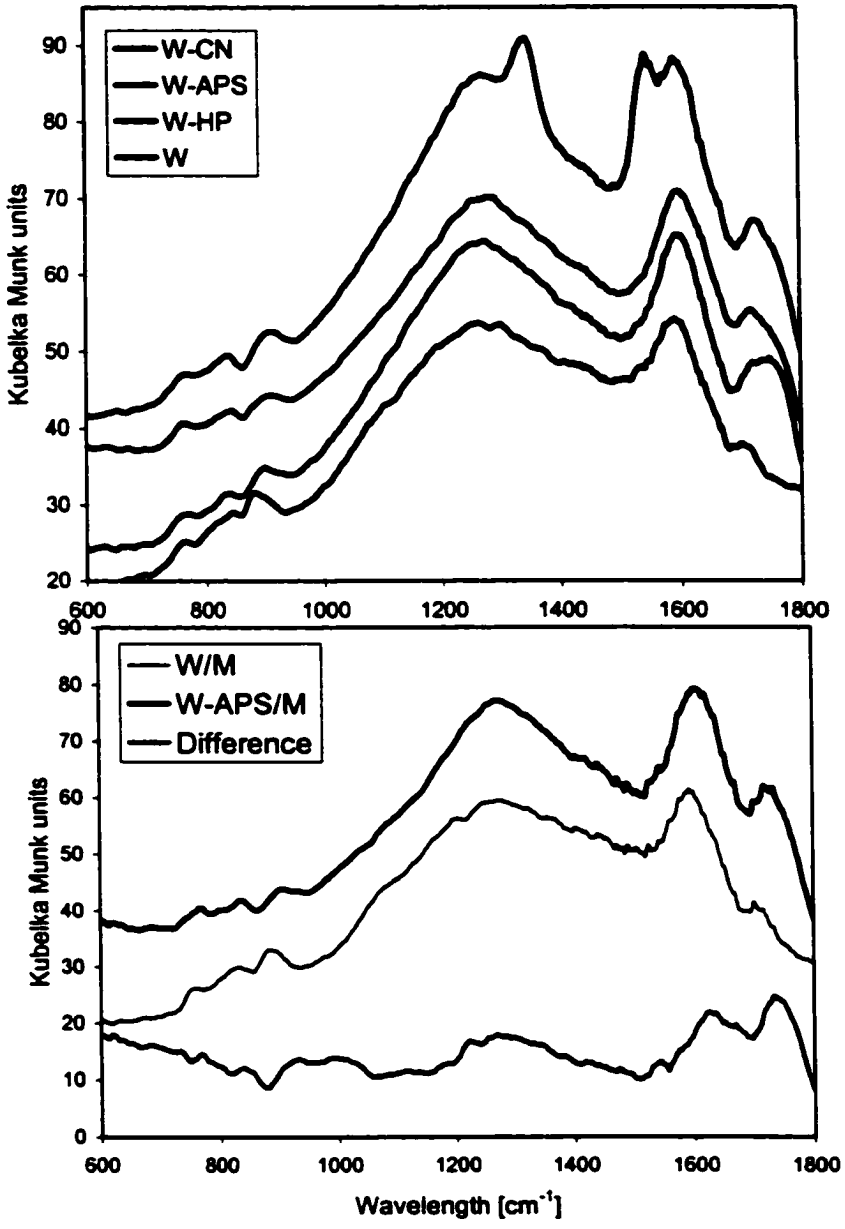

Figure 15. FTIR spectra. The order of the spectra is the same as in legend (from top to Bottom.)

Infrared spectroscopy provides valuable information about the chemistry of the carbon surface. Although FTIR cannot provide quantitative information, it can be used to verify the presence or absence of certain functional groups. The obtained spectra for sample W and its oxidized counterparts and those that are washed with methanol are

presented in Figure 15. The presence of a peak around 1700 cm^{-1} is due to the stretching vibrations of C=O groups which is characteristic of carboxyls, ketones, aldehydes, and esters. The presence of a peak around 1300 cm^{-1} is the result of the stretching vibrations of C---O and is usually attributed to alcohols, phenols, esters, and carboxylic acids [116-117]. After oxidation we observe the appearance of new peaks in the spectra, particularly around 1700, 1550, and 1300 cm^{-1}, along with changes in the intensity of the existing peaks. Those peaks are characteristic of oxygen containing functional groups. The well-defined peaks for the spectrum of sample W show that it possesses, in addition to oxygen containing groups, hydrogen attached to the aromatic ring and hydrogen in aliphatic groups [115].

The spectrum for the sample W-HP shows a band at 1745 cm^{-1} which is consistent with the C=O stretching vibrations. It also reveals a peak at 1275 cm^{-1}, which is due to C--O stretching vibrations along with peak at 1593 cm^{-1}, which is the result of C=O stretching vibrations. The peak at 1275 cm^{-1} shows that phenolic groups exist on the carbon surface. The three peaks combined indicate the presence of carboxylic groups [15, 16, 116, 117]. Similar peaks appear in the spectrum of sample W-APS with the exception that the peak C=O stretching vibration is shifted to around 1710 cm^{-1}. The peaks in the W-APS spectrum are more pronounced and sharper than in the case of W-HP which suggests a higher concentration of carboxylic groups. This is consistent with the results obtained from Boehm and potentiometric titrations. The spectrum for sample W-CN reveals the three peaks around 1719, 1600, and 1255 cm^{-1} that are characteristic of carboxylic and phenolic groups. There are two additional peaks in this spectrum at 1547

and 1341 cm^{-1} which can be attributed to the presence of nitro groups on the carbon surface.

Washing with methanol did not change the relative intensity of the peaks. This could be due to the fact that the total number of groups remains more or less the same after the methanol washing. Boehm and potentiometric titrations showed that methanol washing results in a decrease in the number of carboxylic groups and lactones accompanied by an increase in the number of phenolic groups. This suggests that no new oxygen-carbon bonds are created and that only rearrangement of those bonds occurred. One should note that carboxylic acid groups and esters would produce the same bands which is due to the fact that both possesses a C=O, C=O, and C---O bonds. It follows that one cannot clearly distinguish among those groups based on the FTIR results alone.

Figure 16 presents the IR spectra of samples U and C and their oxidized counterparts. To study the effect of oxidation on the surface chemistry, the spectra of the initial samples were subtracted from the oxidized counterparts (Figure 16) [118, 119]. The spectra obtained for sample C and its oxidized counterpart suggest a high degree of carbonization which it consistent with carbons of coal origin. Similar results are obtained for sample U. A high degree of carbonization makes it very difficult to assess the surface groups using FTIR. Subtraction of the initial spectrum from the oxidized counterpart provides information about the surface of the oxidized sample only in the case of U. The bands obtained are consistent with the presence of carboxylic and lactonic groups due to the pronounced increase in the peak intensity at around 1700 cm^{-1}. This peak represents stretching vibrations of C=O.

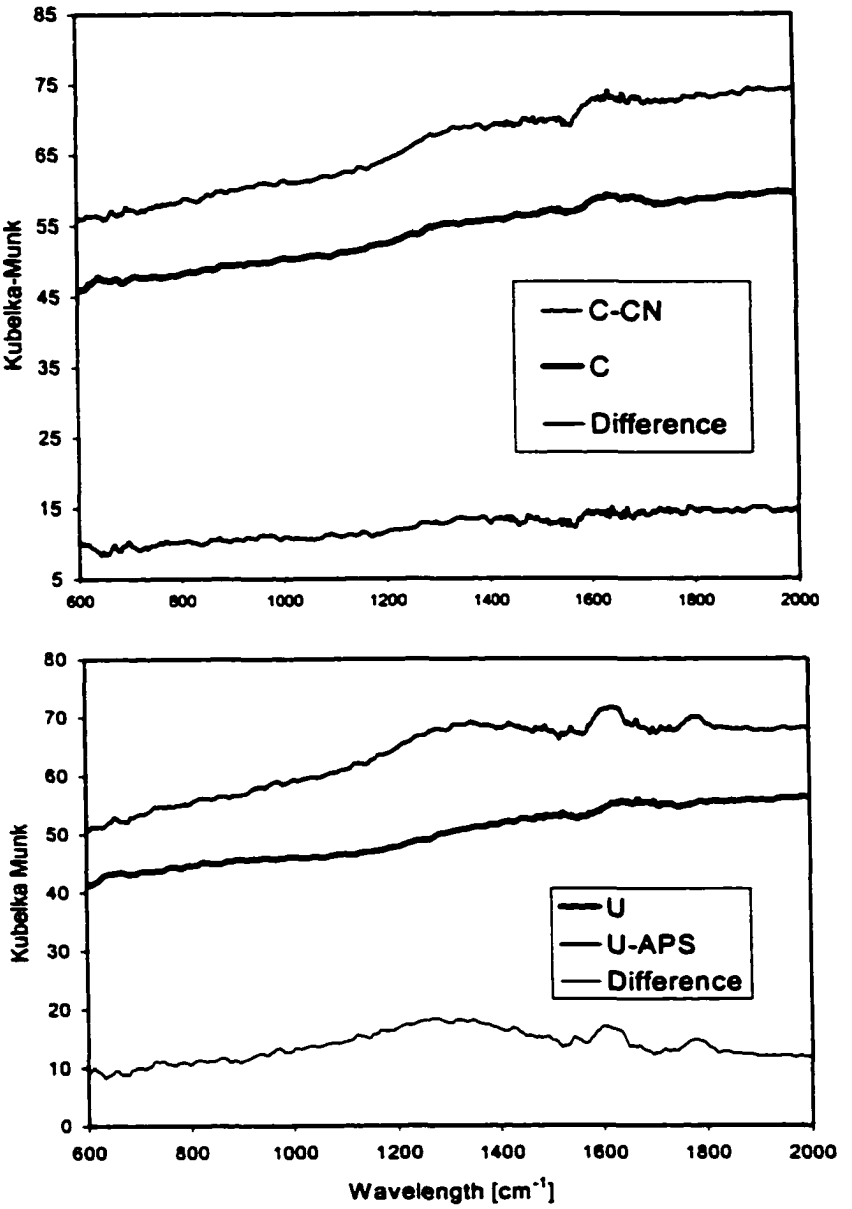

Figure 16. FTIR spectra.

When the temperature programmed desorption (TPD) experiment is performed without any special traps to separate CO and CO_2 [120] or without connection to a mass spectrometer, plots combining all of the desorbed species are obtained (Figure 17) without clear well-defined peaks. The volume of the gases thermally desorbed during heat treatment consists of water, carbon dioxide, and carbon monoxide. It is well known

that the oxygen complexes on the carbon surface decompose to CO and CO_2 at temperatures up to 1250 K [19]. The first two peaks in the spectrum are the result of the decomposition of strong acids such as carboxylic acids at temperatures less than 970 K [19]. At higher temperatures weak acids such as phenols, quinones and organic bases decompose as CO [19]. The temperature at which certain groups decompose is related to the strength of a specific oxygen-containing group. Thus the amount of oxygen containing species released should correspond to the number of oxygen-containing groups on the carbon surface. In order to separate amounts of several types of oxygen groups, the obtained plots were deconvoluted using PeakFit procedure with a Gaussian deconvolution method. The data treatment is described in the experimental section.

Figure 17 shows a comparison of TPD plots obtained for three initial carbons. The plots differ and they show that the most acidic carbon is U carbon with a significant volume of CO_2 representing carboxylic groups that decomposed at low temperatures. These results are consistent with those of Boehm and potentiometric titration. The results also show that sample C contains the smallest number of decomposed oxygen containing species. Furthermore, Figure 17 clearly demonstrates that oxidation leads to a significant increase in the number of desorbed species. It is interesting that this increase is greater for groups decomposed at lower temperatures, which are CO_2 groups, than for CO decomposing groups. This is also consistent with the titration results where mostly carboxylic groups were detected.

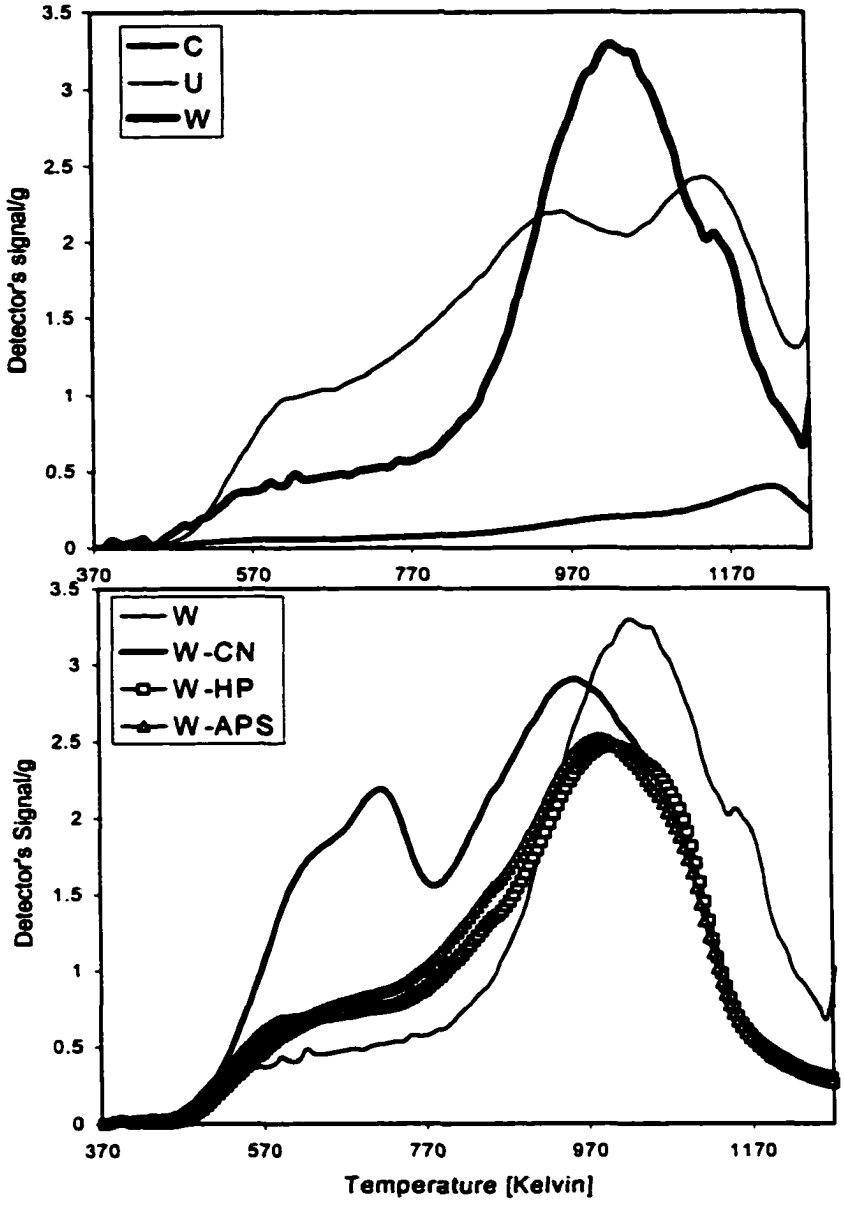

Figure 17. Top: TPD results for initial carbon samples.
Bottom: TPD results for W and its oxidized counter parts.

Examples of the PeakFit deconvolution results are presented in Figures 18 and 19. The first and second peaks are centered around 570 and 750 K, respectively. We assigned those peaks to desorption of CO_2 from the decomposition of carboxylic acids [19], while the peaks at 970 and 1150 K were assigned to desorption of CO [19] from the decomposition of weak acids, weak bases, and other oxygen containing organic species.

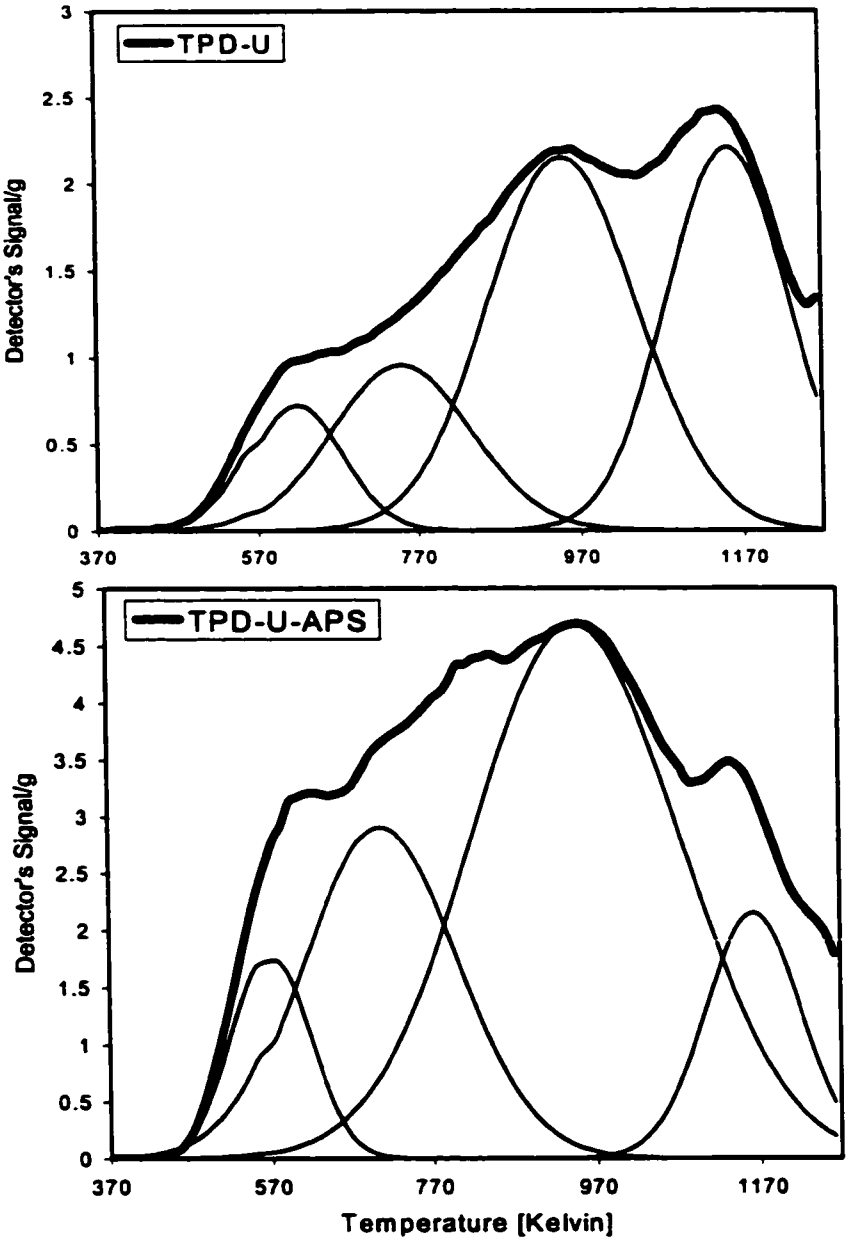

Figure 18. Examples of TPD results for samples U and U-APS.

The results obtained from TPD are presented in Table 6. The amounts of groups are presented in molecule per square nanometer of the carbon surface. For simplification, the results are fitted assuming that four types of species are present and that decomposing gases consist only of carbon dioxide and carbon monoxide. In the case of sample W, the

last peak was assigned to CO. Although it appears as a part of the curve, it is not counted for the total number of groups. This is due to the fact that these species decompose at temperatures higher than the carbonization temperature of this carbon and may consist of hydrocarbons evolved during the aromatization process.

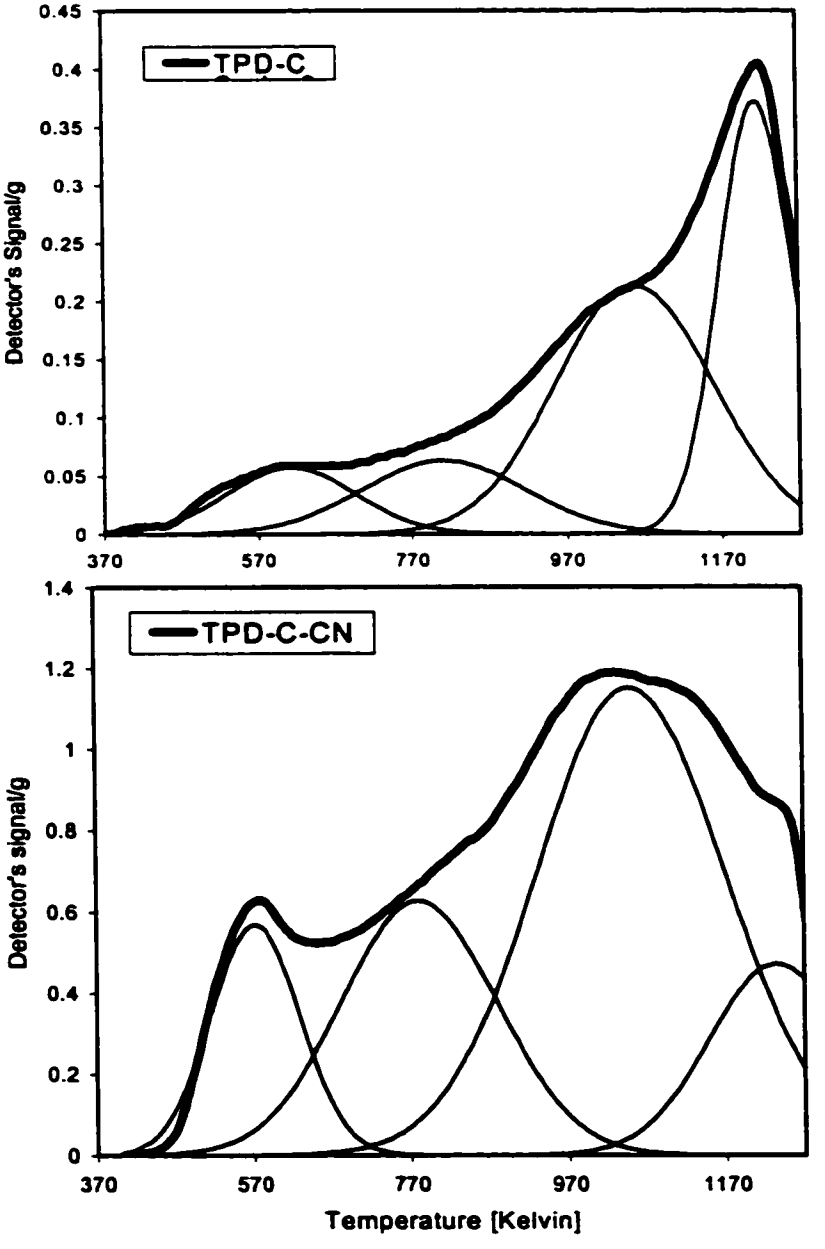

Figure 19. Examples of TPD results for C and C-CN.

Table 6. Results of Temperature Programmed Desorption (TPD) [molecule/nm^2].

Sample	Peak 1 CO_2	Peak 2 CO_2	Peak 3 CO	Peak 4 CO	Peak1+2 CO_2	Peak3+4 CO	Sum
W	0.085	0.152	1.127	0.088	0.237	1.216	1.453
W-APS	0.174	0.486	1.904	0.142	0.661	2.045	2.706
W-CN	0.518	0.632	2.737	0.111	1.150	2.848	3.999
W-HP	0.158	0.436	1.675	0.062	0.594	1.738	2.331
C	0.037	0.051	0.193	0.143	0.088	0.335	0.423
C-CN	0.248	0.476	1.207	0.250	0.724	1.457	2.181
U	0.073	0.147	0.414	0.327	0.220	0.740	0.960
U-APS	0.162	0.550	1.395	0.293	0.712	1.688	2.400

Although, the TPD results follow a similar trend to Boehm and potentiometric titrations, they clearly differ in two aspects. The first aspect is that the overall number of groups determined by TPD is considerably larger than those obtained by Boehm and potentiometric titrations. This is the result of the limitations on Boehm and potentiometric titration methods. Titration methods offer a way of detecting oxygen groups present in the form of carboxylic acids, lactones, phenols and bases. However, they cannot assess all the other groups that can be formed on the surface such as ketones, ethers, aldehydes, and pyrones. Also, groups that contain nitrogen, phosphorus or sulfur cannot be determined by Boehm and/or potentiometric titration. Since sample W is prepared by phosphoric acid activation, a large quantity of phosphorus is expected to remain as functional groups on the surface. Sample U is prepared by KOH activation and as a result potassium ions is likely to be present in very small pores and cannot be detected by either of Boehm or potentiometric titration. Since sample C is prepared by the steam activation method, most of the groups can be determined by both of Boehm and

potentiometric methods. This explains the fact that sample C received comparable results for surface groups from all three techniques used.

The second aspect is that the amount of groups determined using TPD is twice greater than those determined using potentiometric titration for almost all of the carbons except for the C carbon. The number of groups increased by more than five fold for sample C after oxidation with nitric acid as shown from TPD. This is a greater increase than expected based on the titration results. Sample W also shows a significantly larger increase in the number of groups, as compared to Boehm and potentiometric titrations, due to nitric acid oxidation. These can be explained by the fact that nitric acid introduces groups other than those that can be detected by Boehm and potentiometric titration methods. Nitric acid has been known to provide a nitronuim ion capable of nitrating an aromatic ring [121]. Nitronium ion formation occurs as follows:

$$HNO_3 + HNO_3 \Longleftrightarrow NO_2^+ + NO_3^- + H_2O \qquad (27)$$

Since the nitronium ion is a strong electrophile, it can easily attack aromatic rings with activating groups on them. It can also attack a ring that doesn't posses an activating group or even has a deactivating group, although to a lesser extent. Activating groups include groups such as: O^-, NR_2, NHR, NH_2, OH, OR, NHCOR, and aliphatic groups. Deactivating groups include: NR_3, NO_2, CF_3, CN, CHO, COOH, and COOR. The mechanism for the nitration reaction has been long established [122, 123] and the following is a simplified scheme of the nitration mechanism (Figure 20 shows a simplified scheme for the nitration mechanism process of an activated carbon surface):

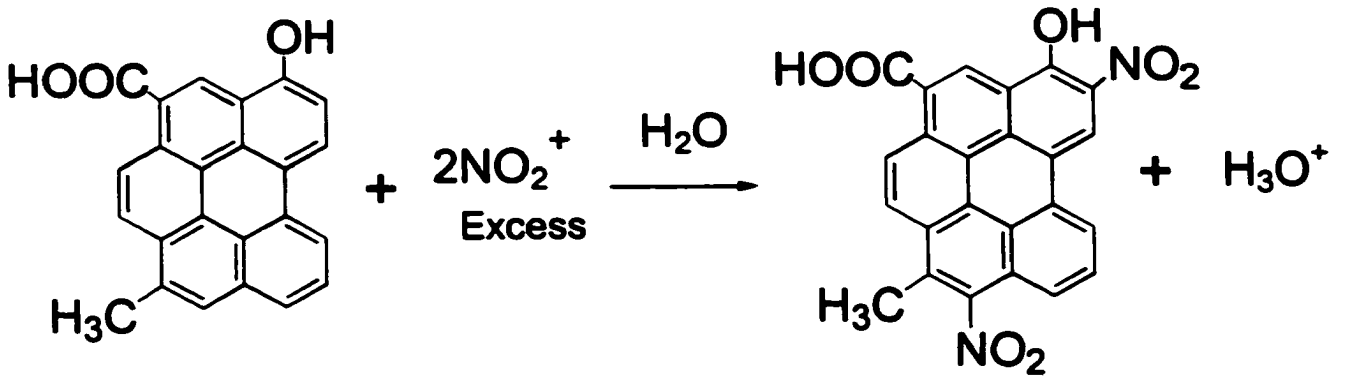

Figure 20. Simplified mechanism of the nitration reaction.

$$ArH + Y^{+} \Longleftrightarrow Y^{+}ArH$$
$$Y^{+}ArH \Longleftrightarrow Y - Ar^{+} - H \qquad (28)$$
$$Y - Ar^{+} - H \Longleftrightarrow ArY + H^{+}$$

where Ar denotes the aromatic ring, Y^{+} represent the nitronium ion.

It is important to note that the nitration reaction has all of the required and favorable conditions to proceed in our systems. The activated carbon structure is made up of aromatic rings. The presence of functional groups on the surface plays a role in the reaction. The reason that sample C has a smaller number of those groups as a result of the oxidation/nitration is due to the structural properties of the carbon. Carbon C is of coal origin and has a high contribution of aromatic condensed rings to the overall structure. On the other hand, sample W is of wood origin and has a significant contribution of aliphatic chains to the total carbon structure. Since aliphatic groups are

activating, that makes the aromatic rings more susceptible to nitration. Consequently, the effect of introducing nitro groups to the carbon surface should be more pronounced for sample W than that for sample C.

Nitro groups begin to decompose at about 550 K resulting in the release of NO_2 [124]. This species contributes to the first peak of the deconvoluted TPD curve where for the C-CN the amount of decomposed species increased about nine fold compared to the initial counterpart (Table 6). A significant increase in the number of groups decomposed in this temperature range is also found for the W-CN sample. Moreover, those nitro groups could not be detected in titration due to their inability to dissociate.

Although FTIR doesn't provide quantitative information about the carbon surface chemistry, it can further verify our hypothesis about nitration reaction. Nitro groups are usually characterized by two strong bands: one is around 1600 – 1500 cm^{-1}, and the other is around 1390 – 1300 cm^{-1} [125]. It is clear from Figure 15 that sample W-CN has the similar stretching vibrations to those of W, W-APS, and W-HP which indicate the presence of carboxyls, lactones and phenols with the exception of the additional two strong bands with the stretching vibrations of 1540 and 1350 cm^{-1}. Those two bands are the result of the presence of nitro groups on the carbon surface [125]. They are only present on the sample oxidized with nitric acid, which means they are a consequence of the oxidation/nitration method. This, in addition to the results obtained from TPD analysis, confirms that nitric acid oxidation not only introduces carboxylic acids, lactones and phenols, but also results in a significant quantity of nitro groups via nitration mechanism.

The FTIR confirmation of the presence of nitro groups cannot be found on DRIFT spectra for C series of samples due to the significant absorption of infrared radiation by a strongly aromatized activated carbon matrix. In Figure 16 we present the spectra for the initial C carbon and after oxidation with nitric acid along with the difference between them obtained by subtraction of spectra from the spectra of sample C [118]. Although the curves show an increase in intensity after oxidation, the results are difficult to interpret.

To further confirm incorporation of nitrogen into the structure of C-CN and W-CN carbons, the CHN analysis was done in a commercial laboratory. The results are presented in Table 7. As expected after oxidation, the content of carbon decreased due to an increase in the amount of oxygen (usually calculated as differences), however, we do not make this interpretation for W due to the presence of a significant amount of phosphorus in this carbon [82]. It is also seen that the content of nitrogen significantly increased, especially for the W-CN carbon where, as expected based on TPD results, a significant amount of nitro groups was incorporated due to the high aliphatic content of this material.

Table 7. Results of CHN analysis [%]

Sample	C	H	N	O*
W	83.98	2.01	0.15	13.86
W-CN	69.38	2.02	2.34	26.26
C	90.44	0.62	0.37	8.57
C-CN	82.13	0.95	0.89	16.03

*From a difference to 100%

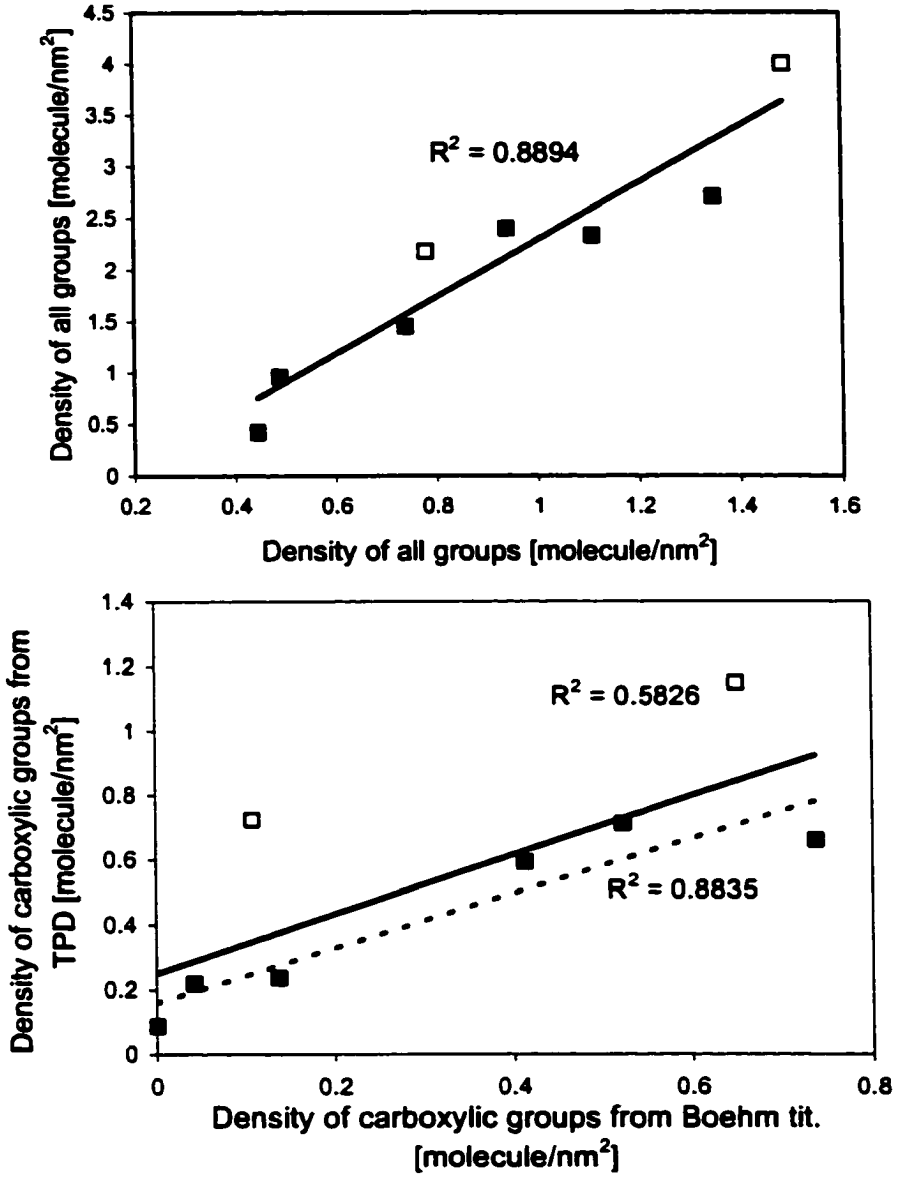

Figure 21. Relationship between the number of groups determined from Boehm titration and TPD.

Figure 21 presents the correlation between the amount of groups determined using Boehm titration and the amount determined using TPD. When all groups are taken into consideration, a good correlation is found (Figure 21, top). The relationship changes when only strong acids are chosen for plotting (Figure 21, bottom). For all carbons studied the correlation coefficient is equal to 0.58. The results presented in Figure

21(bottom) show that two points do not follow the general trend. Those points represent samples oxidized with nitric acid. This is due to the introduction of nitro groups via nitrative mechanism which cannot be assessed by potentiometric or Boehm titration methods. After the exclusion of those points the correlation coefficient is equal to 0.88. These results demonstrate that good correlation between titration and TPD results exists (with slope close to 2.5 for all groups). When a more detailed analysis is required, as for instance the amount of strong acids, the discrepancy exists due to the incapability of titration methods to detect nitro groups.

5.3. Water Adsorption

The results presented in this section show the effect of surface groups and porosity on the adsorption of water. As indicated, this process is very sensitive to the presence of functional groups [27, 37]. Those groups are nucleation sites for the adsorption to begin. As water molecules are adsorbed, they act as secondary adsorption centers where water molecules can further be adsorbed and the cluster formation can occur. Figures 22 and 23 present the water adsorption isotherms for the samples W and W-APS, and W-CN and W-HP, respectively. To clearly show the effect of oxidation on the water uptake, Figure 24 shows the comparison of the isotherms obtained at 283 and 293 K. The water uptake increases in the following order: W < W-HP < W-CN < W-APS. The results follow the same trend as the number of carboxylic acids obtained from the titration methods.

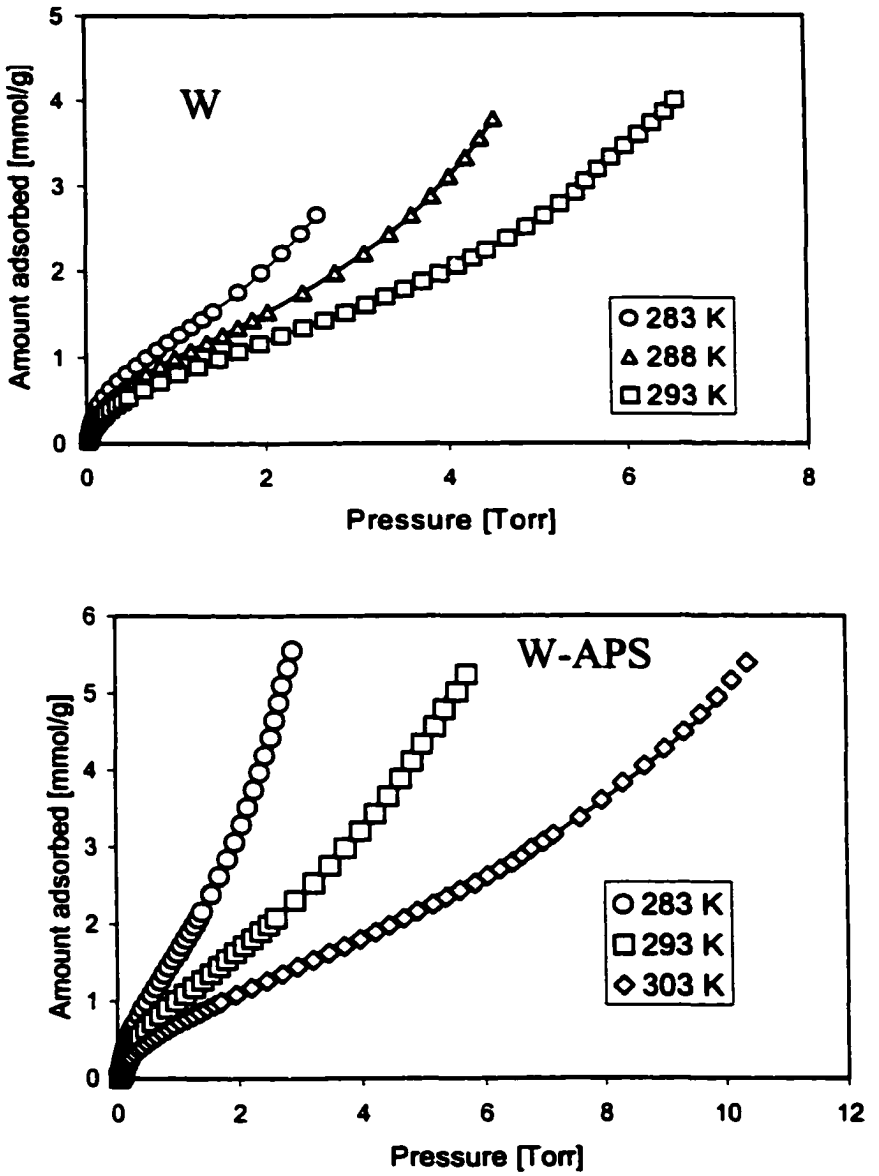

Figure 22. Water adsorption isotherms on samples W and W-APS. The solid lines indicate the goodness of the fit to the virial equation.

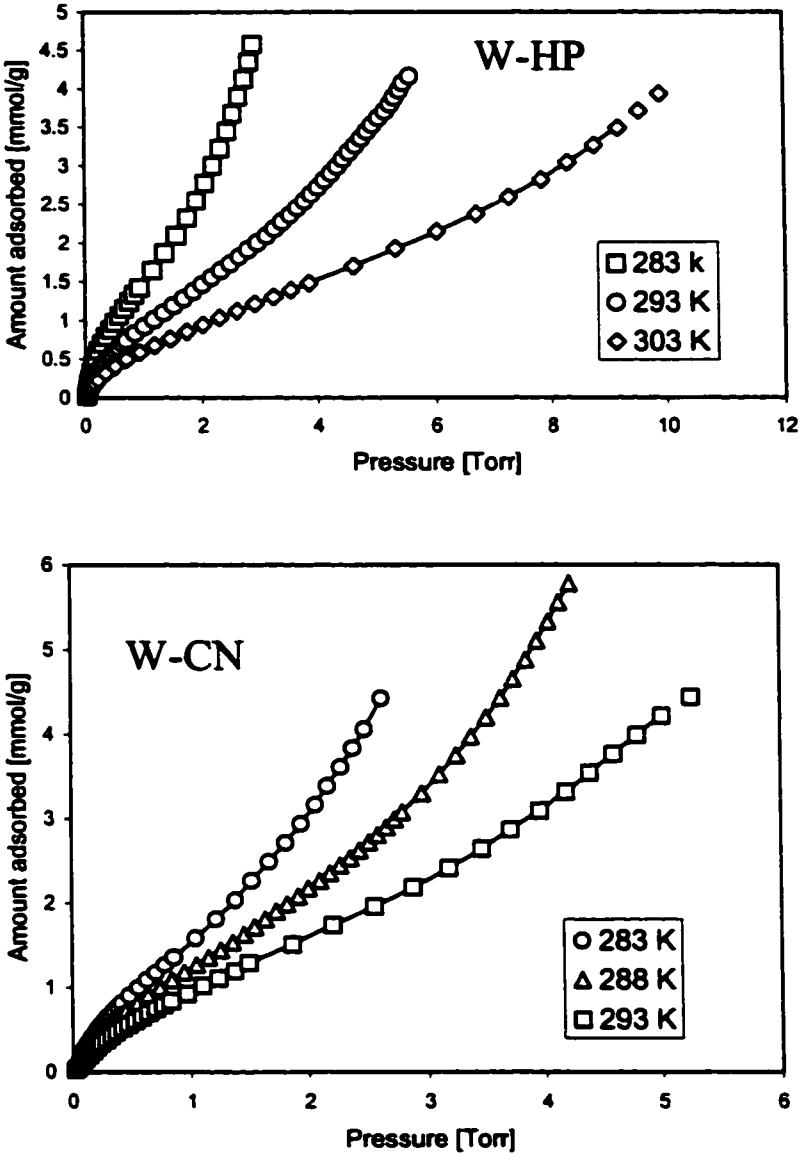

Figure 23. Water adsorption isotherms on samples W-HP and W-CN. The solid lines indicate the goodness of the fit to the virial equation.

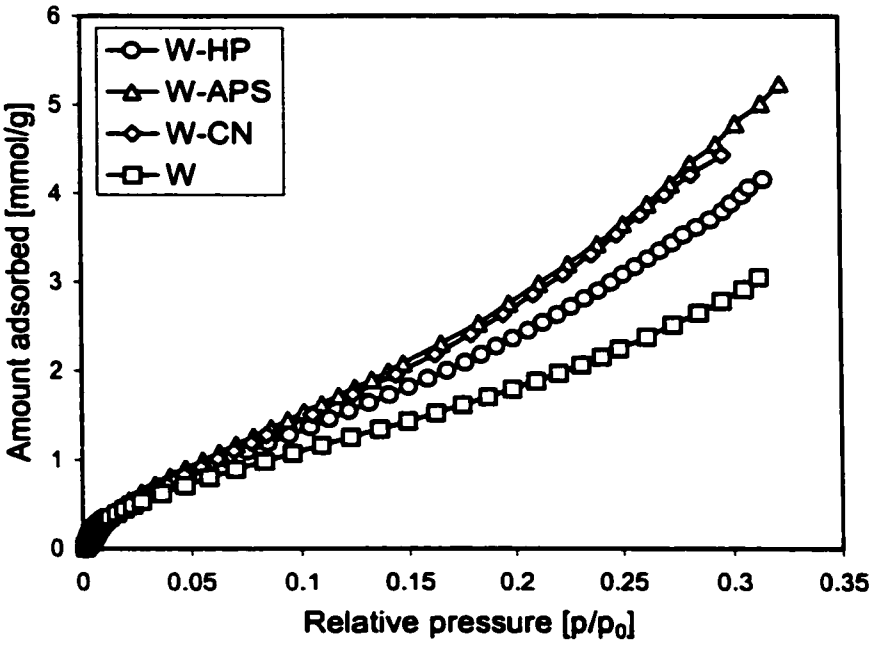

Figure 24. Water adsorption isotherms on the W, W-CN, W-APS, and W-HP at 293 K.

Moreover, the data presented in Figure 25 along with the results obtained from Boehm and potentiometric titrations suggest that there is an apparent relationship between the amount adsorbed and the density of acidic groups. Figure 25 demonstrates a very good correlation between the amount adsorbed at $p/p_0 = 0.1$ and the density of surface groups. The correlation is still good for $p/p_0 = 0.3$. On the other hand, a poor correlation is obtained when sorption amounts at $p/p_0 = 0.01$ are taken into account. This is likely due to the filling of very small pores at low pressure which is the result of the adsorption on secondary sites followed by the cluster formation. At higher pressure, the adsorption occurs in larger pores where functional groups are present. Thus the correlation between the amount adsorbed and the number of functional groups is more apparent. At very low relative pressures, ($p/p_0 < 0.01$) the following order in the amount

adsorbed is observed: W > W-HP > W-CN > W-APS. These results are in the reverse order compared to the amount adsorbed at $p/p_0 = 0.3$. The observed behavior is persistent at all three temperatures measured and that is why we do not consider it as an experimental artifact. We attribute this to the presence of very small pores enhancing water adsorption due to pore filling process.

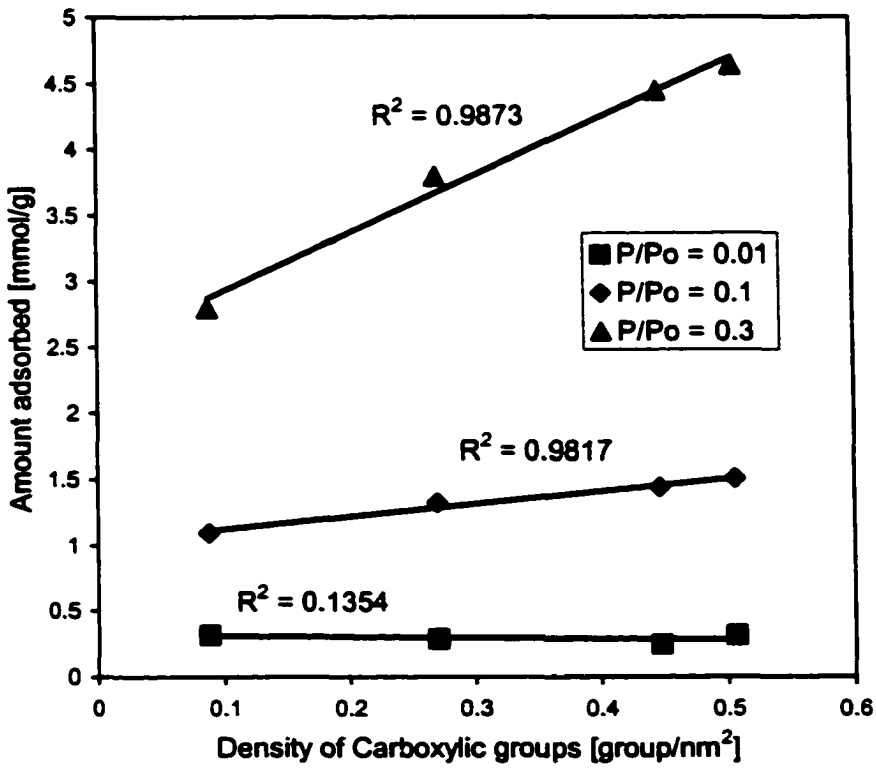

Figure 25. Dependence of the amount adsorbed at different relative pressures on the density of carboxylic groups.

Figures 26, 27 and 28 present the sorption of water on samples C, C-CN, U, and U-APS. In all cases, oxidation causes an increase in the sorption of water. For sample C, the amount adsorbed increased almost six fold as the result of oxidation with cold nitric acid. As mentioned above, the total number of groups calculated from Boehm titration almost doubled for this sample, whereas the number of acidic groups increased more than seven fold. The number of carboxylic groups also increased from 0.0 to 0.108 molecule/nm^2. For sample U, the total amount of water adsorbed increased by about eight fold and the number of carboxylic groups increased by more than twelve fold. This shows that there is a direct relationship between the amount adsorbed and the number of carboxylic groups on a given sample where the rest of the variables are constant.

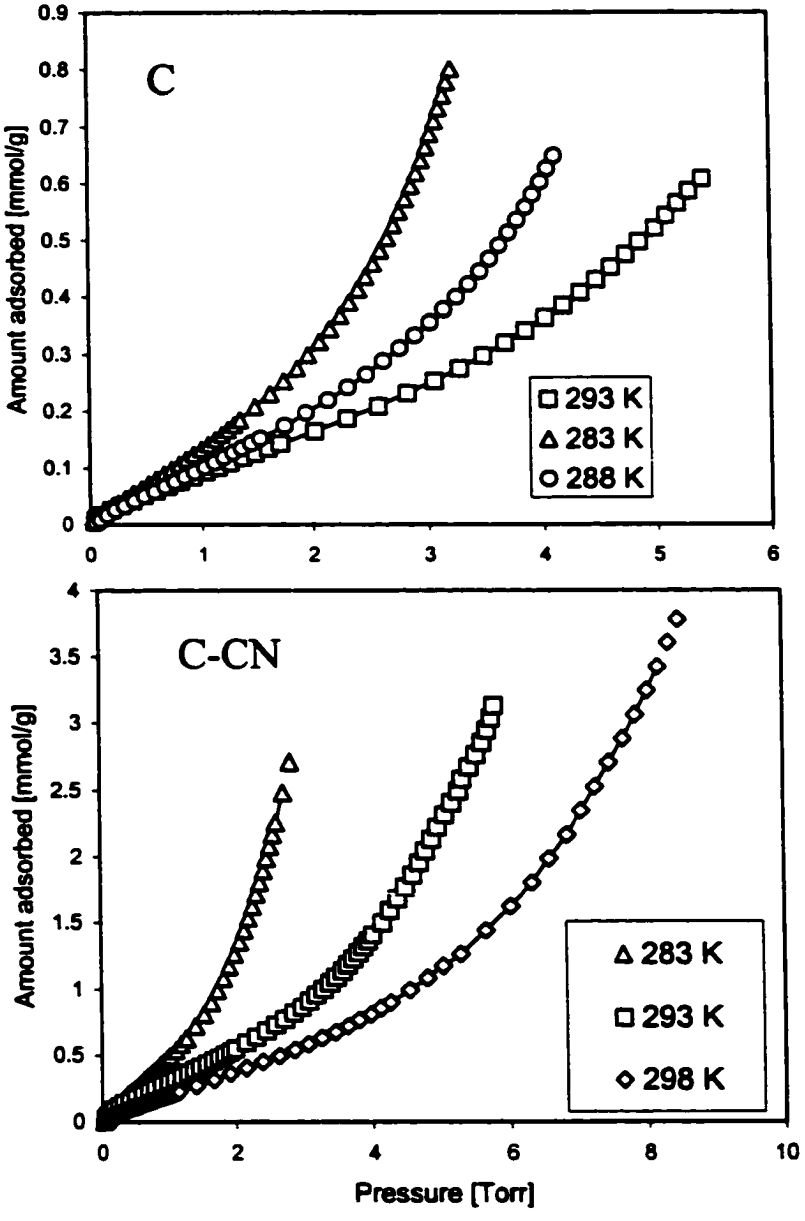

Figure 26. Water adsorption isotherms on samples C, and C-CN. The solid lines indicate the goodness of the fit to the virial equation.

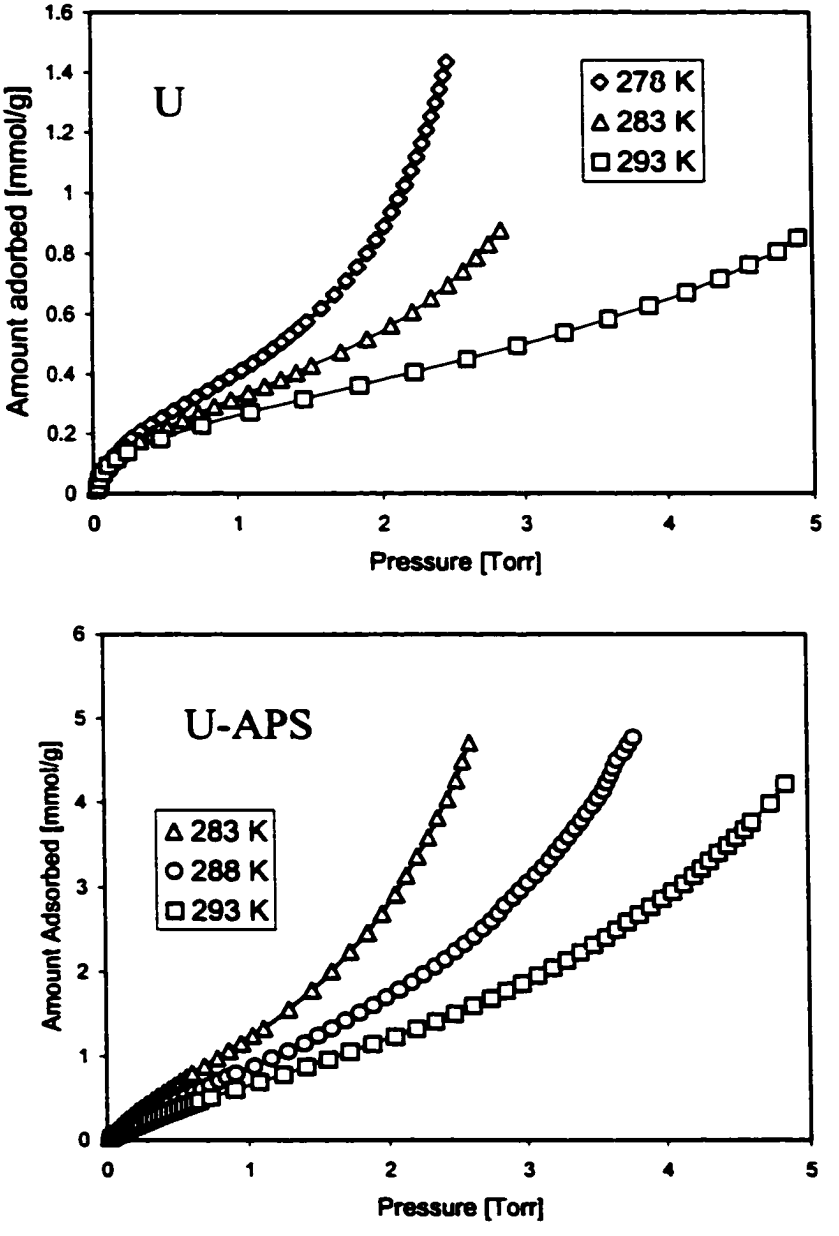

Figure 27. Water adsorption isotherms on samples U and U-APS. The solid lines indicate the goodness of the fit to the virial equation.

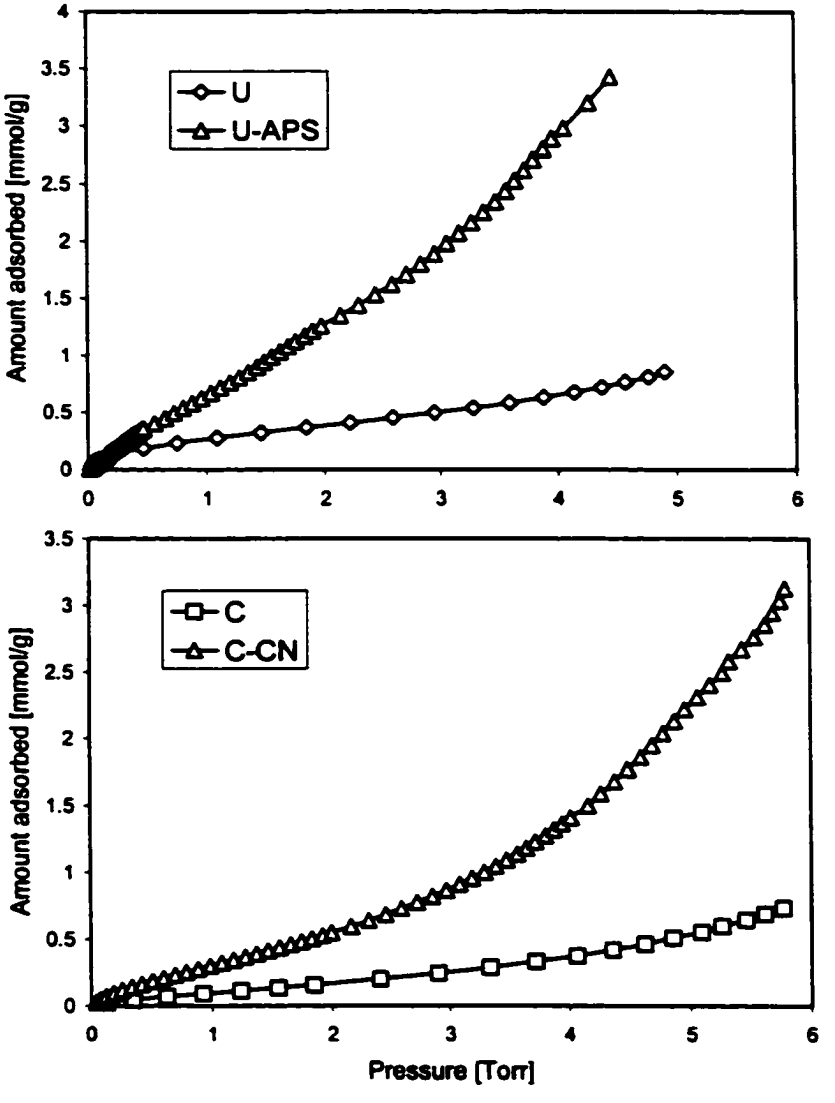

Figure 28. Water adsorption isotherms for samples C, C-CN, U, and U-APS at 293 K.

The total sorption of water on the W sample is much greater than that on sample C. It is obvious that acidic groups contribute to this difference. However, the results clearly show that adsorption is not dependent only upon the density of these groups. It is likely that on the surface of W carbon, due to its higher contribution of micropores, the process of cluster formation is enhanced and occurs to a greater extent filling all space available. This may also explain the slightly higher uptake of water at very low relative pressure for W carbon as compared to its oxidized counterparts. This is due to the larger contribution of the smaller micropores on sample W compared to sample C where adsorption can occur and clusters can be formed.

Differences in the chemical and structural features of U and W carbons influences the sorption uptake of water. For U carbon, reproducible isotherms at very low pressures were not obtained despite many experimental runs. It is worth mentioning that washing this carbon in a Soxhlet apparatus to a constant pH required more than two weeks. The residual KOH was removed very slowly owing to the very small pore sizes. It is likely that potassium hydroxide used for activation was not completely removed during Soxhlet washing and potassium ions, or oxides, reacted with water supplied to the system during the adsorption measurements. In the case of U-APS, the isotherms were measured with good reproducibility. Although small pores are also present in this material, the strong oxidant, ammonium persulfate with sulfuric acid, likely caused the removal of residual potassium compounds.

Although sample U has a larger micropore volume that sample W, its water sorption is about one-forth that of sample W. The density of the acidic groups, especially carboxylic groups is lower for sample U than for W carbon by about a four fold. This

supports our findings about the relationship between the surface density of acidic species and the water uptake by activated carbon. After oxidation, the water uptake on W and U carbons is similar, although the capacity of W is slightly higher at relative pressures below 0.25 as seen in Figure 29. At higher pressures a crossover is noticed. The densities of acidic groups for oxidized carbons are similar and there are pronounced differences in the micropore volumes of carbons. The results suggest that the micropore volume starts to play a role in the adsorption process when the condensation in the pore system starts to occur at a relative pressure of about 0.3.

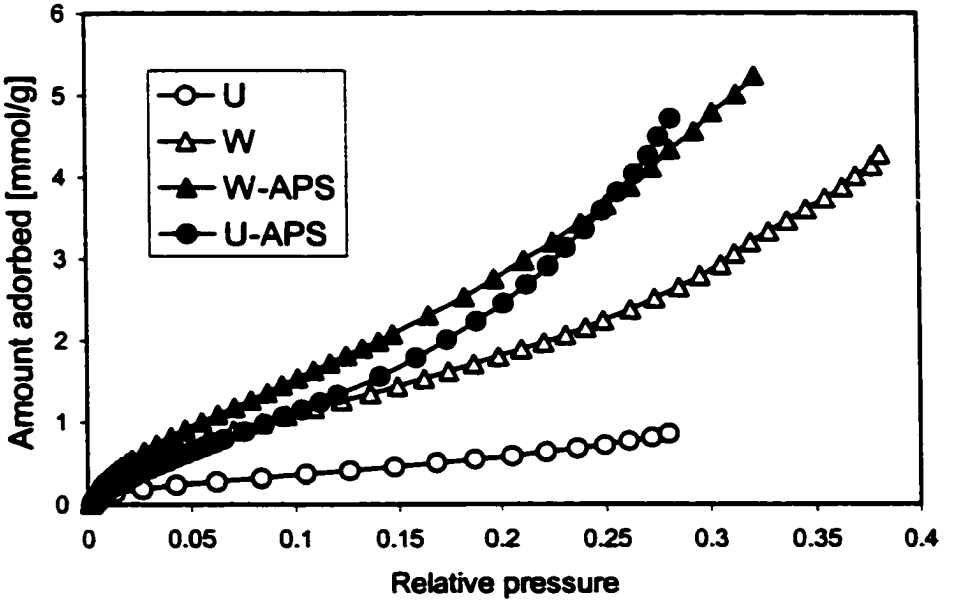

Figure 29. Water adsorption isotherms for sample U, W, W-APS, and U-APS.

Samples W/M and W-APS/M were used to study the effect of washing with methanol on the adsorption of water. As discussed earlier, methanol washing caused an

increase in the number of phenols accompanied by a decrease in lactones and carboxyls detected using various methods. This indicates that during washing with methanol esterification occurs. If the necessary energy is supplied (the system is kept at high temperature, around the boiling point of methanol), the following pathways of reactions are expected [126]:

$$\underset{\text{carboxylic acid}}{R\text{-}COOH} + CH_3OH \rightleftharpoons \underset{\text{ester}}{R\text{-}COOCH_3} + H_2O \qquad (29)$$

$$\underset{\text{lactone}}{R\text{-}COO\text{-}R} + CH_3OH \rightleftharpoons \underset{\text{ester}}{R\text{-}COOCH_3} + R\text{-}OH \qquad (30)$$

Then when exposed to water in "wet" titration methods, hydrolysis occurs:

$$\underset{\text{ester}}{R\text{-}COOCH_3} + H_2O \rightleftharpoons \underset{\text{carboxylic acid}}{R\text{-}COOH} + CH_3OH \qquad (31)$$

Reaction 30 needs an acidic environment, which is easily provided by the acidic nature of the carbon surface [127]. The proposed pathways of reactions can explain changes in the number of acidic groups detected by "wet" titration methods and changes observed using "dry" methods.

If the above mentioned hydrolysis occurs, the indication of it should be revealed on the water adsorption isotherms. The examples of isotherms measured on sample W

and W/M are presented in Figures 30 and 31. Although the temperature dependence of the amount adsorbed looks apparently correct for both samples, the subtle but significant discrepancies are seen in a logarithmic scale at a very low pressure range (Figure 32). Washing with methanol caused a crossover at low relative pressures and it is hard and almost impossible to get good reproducibility. This behavior indicates a lack of equilibrium, which is likely caused by a chemical process (hydrolysis) occurring in the system. When water molecules are adsorbed on the carbon surface decorated with esters, hydrolysis takes place resulting in the production of carboxylic surface groups and methanol molecules. The presence of methanol contributes to the vapor phase pressure and may block some centers for water adsorption. The apparent result of this is the measured isotherm, which represents sorption of the water-methanol mixture. The shape of the isotherm depends on the partial pressure of both components and the amount of esters able to hydrolyze into methanol. The latter is directly dependent on the amount of the carbon sample taken for measurement (if we consider replicate samples). Besides the above-described irreproducibility of the measured isotherms and the inconsistency in their temperature dependence, another indication of the occurrence of the hydrolysis and the presence of methanol as a byproduct is a consistent decrease in the amount of water adsorbed for W/M and W-APS/M compared to the samples without methanol treatment (Figure 27). This happens despite their slight increase in the number of acidic groups. The isotherms were repeated at least three times, and the estimated average standard deviation for three pressures ranges are 0.02 Torr ($p < 0.01$), 0.053 Torr ($0.01 < p < 1$), and 0.11 Torr ($1 < p < 3$).

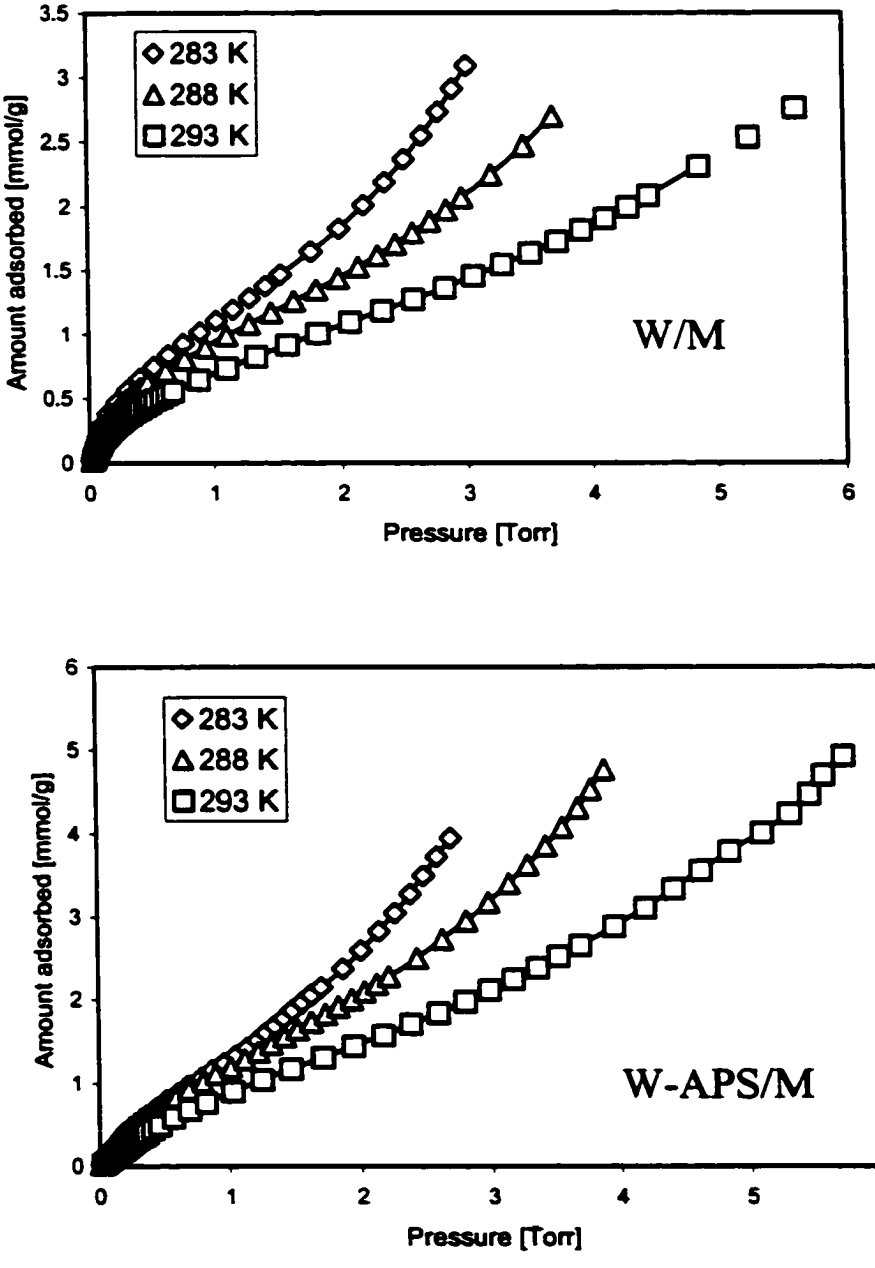

Figure 30. Water adsorption isotherms on samples W/M and W-APS/M. The solid lines indicate the goodness of the fit to the virial equation.

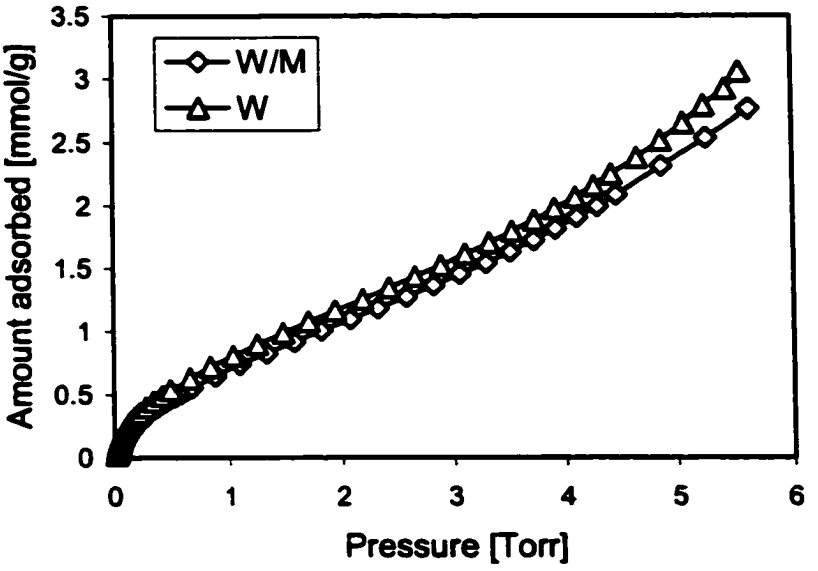

Figure 31. Comparison of water adsorption isotherms at 293 K on carbons before and after washing with methanol.

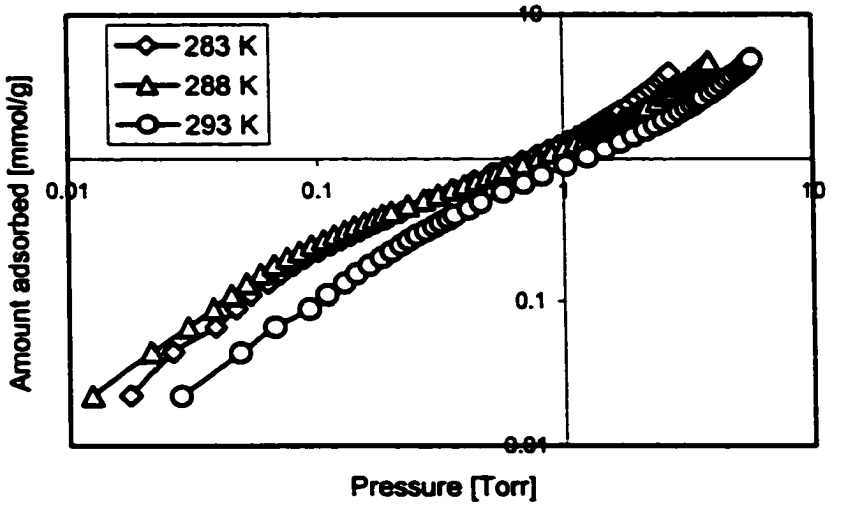

Figure 32. A logarithmic scale plot of W-APS/M water adsorption isotherm.

5.3.1 Isosteric Heats of Water Adsorption

The density of groups and their type should contribute to the adsorption on primary centers, before the process of water-water interaction is predominant. This can be studied by comparing the values of isosteric heats of adsorption and their dependence on the surface coverage. A convenient way to calculate the isosteric heat of adsorption from isotherms measured at different temperatures is by using a virial-like equation [128]:

$$\ln p = \ln v + \frac{1}{T}\sum_{i=1}^{m} a_i v^{i-1} + \sum_{i=1}^{n} b_i v^{i-1} \tag{32}$$

where v, p, and T are the amount adsorbed, pressure, and temperature, respectively. This equation was derived under the assumption that in the limited range of temperatures the isosteric heat of adsorption, Q_{st}, is temperature invariant and that the adsorption isotherms obeys Henry's law in the limit of zero pressure. Fitting equation 32 simultaneously to adsorption isotherms obtained at different temperatures gives a set of temperature-independent parameters a_i which lead to direct evaluation of Q_{st}:

$$Q_{st} = -R\left(\frac{\partial \ln p}{\partial (1/T)}\right)_v = -R\sum_{i=0}^{m} a_i v^{i-1} \tag{33}$$

where R is the universal gas constant. An equation similar to the virial type equation was also used by Avgul and Kiselev for the calculation of Q_{st} [7]. The difference between

equation 32 and their formulation was recently discussed [129]. Equation 32 was successfully applied to several adsorption systems over a broad range of temperatures using relatively low values of m and n [10, 127, 129]. However, due to the numerical instability of higher order polynomials, this equation may only be used for certain shapes of isotherms whose accurate fit does not require polynomials of higher order.

Water isotherms on our carbons are quite complex and difficult to fit accurately by equation 32 over the whole range of pressures. To calculate Q_{st} from such isotherms, the procedure discussed elsewhere is applied [130]. Briefly, equation 32 is fitted into subsets of data points rather than to all experimental data. Each subset comprises N_s data points selected consecutively with respect to v. By considering a sequence of overlapping subsets, one can scan the whole range of data.

To estimate the uncertainties of the calculated Q_{st} values, one needs to know the error variances, σ^2, of the p, v, and T measurements. Since σ values of the experimental errors are usually not known a priori, it is a common practice to estimate their values from the data. In the approach used here we allow for variation of σ between subsets of data. Then independent local estimates of σ for different subsets can be calculated:

$$\sigma_p^2 = (N_s - m - n)^{-1} \sum_{i=1}^{N_s} [(\ln p_i^{exp} - \ln p_i^{eq})]^2 \qquad (34)$$

where superscripts exp and eq refer to the experimental and calculated pressures, respectively. The value σ_p characterizes the error of ln(p), which results effectively from

errors of all measured variables. From σ_p, by applying the law of propagation of errors, we estimate σ_Q of the calculated $Q_{st}(V_s)$:

$$\sigma_Q^2(v_s) = \sigma_p^2 \sum_{j=1}^{m} \sum_{k=1}^{m} v_s^{j-1} S_{jk} v_s^{k-1} \tag{35}$$

where S_{jk} are the elements of the inverse matrix of the normal equation [131].

The advantage of dividing experimental data into subsets, which are analyzed as samples representing local adsorption behavior, is that a simple equation to correlate the data is applied; thus local estimates of errors can be obtained. The number of points, N_s, taken as a sample should be large enough to make the sample representative but not too large in order to retain a local character of the sample. In our calculations, we set the size of the subset $N_s = 15$. In equation 32 we take m = 3 and n = 1. It was found that these orders of polynomials are sufficient to fit the data of subsets of selected size within experimental accuracy [130]. Increasing m and n above 3 and 1 did not change significantly the results obtained.

Figure 33 presents the calculated heats of adsorption for samples W, W-CN, W-APS, and W-HP. Due to the complexity of the water adsorption mechanism, the differences in the surface chemistry of the carbon samples, and in the pore size distributions, the amount of water adsorbed is not representative of the surface coverage in the traditional meaning of this parameter. For strongly oxidized samples, the obtained heats of water adsorption start from about 27 kJ/mol, while for sample W the value of Q_{st} is slightly lower (about 22 kJ/mol). It was demonstrated by Avgul and Kiselev that the

energy of interaction of water molecules and a pure graphite-like surface is very low [7]. It is reported that the heat of water adsorption at zero surface coverage for carbons without any water-surface groups interactions is 17 kJ/mol [7, 26]. The maximum heat of adsorption calculated by taking into account the hydrogen bonding interactions between water molecules in the monolayer is reported to be around 28 kJ/mol [41]. The presence of functional groups, their type, number and strength enhances the energetics of the process due to hydrogen bonding to surface active sites. Then cluster formation occurs, water molecules interact with each other (3-D hydrogen bonding) resulting in the heat effectively equal to the heat of water condensation of 45 kJ/mol [43]. Similar behavior of water has been recently reported by Harding et. al based on the study of the activation energy [40].

The isosteric heats of water adsorption on samples C and C-CN, and W and W-CN are presented in Figure 34. The heats of adsorption at zero surface coverages were not evaluated; however, Figure 34 indicates that the initial heats of adsorption are 27, 21, 23, and 30 kJ/mol for C, C-CN, W, and W-CN, respectively.

The observed initial rise is due to the interactions of water molecules with the primary adsorption centers, surface groups. Since carbons are outgassed at 393 K when only physically adsorbed water was removed (hydrogen bonded to the surface groups), the obtained heats of adsorption are smaller than the heat of water condensation (3-D hydrogen bonding). In small pores, during the process of occupying of the primary centers by water molecules, horizontal and vertical water-water interactions gradually take place and thus raising heats of adsorption to its limited value, 45 kJ/mol, which represents the heat of water condensation [43].

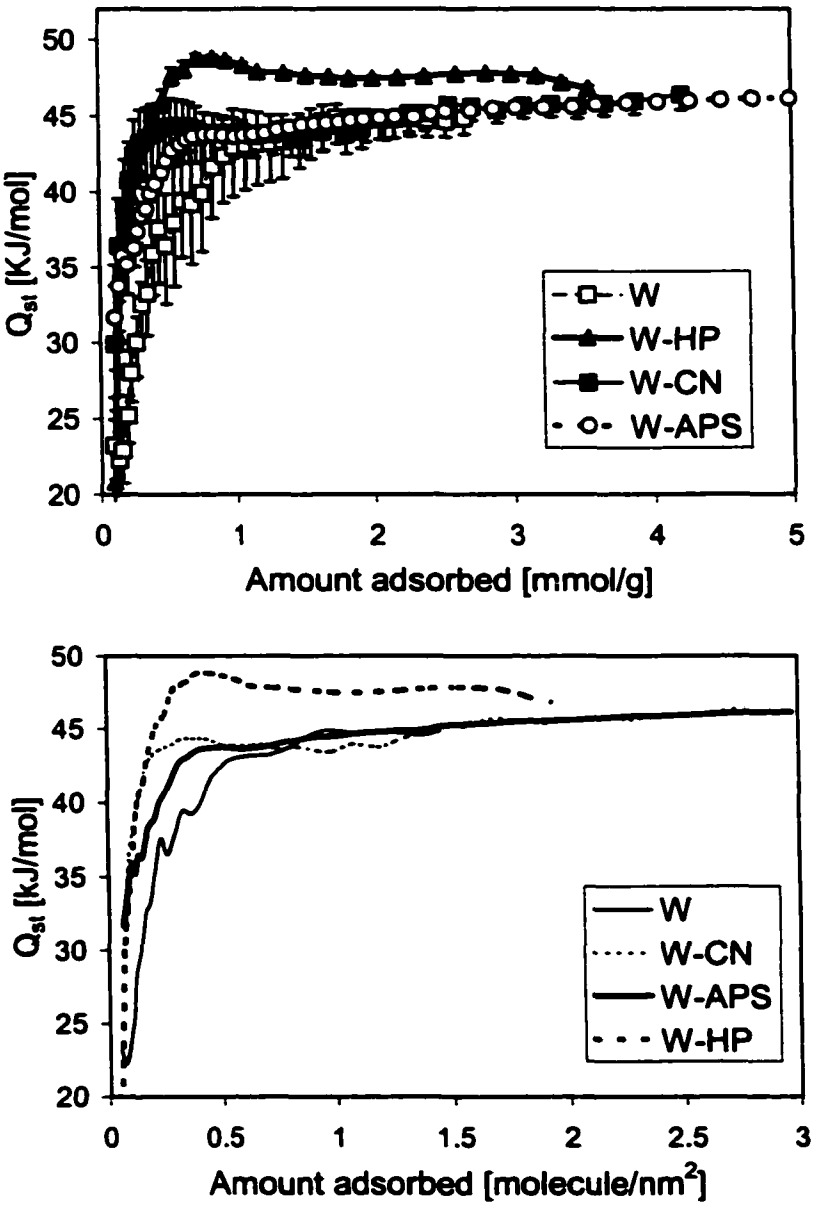

Figure 33. Isosteric heats of water adsorption in (mmol/g) and (molecule/nm^2).

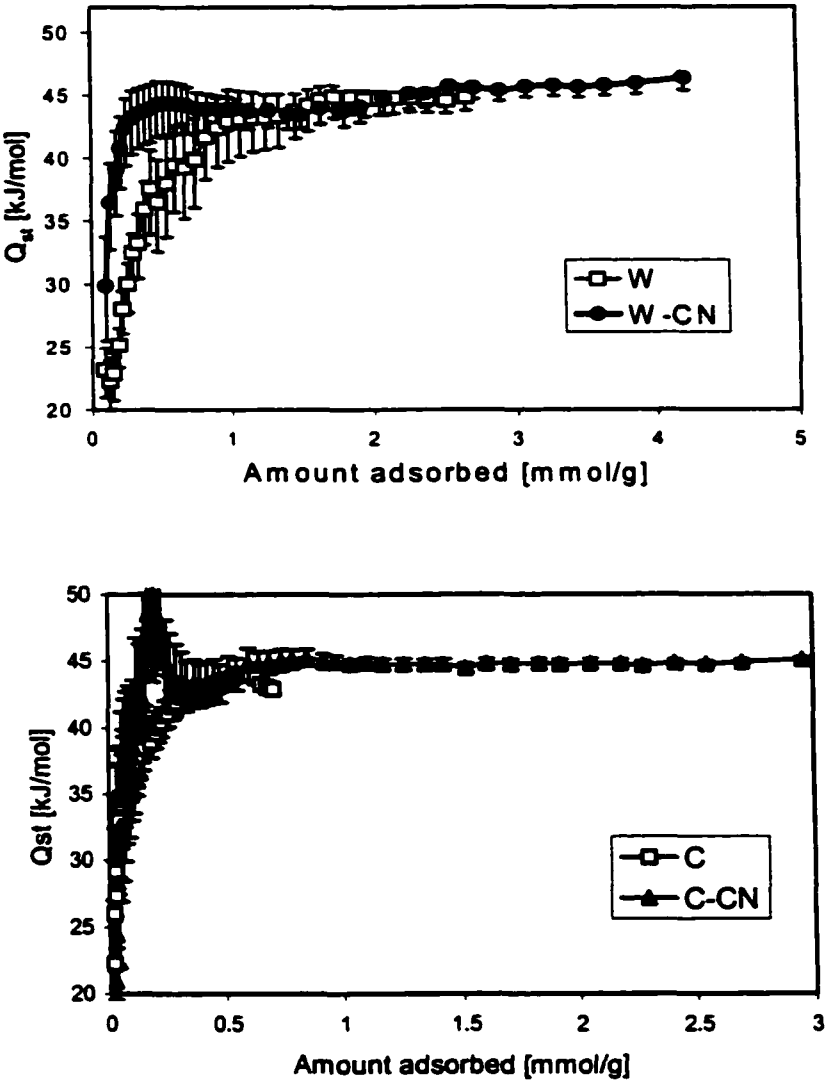

Figure 34. Isosteric heats of adsorption for samples W, W-CN, C and C-CN.

Figure 35 shows the dependence of surface coverage (molecule/nm^2) at which Q_{st} reaches its limiting value of 45 kJ/mol on the density of acidic groups. The linear correlation is obtained either for carboxylic or acidic species, however, the correlation coefficient is much better in the case of carboxylic species. They are considered as the strongest adsorption centers with a significant contribution to the heat of adsorption. No

correlation exists for the surface coverage where Q_{st} reaches 45 kJ/mol when it is plotted against the micropore volume or the volume of pores smaller than 5 Å. This suggests that at very low surface coverage the energetics of the adsorption process are mainly governed by surface chemistry.

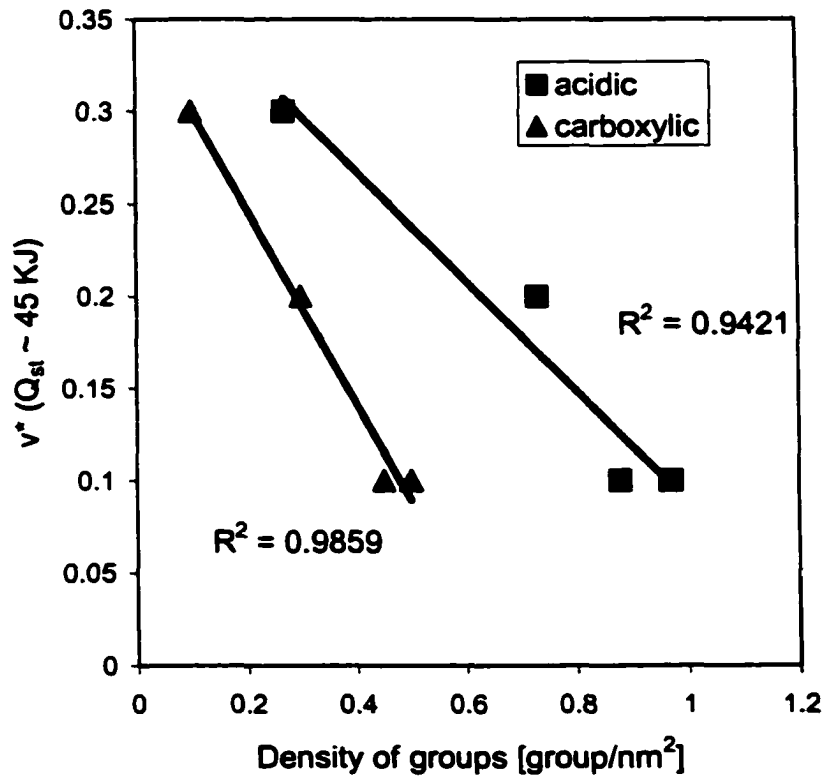

Figure 35. Dependence of surface coverage at Q_{st} equals to 45 kJ/mol on the density of acidic groups.

It is noteworthy that the water-water interactions become predominant at very low surface coverage as more water molecules are adsorbed. Since water molecules are most likely to occupy the most favorable positions and water-water interaction could be stronger than water-functional group interactions, then water molecules adsorb onto already adsorbed water molecules as compared to being adsorbed onto surface functional

groups. It follows that the energetics of the adsorption process become insensitive to the structural and chemical features of the carbon surface. For oxidized carbons the rise at the beginning is more steep due to the high density of acidic groups. This rise is less steep for the initial carbons where the adsorption on oxygen groups gradually takes place reaching the limited value at higher surface coverage than for that of the oxidized counterpart. This can be explained by the distribution of groups with relatively large distances between them which prevents the direct interactions of water-water at a very low surface coverage.

Another factor which is likely to play a role in determining the behavior of the heats of adsorption is the porosity of the carbon material. The contribution of small pores should enhance the cluster formation even when total acidity increases as happened in the case of C-CN carbon. Its density of groups is almost twice as small as in the case of W-CN; however, the energetics of the adsorption process are similar. It is interesting to compare the behavior of the initial W and C carbons. The densities of groups calculated from either Boehm or potentiometric titrations are similar; however, the isotherms differ significantly in the water uptake. The trends of the heats of adsorption are similar, but the W sample reaches the limiting value of the heat of water condensation at lower surface coverage than C. This is probably due to the different strength and type of groups which are predominately acidic in the case of the W carbon material. It was proposed that these groups mainly contribute to the water adsorption process [23]. The factors which make the shape of the isosteric heat of adsorption at very low surface coverage slightly steeper for the C sample than the one for the W sample are likely its microporosity and the significant volume of the pores smaller than 5 Å.

The effect of the number and density of groups on the heats of adsorption can be considered when two groups of samples of different origins are discussed independently. This is due to the significant differences in their porosity. In the case of the W materials, the limiting values of the heats of water condensation are reached much earlier for sample W-CN than sample W. As expected, this is in reciprocal relationship to the differences in the number and density of acidic surface groups. When carbon C is considered, the limiting value is also reached earlier for sample C-CN than sample C, which also follows the trend in the changes in the densities of their surface groups.

The validity of our discussion of the changes in the heats of adsorption is supported by the analysis of the experimental error [130]. It is well-known that the calculation of Q_{st}, especially at low surface coverage, is usually accompanied by a certain level of error due to the uncertainties of the experimental measurement and the variations in temperature. The error is about 5 kJ/mol at low surface coverage and for higher sorption uptake, where water-water interactions are predominant, it becomes smaller than 1 kJ/mol.

The heats of adsorption for sample U-APS along with W and W-APS are presented in Figure 36. Compared to Q_{st} of W-APS, the heat of adsorption obtained for U-APS sample shows a very interesting trend. The first recorded point starts at 45 kJ/mol, and then at very low surface coverage (fewer than 0.3 molecules of water/nm^2), a slight increase of about 10 kJ/mol is noticed. For the W sample, at this surface coverage the hydrogen bonding contribution gradually increases, causing an increase in the heat. The differences in the heats of adsorption between U-APS and the W-APS series of samples are likely the result of the significant differences in the porous structure of both carbons.

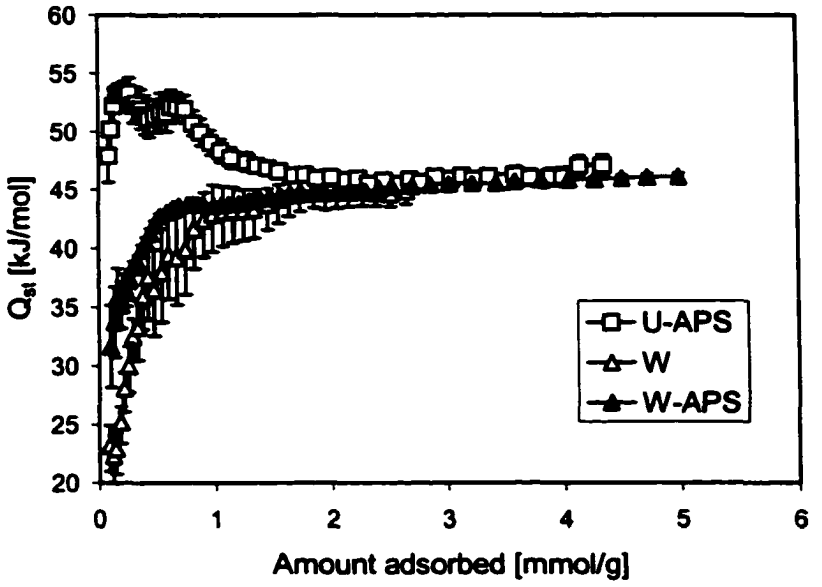

Figure 36. Isosteric heats of adsorption for U-APS, W, and W-APS.

As mentioned earlier, the volume in small pores as determined by DFT calculations is much higher in the case of U-APS than for W-APS. The sizes of pores are also smaller for the former material. Although the energy of water-carbon interaction is very small compared to the energy of hydrogen bonding [7], water molecules when adsorbed on a functional group in a pore no wider than a few water molecules (<10 Å in width) can create a specific cluster [29]. This cluster may be capable of interacting with surrounding pore walls, which results in a slight increase in the adsorption energy. When those very small pores are filled, only 45 kJ/mol, equal to the heat of condensation, is released owing to the relatively homogeneous microporous structure of this material. In the case of the W series of samples, the contribution of molecular size pores is smaller and their effect, if present, is evident only at the surface coverage lower than that measured in our experiment.

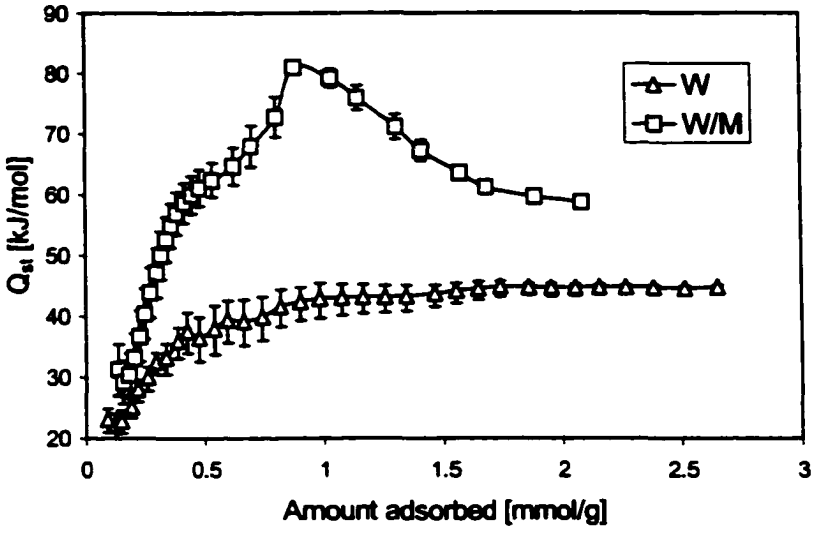

Figure 37. Isosteric heats of water adsorption for W and W/M.

To underline the importance of the proper conditions for the calculation of the isosotric heat, Figure 37 presents the isosteric heats of water adsorption on samples W and W/M. For W/M sample, heat starts from a much higher value than the other samples (~31 kJ/mol), reaches its maximum at about 80 kJ/mol, and decreases to about 60 kJ/mol. That Q_{st} does not represent the isosteric heat of water adsorption, but rather a combination of water adsorption and another mechanism that involves bond formation, such as hydrolysis of an ester group. The discussion of hydrolysis is presented in section three of chapter five of this thesis.

The presence of esters or other groups that can react with water may result from other surface treatments or carbon production methods. Recently, high values for the heat of water adsorption on activated carbons, initial and oxidized, have been reported by some researchers [132]. Those high heats, ~100 kJ/mol, are obtained when the calorimetric technique is used (flow calorimetry). In this approach the cumulative heat effect of the process is measured. Such high values may indicate the heat of the chemical

reaction of water with carbon surface functional groups, which is beyond the physical adsorption process. The discussion presented in this thesis indicates that the surface functionality of activated carbon used for an experiment strongly depends on the pretreatment procedures and the history of the samples. In our case we pointed out the hydrolysis. However, the heat effect of this reaction is not high [129], we evaluated it to be a maximum of 12 kJ/mol for esters involved in aromatic rings. The probability for the hydrolysis of esters during water sorption seems to be high when carbons are unwashed (as received) and oxidized using "dry" methods such as heating in air. In some cases, especially when the surface is very complex from a chemical point of view and susceptible for reaction with water, it is practically impossible to be aware of all reactions occurring in the system. In such a situation, adsorption of byproducts such as methanol occurs, which may contribute to the measured heat effect. The hydrolysis of esters presented in equation 31 is just an example for consideration.

5.4. Methanol Adsorption

Examples of methanol adsorption isotherms of W, W-APS, and U-APS carbons are presented in Figures 38 and 39.

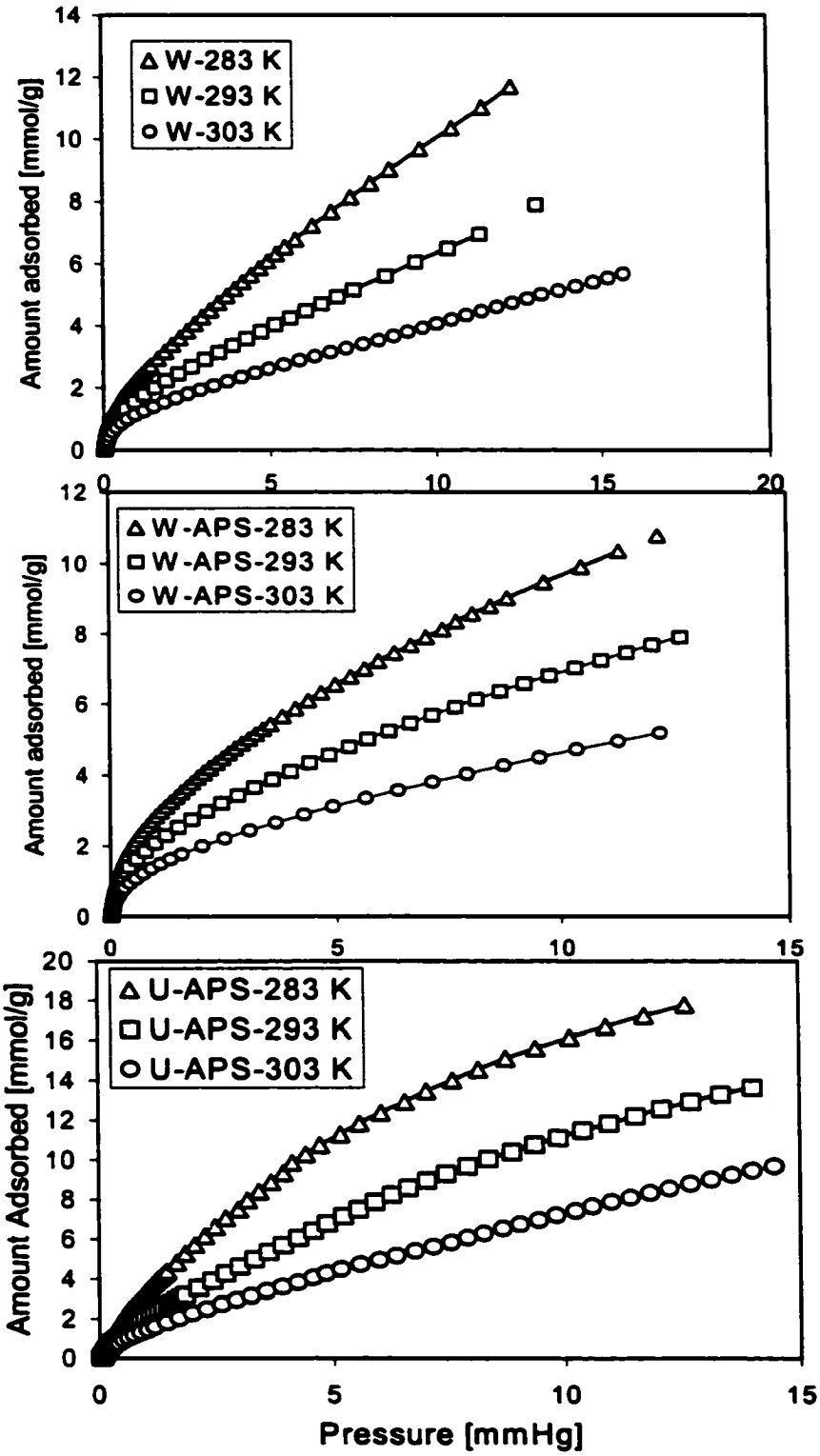

Figure 38. Methanol adsorption isotherms on samples W, W-APS, and U-APS. The solid lines indicate the goodness of the fit to the virial equation.

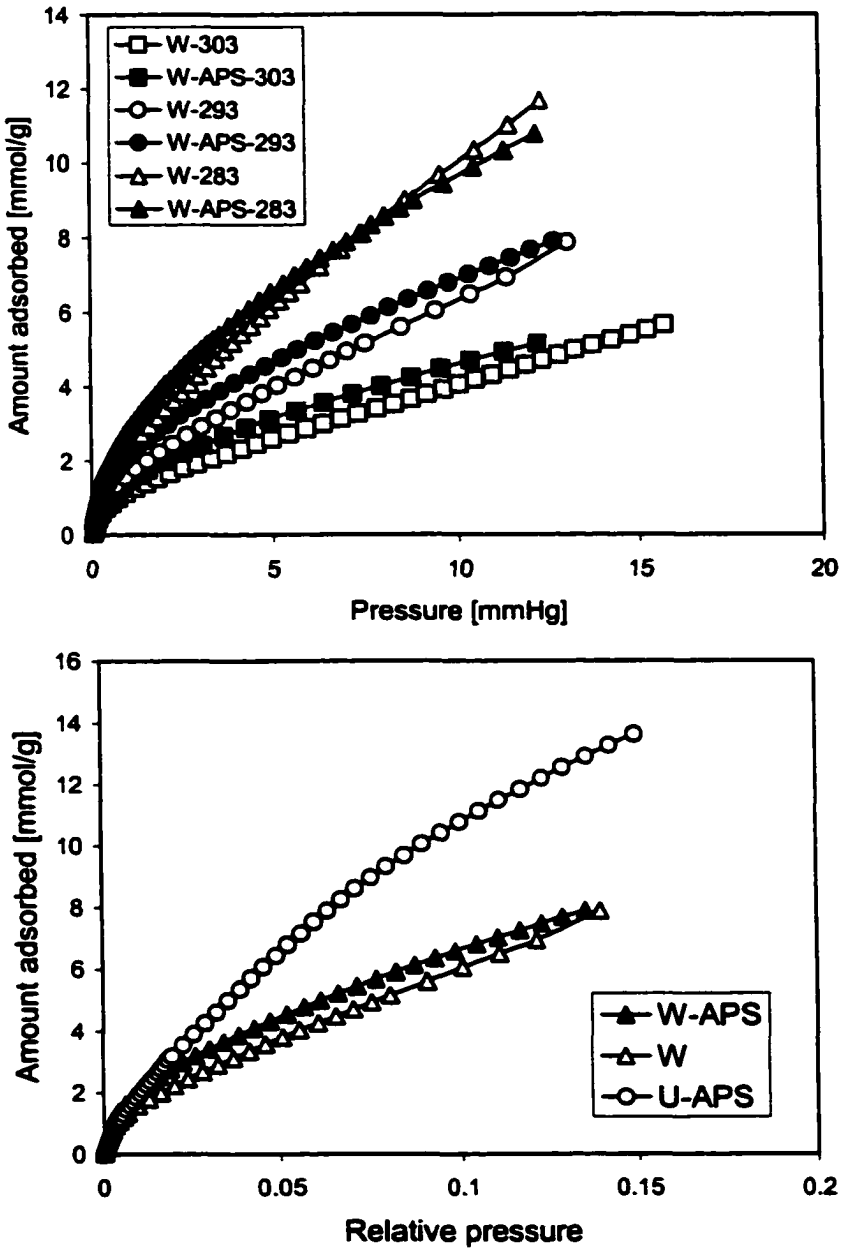

Figure 39. Methanol adsorption isotherms: Top on samples W and W-APS. Bottom: Methanol adsorption isotherms at 293 K on samples W, W-APS, and U-APS.

The shapes of the isotherms at the relative pressure range smaller than 0.3 is different from the shape of water isotherms and the indication of condensation in pores is

not noticed. It is interesting to note that oxidation of a carbon does not significantly change the sorption uptake at low relative pressure (Figure 39). The uptake is only slightly higher, in spite of the significant increase in the density of polar groups [32].

At p/p_0 around 0.15 (noticed at all temperatures) the crossover occurs as seen in Figure 39. This behavior can be explained by the specific mechanism of methanol sorption, different from that for water. The methanol molecule, besides possessing an OH group capable of hydrogen bonding, contains a hydrocarbon moiety with a high affinity to dispersive interactions with the activated carbon surface [23]. As a result, methanol is more likely to choose the more energetically favorable interactions depending on the accessibility of pores and surface coverage. The obtained results suggest that at low surface coverage sorption of methanol is a combination of the effect of both dispersive interactions of the hydrocarbon moiety and hydrogen bonding. When hydrogen bonding capacity is exhausted only dispersive interactions play a role. This is reflected in the observed crossover at p/p_0 around 0.15 and a decrease in the amount adsorbed for the oxidized sample whose micropore volume decreased as a result of oxidation.

Figure 40 presents a comparison of methanol and water adsorption isotherms at 283 K for samples W, W-APS, and U-APS. The highest uptake of methanol observed for U-APS is the result of its higher micropore volume. It is noteworthy that for this carbon the amount adsorbed at $p/p_0 < 0.025$ is smaller than that for the W series of samples. This is likely the result of the high density of acidic groups in the case of the mesoporous carbon, W, and its larger pores. This suggests that at a very low relative pressure, methanol tends to create hydrogen bonds with the surface groups and then microporosity and interactions with the pore walls become predominant. Comparison of water and

methanol uptake at the same relative pressure clearly shows the differences in the nature of interactions due to the different chemical nature of the sorbate molecules.

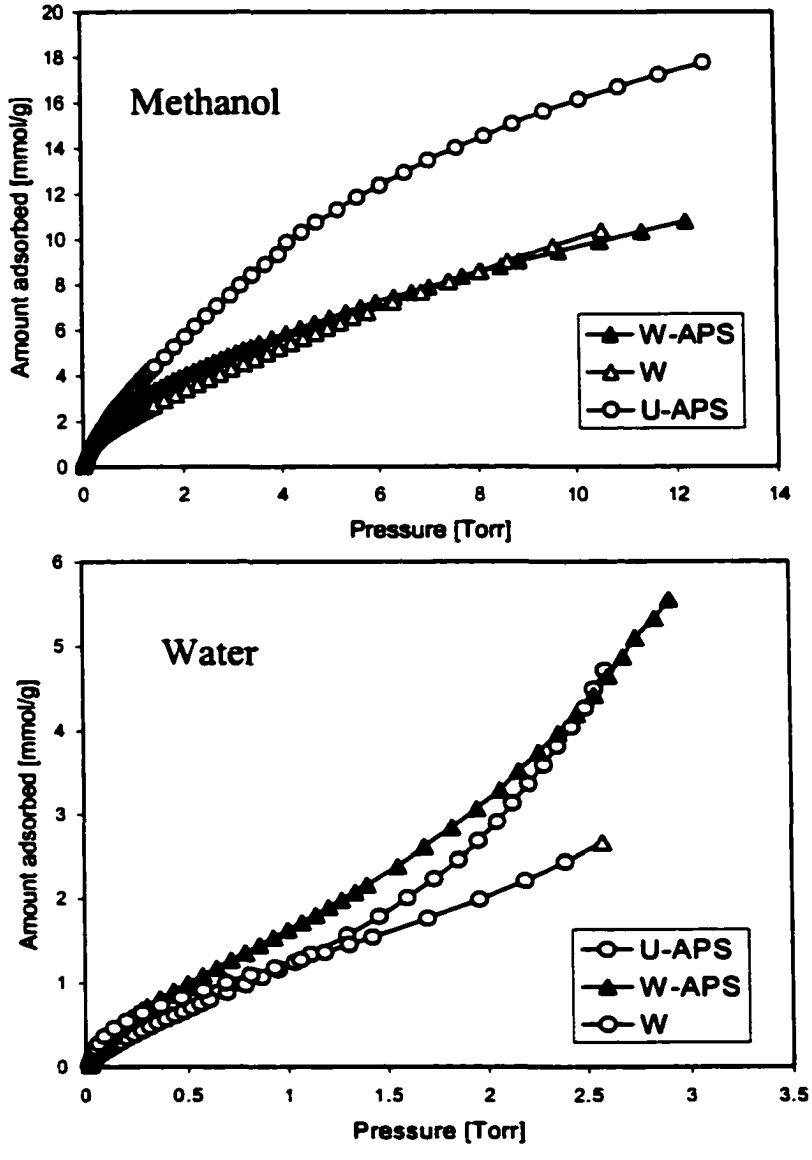

Figure 40. Comparison of methanol and water adsorption isotherms at 283 K for W, W-APS and U-APS.

5.4.1. Isosteric Heat of Methanol adsorption

The isosteric heats of methanol adsorption are collected in Figure 41. In the case of W sample, at very low surface coverage the heat of adsorption decreases. It is a typical behavior for heterogeneous surfaces where dispersive interactions occur. Such a trend is likely the result of adsorption of methanol in small pores where functional groups cannot exist and where only dispersive interactions are possible. As a result of this, heat decreases due to an increase in the pore size occupied by the methanol molecule. Since the number of those small pores is limited, at higher coverage methanol enters pores where polar groups are present and hydrogen bonding starts to play a role. When the coverage increases the heat gradually decreases as a result of adsorption in larger pores. For the oxidized sample W-APS, due to the changes in size and volume of small pores and the higher density of polar groups, methanol does not adsorb in pores similar to its size but it starts to interact with oxygen containing groups in slightly larger pores causing an increase in Q_{st}. When the density of oxygen containing surface species is higher and the pores small enough, the heat reaches 55 kJ/mol [42]. Then the adsorption in larger pores - where interactions of methanol with carbon walls is weaker – occurs.

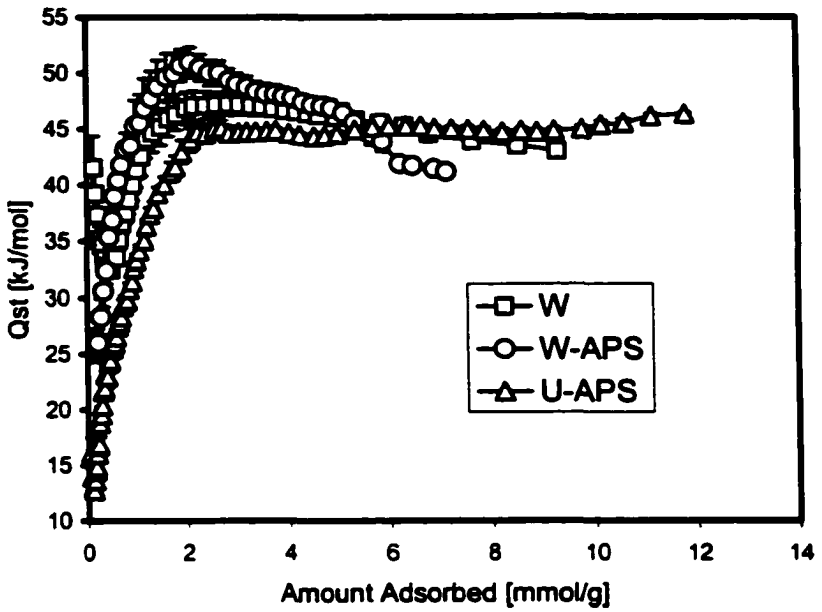

Figure 41. Isosteric heats of methanol adsorption on W, W-APS, and U-APS.

At higher surface coverage the heat decreases and dispersive interactions with larger pores become predominant. This was demonstrated in a decrease in the amount adsorbed for oxidized sample.

For sample U-APS, the isosteric heat of adsorption sharply increases until it reaches a plateau of 45 kJ/mol at low surface coverage. The steep rise is the result of interactions between methanol and surface groups in relatively homogeneous pores. Methanol molecules, owing to the methyl group, cannot create the spherical cluster in very small pores as may happen in the case of water where enhancement in the energy of interaction was observed. The heat at higher surface coverage does not decrease as it occurred for W and W-APS due to the high pore volume in homogeneously small pores and interactions between adsorbed methanol molecules. It is expected that at higher

surface coverage, not reached in our experiments, the heats are likely to decrease due to the interactions of methanol with carbon walls.

5.5. Ether Adsorption

Examples of the isotherms of diethyl ether adsorption on the initial W, W-APS, U, and U-APS samples are presented in Figures 42 and 43. The isotherms are calculated from chromatographic peaks according to the method described above [100]. Very small pressure values indicate that the surface coverage is low. Figure 44 shows the comparison of the isotherms for four carbons studied obtained at a common temperature, 393 K. In order to study the effect of surface chemistry and pore structure on the diethyl ether uptake, the adsorption at an arbitrary pressure, equal to 0.05 torr, was compared.

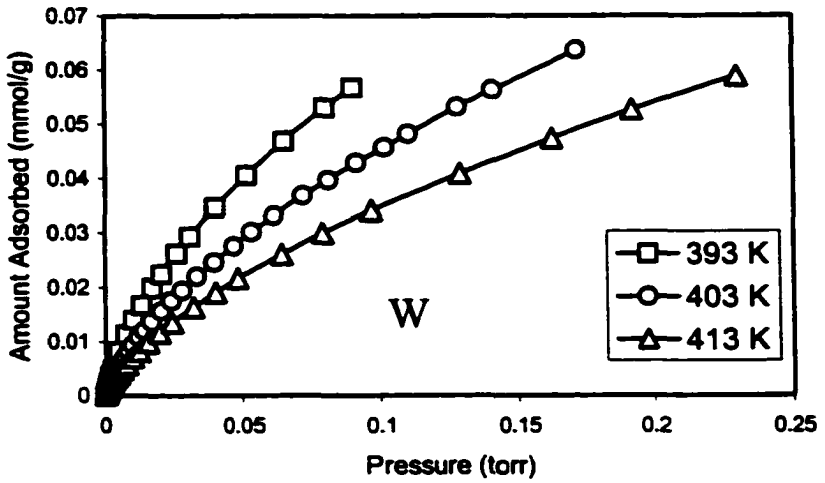

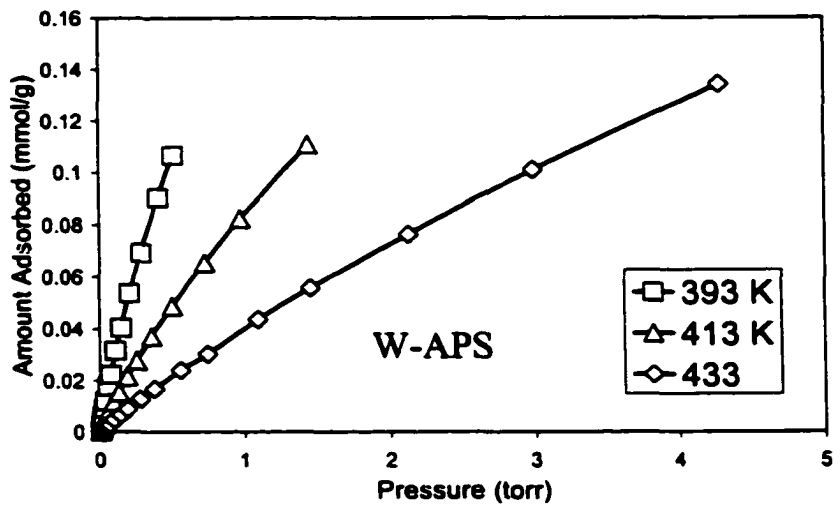

Figure 42. Ether adsorption isotherms on samples W and W-APS.

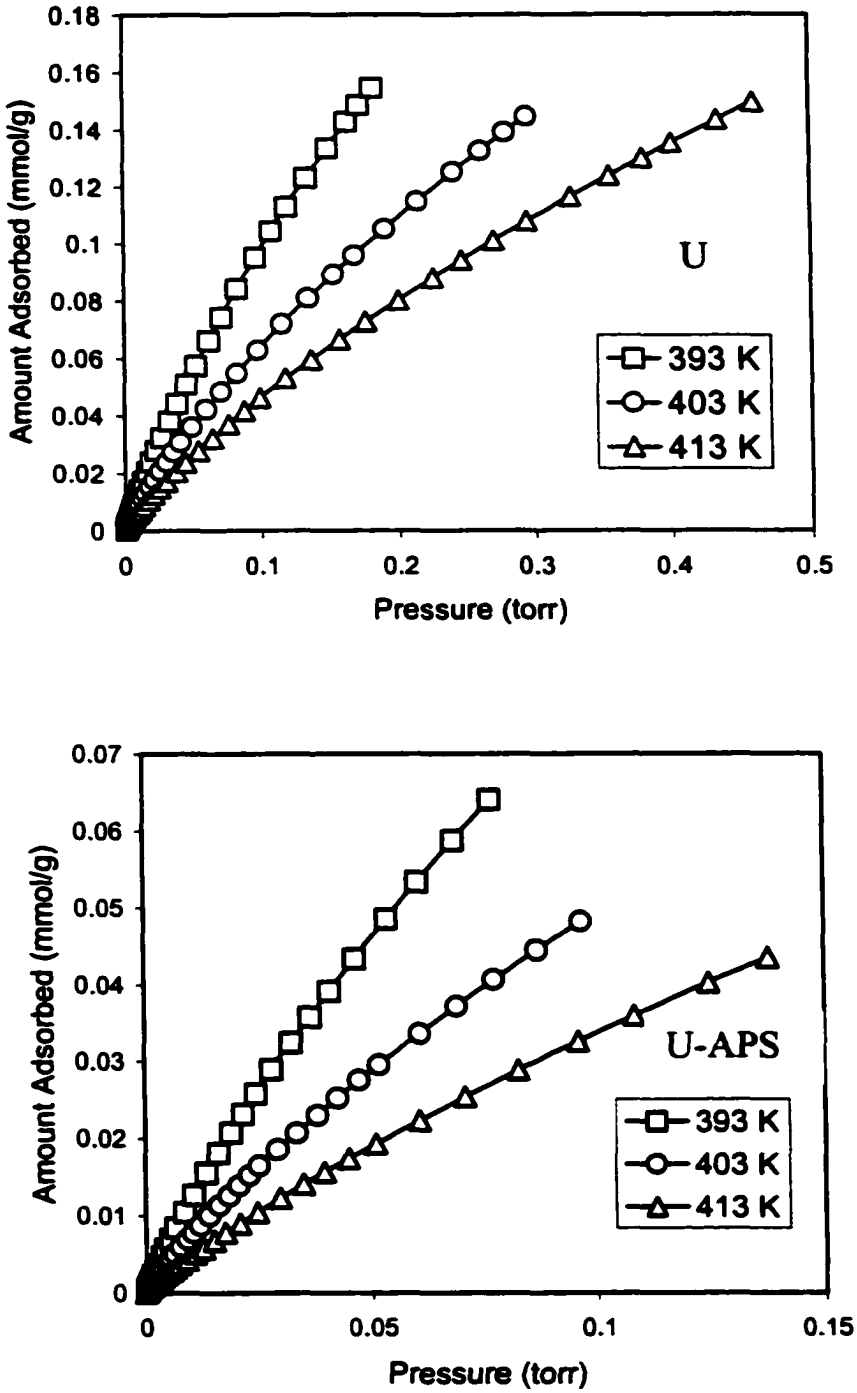

Figure 43. Ether adsorption isotherms on samples U and U-APS.

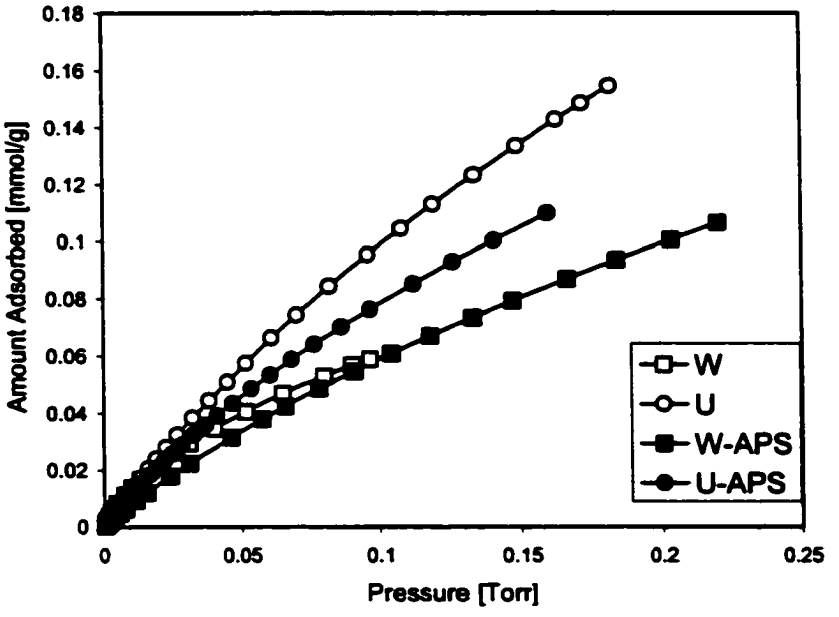

Figure 44. Comparison of ether adsorption isotherms at 393 K.

Figure 45 shows the dependence of the amount adsorbed at 0.05 torr on the micropore volume of carbons and volume of pores smaller than 10 Å. In both cases good correlation coefficients were obtained (R^2= 0.90, and R^2= 0.95 for V_{mic}, and $V_{<10Å}$, respectively). It is interesting that the amount adsorbed does not correlate with the surface density of acidic groups, either specific as phenolic or carboxylic, or all acidic groups reported from Boehm and potentiometric titrations (correlation coefficients equal to 0.36 and 0.62, respectively). These results suggest that at the arbitrary chosen pressure the pore volume is a predominant factor governing the behavior of carbons as diethyl ether adsorbents. A closer look at the isotherms plotted in the logarithmic scale (Figure 46) shows that at very small pressure, for extremely low coverage, the adsorption uptake on W is higher than that on U, however, the trend in the pore volume is opposite. This

suggests that surface chemistry can be a driving force for adsorption phenomena only at the beginning of the process. Indeed, the density of surface acidic groups is twice as high for W compared to that for the U carbon.

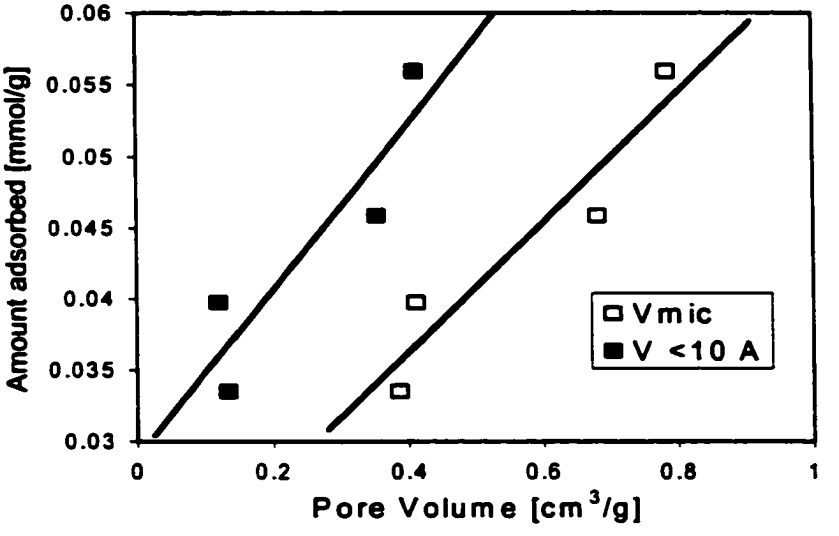

Figure 45. Dependence of amount adsorbed at 393 K and p = 0.05 torr on the pore volumes of the carbon studied.

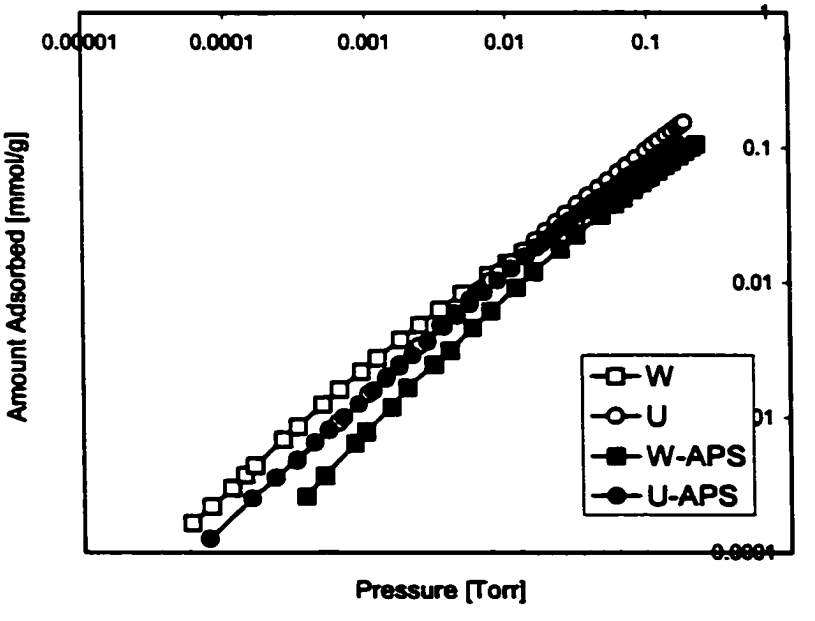

Figure 46. Comparison of ether adsorption isotherms at 393 K (logarithmic scale).

In the discussion of the mechanism of diethyl ether adsorption on activated carbons it is important to emphasize the balance of the adsorption forces which play a role in this process. Those forces are very strong dispersive interactions of hydrocarbon moiety with carbon pore walls, which were found to be equal to 36 kJ/mol on a flat carbon surface [7], and hydrogen bonding of diethyl ether oxygen with surface functional groups such as carboxyls or phenols. The latter interactions are weak compared to the former ones (less than 12 kJ/mol [7]). It follows that even though the dispersive interactions and hydrogen bonding can coexist the overall effect can give the energy value where it may be impossible to distinguish between the two phenomena.

Based on the analysis of the shapes of isotherms and a crossover observed at very low surface coverage, we can conclude that the mechanism of adsorption is somehow different at low coverage than at high coverage. This causes the small contribution of hydrogen bonding to be visible. Information about the mechanism of the adsorption process can be obtained from analysis of isosteric heats of adsorption, Q_{st}.

5.5.1. Isosteric Heats of Ether Adsorption

Based on the result published in the literature, we would expect the heat of diethyl ether adsorption to be smaller than 72 kJ /mol. It follows the assumption that the heat of adsorption on microporous carbons should be double that on a flat carbon surface [133]. According to Avgul and Kiselev, the heat of diethyl ether adsorption on a flat surface is equal to 36 kJ/mol [7]. Moreover, it should be close to the heat of butane adsorption which was reported to be in the range of 50 kJ/mol [134] (the same number of carbon atoms, however, different size of molecules). Indeed, the calculated heats are in the

expected range. The dependence of the isosteric heats of adsorption on the amount adsorbed in mmole per gram of surface is presented in Figure 47.

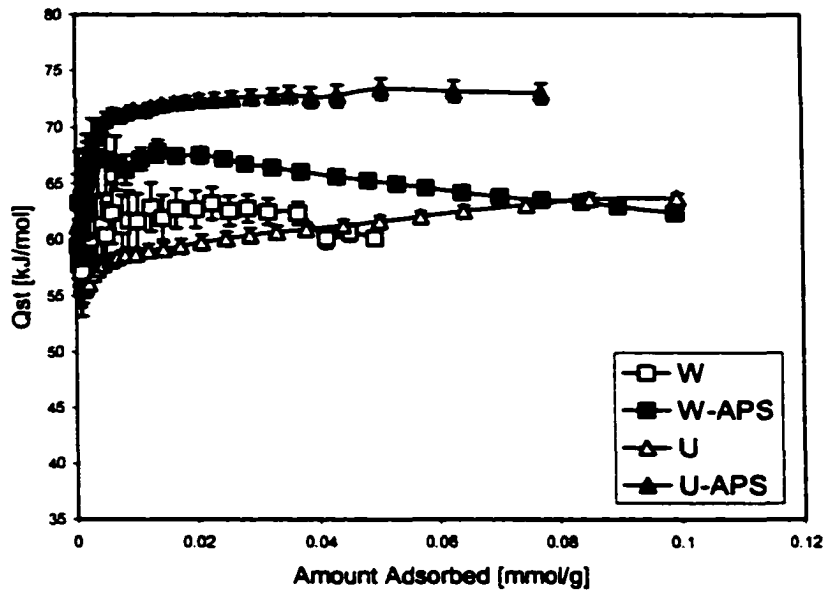

Figure 47. Isosteric heats of ether adsorption.

Trends in the heats show some similarities and differences. Surprisingly, for all samples a small increase in the heat of adsorption at the beginning of the process (from 5 kJ to 10 kJ) occurs. Then, for the W series a monotonic decrease is found, as expected for heterogeneous surfaces. On the other hand, in the case of the U carbons, after an initial increase, the heats reach some kind of plateau in their values close to 70 kJ/mol. It is noteworthy that for all carbons the heats of diethyl ether adsorption are between 60 and 70 kJ/mol which is close to a two fold increase compared to the heat measured on carbon black and reported by Avgul and Kiselev (36 kJ/mol) [7]. This indicates that the adsorption occurs in very narrow pores, similar to the sizes of diethyl ether molecule

which is in fact expected for the low surface coverages such as those reached in our experiments.

An increase in heats of adsorption with surface coverage was also found for adsorption of water and methanol [31, 32, 44, 84, 85, 113, 119]. In the case of those systems, an increase was possible due to the weak interactions of sorbates with the carbon surface and a strong contribution of hydrogen bonding. The initial heats of adsorption, in those cases were smaller than the heat of condensation. In the case of diethyl ether adsorption the initial heat is much higher than the heat of condensation (26 kJ/mol) which can be explained by strong interactions of the hydrocarbon moiety with the narrow pores of activated carbons. To explain an initial increase in the heat is a challenge. If dispersive interactions of the hydrocarbon moiety are the predominant force of adsorption, the heat should have a decreasing trend. In our view, this small increase at very low coverages can be explained only by an affinity of ether to bond to surface groups present in small pores. Those pores are similar in size to diethyl ether molecule (x, y, z, = 4.027 Å, 8.822 Å, 4.556 Å, respectively, [135] (σ =4.722 Å)) but big enough to accommodate functional groups. In this case the dispersive interactions are enhanced by the presence of hydrogen bonding. After this stage, which in fact may be only temporary, diethyl ether tends to occupy pores closest to its size and the maximum in the heat of adsorption is reached.

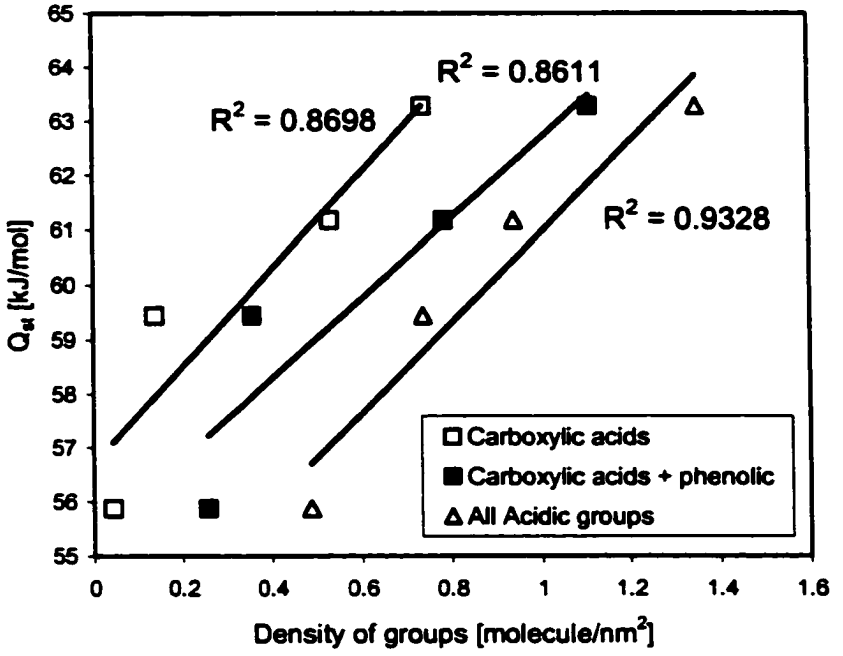

Figure 48. Dependence of the initial heat of ether adsorption on the density of acidic groups.

Supporting the above mentioned hypothesis is the fact that the initial heats increased after oxidation. The initial rise is also steeper after oxidation than that for the initial samples. The dependence of the initial heat of adsorption on the density of surface groups (all and carboxylic and phenolic) is presented in Figure 48. Good correlation coefficients (R^2 = 0.87, R^2 = 0.86, R^2 = 0.93 for carboxylic, phenolic and all acidic groups on the surface, respectively) indicate that hydrogen bonding makes a contribution to the adsorption in narrow pores. No correlation with pore volume was found, since pore sizes, not volume, are important for the energetics of the process. It is important to mention here that the amount adsorbed is very small, around 10 times smaller than the average density of surface groups. This suggests that only narrow pores take part in the adsorption. After the first stage of the process, it is likely that adsorption becomes more

stable and interactions of hydrocarbon moiety are predominant, and the effect of hydrogen bonding cannot be distinguished due to its low energy.

The differences in the observed trends in the heats of adsorption between W and U carbons can be explained by the differences in their pore structure. As shown in Figure 7 the sizes of narrow pores are similar in both groups of carbons, however, in the case of U and its oxidized counterpart the volume is much larger. Since the coverage is less than 0.1 molecule/nm^2, adsorption likely occurs in the range of very narrow pores, as mentioned above, close in size to the diethyl ether molecule. Differences in the volumes of these pores shows that in the case of W we observe a monotonic decrease in the heat whereas for U the heats are at the constant, maximum level. The latter can be explained by the fact that pores are very similar in sizes and when smaller pores are filled adsorption occurs in slightly larger ones with the contribution of hydrogen bonding (around 12 k/mol [7]) which enhances the adsorption energy. In the case of W and W-APS the pore structure is more heterogeneous than for the U samples (Figures 8 and 9) and, at the same coverage, the larger pores have to be filled which results in a slight decrease in the heat of adsorption. This decrease occurs since the contribution of hydrogen bonding is small compared to the interaction of the hydrocarbon moiety with carbon surface (36 kJ/mol for carbon blacks [7]).

5.6. Phenol Adsorption

Phenol adsorption isotherms measured at 303 K and 333 K on samples W, W-APS, U and U-APS are presented in Figure 49 along with the fit to the Freundlich equation (26). The uptake at lower temperature is higher, which is expected. It is interesting to note that sample U, which is highly microporous and has a smaller number of acidic groups than sample W, has a significantly larger uptake. This can be attributed to two factors: 1) there is a difference in the volume of pores smaller than 10 Å between the carbons studied, which suggests that those pores play a role in the adsorption of phenol, and 2) sample W has twice as much acidic groups as sample U. It has been shown in the literature that the introduction of oxygen groups to the carbon surface causes a decrease in the uptake of phenol [50-52, 55, 56]. Our experimental results are in agreement with this since oxidation resulted in a decrease of phenol uptake for all of the samples studied. This is due to an increase in the number of surface oxygen groups which localize the free electrons on the carbon basal planes [52]. It is worth mentioning that oxidation decreases the micopore volume and volume of pores smaller than 10 Å and it also has an effect on the decrease in the uptake of phenol. Furthermore, oxidation caused a larger decrease in uptake for sample U-APS than that for sample W-APS. Two factors may cause this behavior. First, the effect of oxidation on U seems to be more pronounced than on sample W. Sample U-APS showed an increase of three fold in the number of acidic groups per gram of carbon whereas W-APS showed an increase of only two fold. Second, the volume of pores smaller than 10 Å increased for sample W-APS while a

decrease is noticed for U-APS. The above two factors clearly influence the phenol adsorption process.

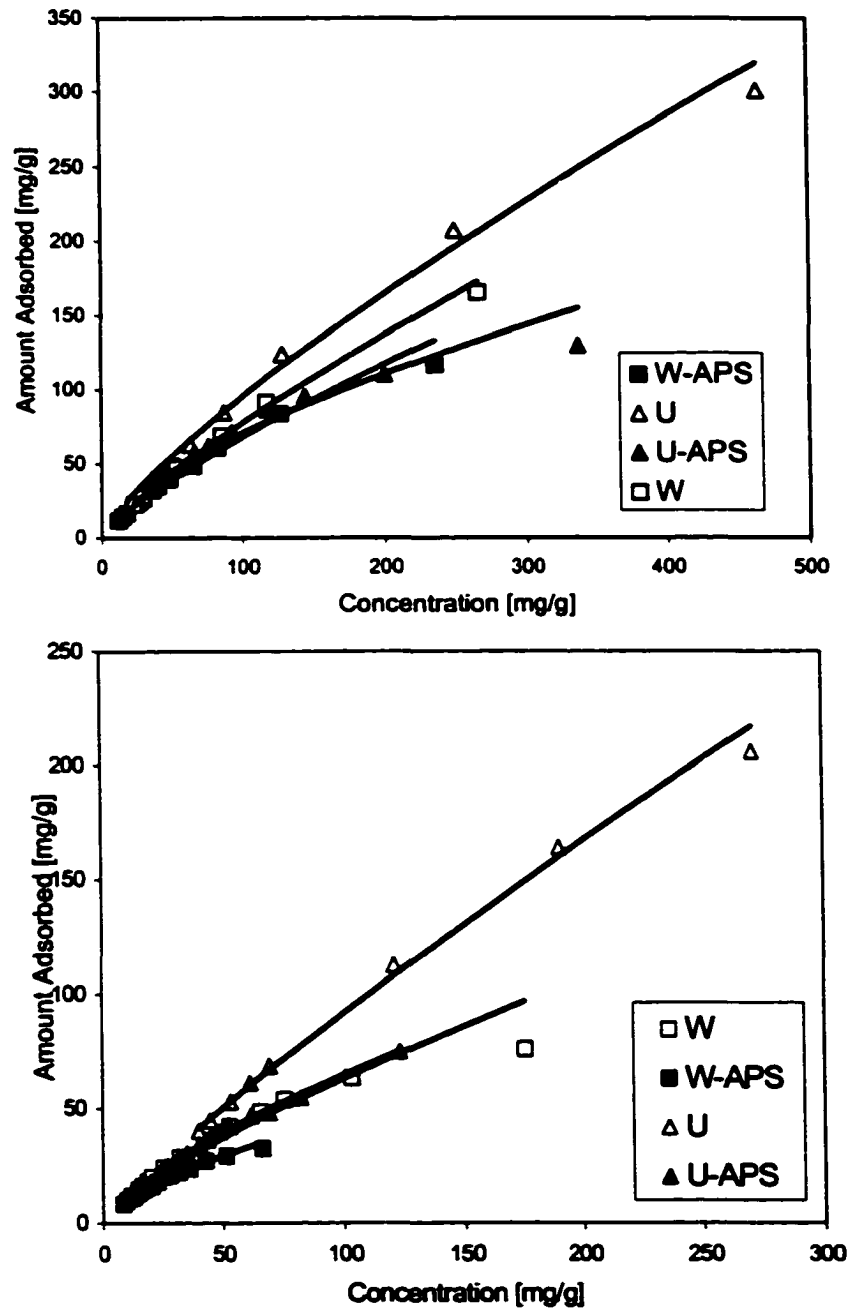

Figure 49. Phenol adsorption isotherms from solution. Top: 303 K. Bottom: 333 K. The solid lines indicate the goodness of the fit to the Freundlich equation.

It was indicated in the literature that phenol adsorption depends on both the porosity and the presence of surface groups, their type and density [49-55]. However, based on our results, no correlation of the uptake could be found with the carbon micopore volume, volume of pores smaller than 10 Å, or carbon surface area. Furthermore, no correlation could be found between the uptake and the surface functional groups: carboxylic, phenolic, lactonic, acidic, basic, or all.

Table 8 presents the values of n, K_F, and R^2 (the correlation coefficient) obtained from fitting of the experimental data to the Freundlich equation. For almost all of the carbons studied, the experimental data fit to the Freundlich equation with R^2 values greater than 0.97. Analyzing the fit, it is clearly seen that the Freundlich isotherm overestimates the amount adsorbed at high concentration of phenol in the solution. This is due to the fact that the Freundlich equation does not impose any requirements that the coverage must approach a constant value corresponding to one complete monolayer as C becomes large. Hence, the Freundlich equation is expected to fail at high concentrations of adsorbate [136].

The results in Table 8 show that oxidation resulted in a decrease in the values of n and an increase in the values of K_F for all of samples studied. Since n is related to the energetic heterogeneity (average energy of sites) and K_F is the unit-capacity parameter, oxidation caused an increase in the unit-capacity and a decrease in the energetic heterogeneity. This is caused by an increase in the number and density of acidic functional groups and a decrease in the volume of micropores. As the number of acidic surface groups increases, the π-electrons are removed from the carbon matrix [53]. Since these electrons play a role in phenol adsorption via dispersive interactions [52], their

removal causes a decrease in the average energy of the adsorption sites decreasing the value of n after oxidation.

Table 8. Fitting parameters of the experimental results to the Freundlich isotherm at 303 K and 333 K.

Sample	N (303 K)	K_F (303 K)	R^2(303 K)	n (333 K)	K_F (333 K)	R^2(333 K)
W	0.8221	1.758	0.9700	0.7673	1.836	0.9814
W-APS	0.7883	1.802	0.9917	0.6483	2.298	0.9857
U	0.7878	2.534	0.9916	0.8679	1.679	0.9973
U-APS	0.5466	5.531	0.9672	0.7159	2.391	0.9939

We should mention here that the amount of phenol adsorbed on all carbons was smaller than the total number of carboxylic groups present on the surface. This has an important implication since carboxylic groups can react with phenol via an ester formation route, thus causing a chemisorption on the carbon surface. The chemisorption reaction will take place only if the energetics of the process are higher than those of the physisorption. It is expected that the heat of adsorption of phenol on activated carbons should be similar to that of benzene, which was found to have a heat of adsorption of 42 kJ/mol on carbon black [7]. Assuming a two fold enhancement as the result of the existence of small pores [133], the heat of adsorption should reach a maximum value of about 84 kJ/mol on porous activated carbons. The fact that phenol possesses an OH group, not present on benzene, should not have a significant effect on the energetics of the process. This is because the hydrogen bonding contribution to the adsorption process should not exceed 12 kJ/mol [7] which is a small value in comparison to the heat of

adsorption due to dispersive interactions. Assuming that a functional group is present in a small pore where phenol can adsorb, the size of the pore has to be greater than the size of the phenol molecule. This will cause the energy of dispersive interactions to be smaller than the maximum expected value [133]. Since the pH values of the carbon suspensions were between 3.6 and 6.8, and an acidic environment promotes ester formation, and the energy of this reaction is estimated to be around 74 kJ/mol for esters involved in aromatic rings [127], esterification is possible in our systems. Although, the heat of ester formation is smaller than 84 kJ/mol, we should note that the maximum heat due to dispersive interactions can be released only when adsorption in pores similar to the size of phenol molecule occurs. When those high energy centers are occupied, the heat of adsorption dramatically decreases. Furthermore, ester formation should be accompanied by some dispersive interactions between the aromatic part of the phenol molecule and the carbon surface. This can release heat much higher than 84 kJ/mol. We should note that water, due to its weak interactions with the carbon basal planes, and weak hydrogen bonding energy with the surface oxygen containing groups [7, 31, 32] is not expected to compete with phenol for adsorption centers.

Ester formation on carbons after oxidation would also explain the increase in the parameter K_F. Figure 50 presents the correlation between either carboxylic groups or acidic groups and the unit-capacity factor, K_F. A good correlation exists with R^2 values of 0.9288 and 0.9881 for carboxylic and acidic groups, respectively. More carboxylic groups on the carbon surface should react with more phenol molecules from solution. It should be noted that we do not exclude physically adsorbed phenol from its contribution to the value of the unit capacity factor.

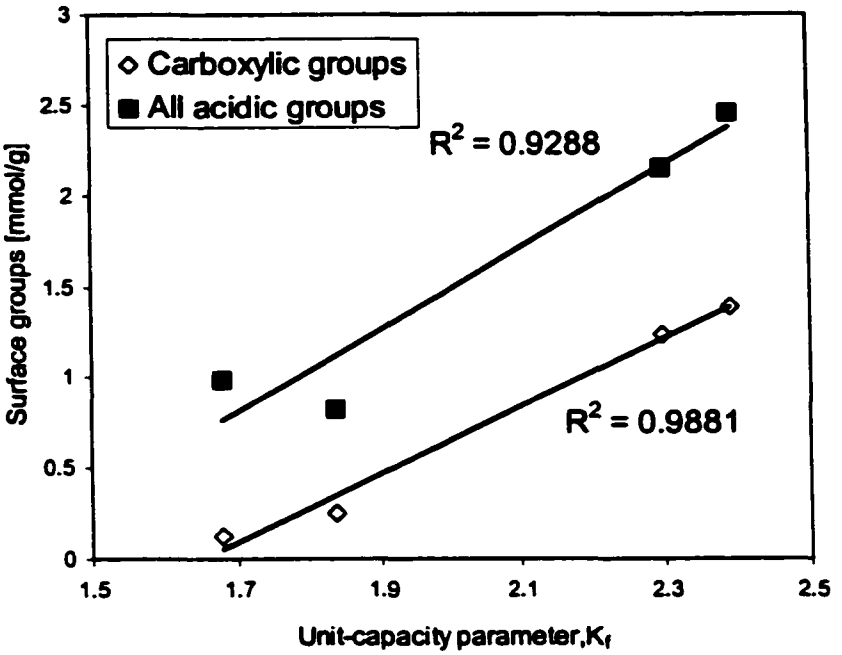

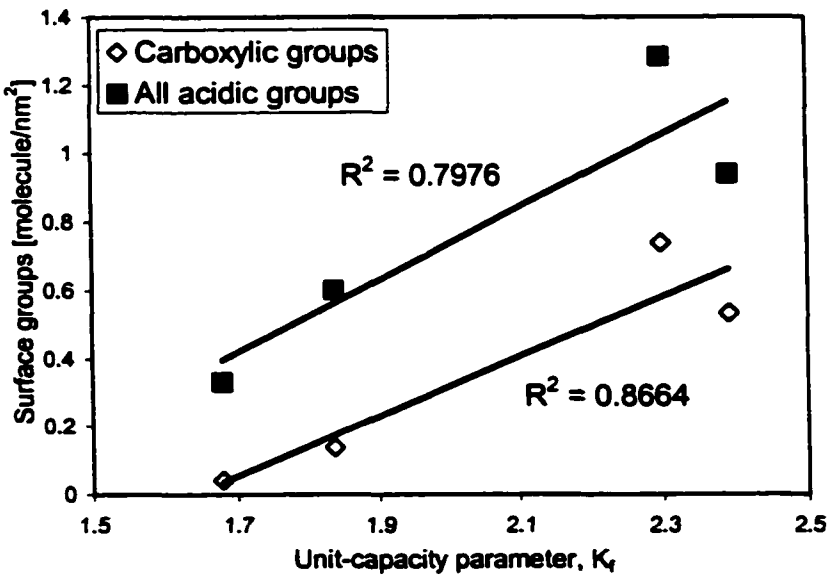

Figure 50. Correlation between unit-capacity parameter, K_F, for phenol and carboxylic and acidic surface groups.

We can also use the ester formation to explain the decrease in the values of n, related to the energetic heterogeneity. Figure 51 presents the dependence of the n parameter on the numbers of either carboxylic or acidic groups. The correlation coefficients are 0.8829 and 0.9642, respectively. Although the number of carboxylic groups increase, n decreases because the adsorption of phenol on our carbons is a combination of physical and chemical adsorption. The chemical adsorption is represented by ester formation between the OH group of the phenol and the carboxylic groups on the carbon surface. The physical adsorption occurs due to the dispersive interaction between the benzene ring of the phenol and the carbon's basal planes. Carboxylic groups act as electron acceptors, thus causing a decrease in the π-electron density in the carbon planes. This decreases the strength of the interactions between the aromatic ring of the phenol molecule and the carbon surface. As a result, the average energy of the sites decreases causing a decrease in the values of n even though we have a larger numbers of sites present.

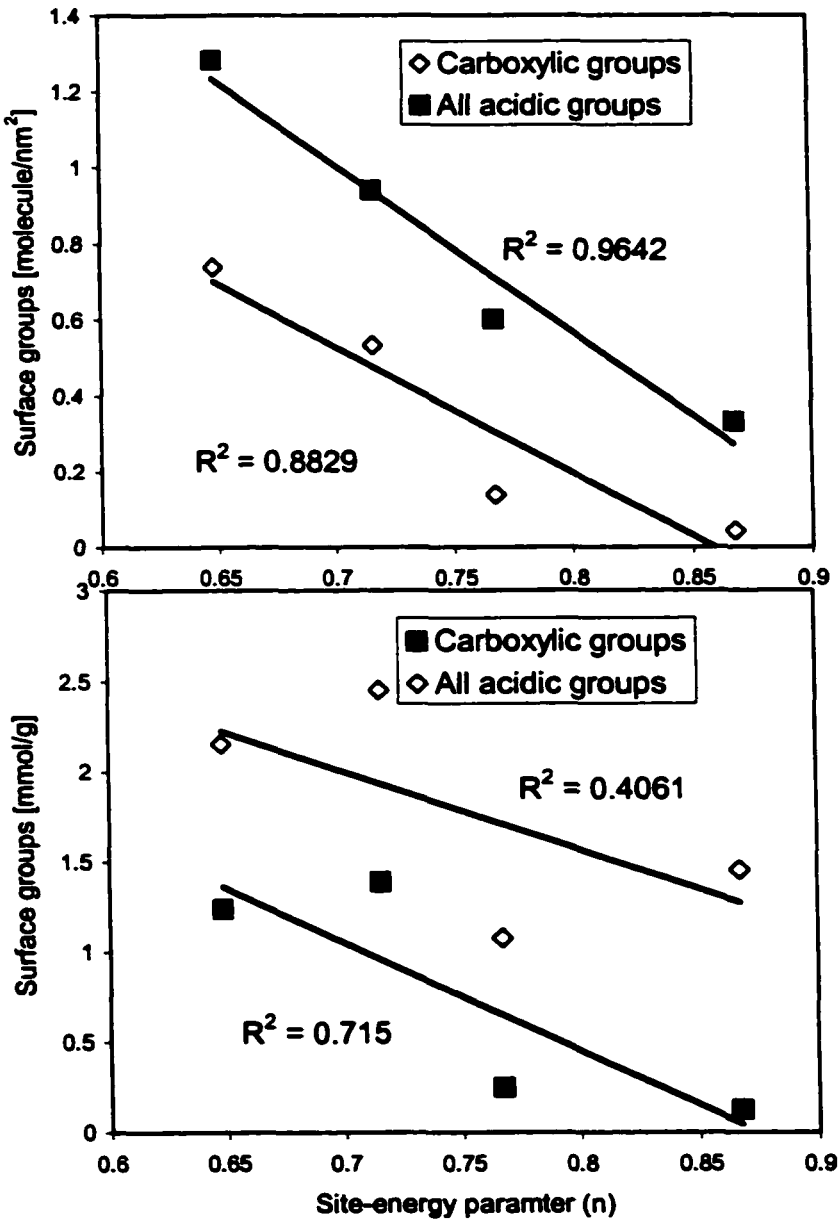

Figure 51. Correlation between carboxylic groups and the average energy of the sites.

6. CONCLUSIONS

Nitric acid interacts with the carbon surface via two distinct mechanisms: oxidative and nitrative routes. In the oxidative route, oxygen surface complexes are introduced to the carbon surface, which can be determined using Boehm and potentiometric titration. Nitration introduces nitro groups, NO_2, to the carbon surface. Those groups cannot be evaluated using Boehm or potentiometric titration, but could be easily detected through FTIR in conjunction with TPD analysis. Nitro groups possess a positive charge on the nitrogen and a negative charge resonating on the oxygen atoms making them excellent candidates for adsorption where ionic species are involved.

In this research, water, methanol, and ethyl ether were chosen as probe molecules because we expect them to interact with the carbon surface in different, however systematic, ways. Water possesses no hydrocarbon moiety and can interact with the carbon surface predominantly via hydrogen bonding. Whereas, ethyl ether has two ethyl groups which allow for strong interactions with the carbon pores and an oxygen atom that provides a center as a hydrogen bond acceptor. Furthermore, ether is analogous to water in the sense that the two hydrogen atoms in water are replaced with two ethyl groups. Methanol is a unique molecule because it has an OH group capable of hydrogen bonding (similar to that of water) and a small methyl hydrocarbon moiety (similar to that of ethyl ether) that can interact with the carbon pore wall via dispersive interactions.

We found that water adsorption shows a strong dependence, at low surface coverage, on the surface chemistry and to a lesser extent on the porosity of the carbons. The calculated heats of adsorption show a significant contribution of water-water

interactions even at very low relative pressure. This is significant because it shows that there are interactions between water molecules at low surface coverage as compared to water being adsorbed on primary adsorption sites until all those sites are occupied. This conclusion contradicts the DS theory, where water molecules are first adsorbed on primary adsorption centers. Once those centers are occupied, adsorbed water molecules act as adsorption sites for other water molecules. Our research shows that water-water interactions play an important role in the adsorption process at low surface coverage where primary adsorption centers are still available.

When very small pores are present, water-molecules are likely to create small, few-Angstrom clusters on which further molecules are adsorbed, releasing more heat than the heat of condensation. Only at the very initial stage of the adsorption process, analysis of the energetics can give some information about the water-surface site interactions. With an increase in the surface coverage, adsorption occurs in small pores where functional groups are able to exist, resulting in an increase in the heat of adsorption, owing to the increased contribution of water-functional groups and water-water interactions. The differences observed for the carbons of particular origin are consistent with the treatment methods and changes in the chemical and structural characteristics of the samples. The heats of adsorption reach a limiting value equal to the heat of water condensation at very low relative pressure when adsorption on primary centers is accompanied by filling of the smallest pores. As the adsorption proceeds in larger pores ($p/p_0 > 0.3$), a decrease in the values of the heat of adsorption is observed due to the adsorption on less energetically favorable centers. The differences in the heats of adsorption observed are due to the differences in the activation and oxidation methods of

the carbons which lead to a variety of surface groups. In the case of water adsorption at $p/p_0 < 0.3$, the density of groups is more important than porosity.

Washing the carbon samples with methanol causes significant changes to the surface chemistry of the carbons. These are due to esterfication, leading to an increase in the number of phenols and esters. The esters, when in contact with water, are hydrolyzed, giving carboxylic acids and methanol as products. When such reaction exists, one cannot use the isotherms to calculate the heats of adsorption owing to irreversibility, non-equilibrium conditions, and the presence and adsorption of another component, methanol. The Clausius-Claperyon equation can give accurate results in the case of water adsorption. But applying it, one has to consider the history of the samples, their surface chemical inventory, reproducibility of isotherms, and the analysis of their thermodynamic dependence. In the case where only physical adsorption is considered, the calculated heats of adsorption represent meaningful quantities.

There are differences between adsorption of methanol on activated carbons with micro- and mesoporous structures. Methanol adsorption is more dependent on the carbon microporosity at low surface coverage than on the surface oxygen groups. As surface coverage increases, the contribution of surface groups to the adsorption process begins to play a recognized role. Although only one method of oxidation was used, the changes in the pore sizes and surface chemistry follow the general expected trend for oxidized carbons. When very small pores are present and the density of surface groups is not very high, methanol adsorbs in pores similar in size to its molecular size via dispersive interactions. As a result of this, the heat of adsorption is higher than the heat of methanol condensation. When pores are large enough to accommodate functional groups, the heat

increases to maximum value of 50 kJ/mol owing to the combined effect of hydrogen bonding and microporosity. At higher coverage, when larger pores are occupied, interactions of methanol decrease. Methanol is sensitive to the density of groups only at low surface coverage, and, with increasing pressure, the micropore volume becomes critical for the adsorption process.

Our research demonstrated that structural heterogeneity, the sizes and volumes of pores, is the predominant factor governing diethyl ether adsorption on activated carbons. Hydrogen bonding in this case is weak compared to the interactions of hydrocarbon moiety with the pore walls. Surprisingly, at very low surface coverage and low pressure, diethyl ether molecules tend to adsorb in pores that are very narrow but wide enough to accommodate an oxygen-containing functional group. Then, adsorption in pores similar in size to the diethyl ether molecule occurs. This results in an increase in the heat of adsorption. With increasing surface coverage, the diethyl ether molecules adsorb in larger pores, where functional groups contribute to the heat of adsorption: however, this contribution is not distinguishable because of the low energy of the process compared to that of dispersive interactions. The high value of the heat of adsorption on very microporous carbon (exactly twice that obtained on carbon black) indicates that only pores similar in size to the ether molecule take part in the process under our experimental conditions. When the process proceeds further, the heat of adsorption is expected to decrease as observed for carbon with more heterogeneous pore structure.

The mechanism of adsorption of small organic molecules from the gas phase on activated carbons depends on the nature of the adsorbate. This includes the polarity of the adsorbate, hydrophobicity (contribution of hydrocarbon moiety), the size of the molecule

(especially the hydrocarbon moiety), acidity, basicity, and functional groups present and their capabilities to hydrogen bond with the carbon surface. The smaller the molecule with hydrogen bonding capability, the more its adsorption would depend on the presence of surface functional groups on the carbon. For example, we would expect molecules such as formaldehyde and formic acid to follow similar adsorption patterns as that of water on activated carbons. On the contrary, larger molecules with no functional groups or a functional group that cannot strongly hydrogen bond to the carbon surface will follow an adsorption mechanism similar to that of ether. In this case the adsorption will be strongly influenced by the carbon microporosity, hydrophobicity, and the pore size distribution. For example, we would expect molecules such as n-pentanone and n-hexanone to follow an adsorption mechanism similar to that of ethyl ether.

The results indicate that phenol adsorption from solution on carbons with acidic pH is dependent on the porosity, but more importantly, on the surface chemistry of the carbons. Oxidation resulted in a decrease in the uptake of phenol due to the decrease of the average energy of the adsorption sites. This decrease is attributed to a combination of two factors. The first factor is a decrease in the micropore volume due to the destruction of very small pores as a result of the oxidation. The second factor is an increase in the number of acidic groups on the carbon surface. Those groups remove the π-electrons from the carbon matrix and thus cause a decrease in the average energy of the sites. Phenol adsorption follows two routes: 1) physical adsorption which occurs as a result of dispersive interactions between the aromatic part of the phenol and the carbon's basal planes, and, 2) chemisorption which takes place via ester bond formation between the OH group of phenol and the carboxylic groups on the carbon surface. Those two routes are

possible from an energetic point of view. Although oxidation causes an increase in the number of carboxylic groups, the uptake decreases due to the ability of carboxylic groups to remove π-electron density from the carbon matrix and thus decreases the average energy of the sites which ultimately leads to a weaker interaction between the benzene ring of phenol and the carbon's basal plane.

7. FINDINGS

7.1. Surface Chemistry Characterization

A. Carbons of wood origin that are prepared using KOH activation have a relatively homogeneous microporous structure. Moreover, they have a high surface area and a predominantly acidic surface. This combination of structural and chemical features could open new possibilities for applications of wood based carbons as separation media for small basic molecules.

B. Combining Boehm, potentiometric titration, TPD and FTIR methods provides qualitative information about groups introduced to the carbon surface other than acidic groups such as nitro groups. Those groups are formed on the carbon surface as a result of nitric acid oxidation.

C. Nitric acid interacts with the carbon surface via two distinct mechanisms: oxidative and nitrative routes. The nitrative route introduces nitro groups to the carbon surface, which can be detected by FTIR in conjunction with TPD.

7.2. Water Sorption

A. Water adsorption at low surface coverage is dependent on both the surface area and porosity of the carbon.

B. There is a significant contribution of water-water interactions to the heat of water adsorption even at low surface coverage.

C. Surface group density is more important than porosity when $p/p_o = 0.1\text{-}0.3$ is taken into account.

D. Heats of water adsorption provide information on the water-surface interactions only at initial stage of the process.

E. In very small pores, water molecules are likely to create clusters of a few Å in size, which are further adsorbed releasing heat higher than that of water condensation.

F. The increase in the surface coverage in small pores where functional groups are able to exist results in an increase in the heat of water adsorption due to an increased contribution of water-functional groups and water-water interactions.

G. The limiting values for the heats of water adsorption is the heat of water condensation and it is equal to 45 kJ/mol.

H. Methanol washing of the carbons results in changes in surface chemistry which are due to the reaction of esterification. This causes an increase in the number of phenols and esters. Esters, when in contact with water, are hydrolyzed.

I. The water sorption isotherms obtained after methanol washings cannot be used to calculate the isosteric heats of adsorption due to the irreversibility, non-equilibrium conditions and the adsorption of another species that resulted in the hydrolysis of esters, methanol.

7.3. Methanol sorption

A. When very small pores are present and the density of surface groups is not high, methanol adsorbs in pores similar in molecular size to its molecule via

dispersive interactions which results in heats of adsorption higher than the heat of methanol condensation.

B. When the pores present are large enough to allow the presence of functional groups, the heat increases to a maximum of about 50 kJ/mol due to the combined effect of hydrogen bonding and microporosity.

C. At higher coverage, and when pores are larger, interactions of methanol with the surface are weaker and thus the heat of adsorption decreases.

D. Methanol sorption is sensitive to the density of groups only at low surface coverage and with increasing pressure the micropore volume becomes critical for the adsorption process.

7.4. Ether Sorption

A. The sizes and the volumes of pores are the predominant factors that govern the diethyl ether adsorption.

B. At low surface coverage and low pressure, the diethyl ether molecule tends to adsorb in very narrow pores but wide enough to accommodate an oxygen-containing group.

C. With increasing surface coverage, diethyl ether adsorbs in larger pores, where functional groups contribute to the heat of adsorption, however their contribution is not distinguishably marked due to the low energy of the process compared to dispersive interactions.

D. The initial heat of adsorption shows a very good correlation with the carboxylic, phenolic and acidic groups. The process of adsorption at low surface coverage is dependent on the presence of oxygen surface groups.

7.5. Phenol Sorption

A. Oxidation decreases the phenol uptake due to the increase in the number of oxygen surface groups, which are electron withdrawing, that localize the free electrons on the carbon basal planes.

B. Oxidation caused an increase in the unit-capacity parameter and a decrease in the average energy of adsorption sites.

C. Carboxylic groups on the carbon surface can react with phenol via an ester formation route and thus causing a chemisorption reaction on the carbon surface.

REFERENCES

1. Bansal, R. C., Donnet, J. B., Stoeckli, F. "Active Carbon," Marcel Dekker, New York, 1988.

2. Boehm, H. P. In "Advances in Catalysis," Academic Press, New York, 1966, Vol. 16.

3. Boehm, H. P. Some Aspects of the Surface Chemistry of Carbon Blacks and Other Carbons. *Carbon* **32,** 759 (1994).

4. Puri, B. R., In "Chemistry and Physics of Carbon," Walker P. J., Ed., Marcel Dekker, New York, 1970, Vol. 6.

5. Donnet, J. B., Papirer, E., Wang, W., Stoeckli, H. F. The Observation of Activated Carbons by Scanning Microscopy. *Carbon* **32,** 183 (1994).

6. Marsh, H., Heintz, E. A., Rodriguez-Reinoso, F. Eds. "Introduction to Carbon Technologies," University of Alicante, Alicante, Spain, 1997.

7. Avgul, N. N., Kiselev, A. V., In "Chemistry and Physics of Carbon," Walker P. J. Jr. Ed., Marcel Dekker, New York, 1970, Vol. 6.

8. Adib, F., Bagreev, A., Bandosz, T. J. Effect of the pH and Surface Chemistry on the Mechanism of H_2S Removal by Activated Carbons. *J. Colloid Interface Sci.* **216,** 360 (1999).

9. Adib, F., Bagreev, A., Bandosz, T. J. Adsorption/Oxidation of Hydrogen Sulfide on Nitrogen-Containing Activated Carbons. *Langmuir* **16,** 1980 (2000).

10. Bandosz, T. J., Jagiello, J., Schwarz, J. Effect of Surface Chemical Groups on Energetic Heterogeneity of Activated Carbons. *Langmuir* **9,** 2518 (1993).

11. Byrne, J. F., Marsh, H. "In Porosity in Carbons: Characterization and Application," Patrick, J. W., Ed., Edward Arnold, London, 1995.

12. Bandosz, T. J., Jagiello, J., Contescu, C., Schwarz, J. A. Characterization of the Surfaces of Activated Carbons in Terms of Their Acidity Constant Distributions. *Carbon* **31,** 1193 (1993).

13. Jagiello, J., Bandosz, T. J., Schwarz, J. A. Carbon Surface Characterization in Terms of Acidity Constant Distribution. *Carbon* **32,** 1026 (1994).

14. Contescu, A., Contescu, C., Putyera, K., Schwarz, J. A. Surface Acidity of Carbons Characterized by Their Continuous pKa Distribution and Boehm Titration. *Carbon* **35,** 83 (1997).

15. Zawadzki, J. In "Chemistry and Physics of Carbon," Thrower, P. A., Ed., Marcel Dekker, New York, 1989, Vol. 21.

16. Fanning, P. E, Vennice, M. A. A DRIFTS Study of the Formation of Surface Groups on Carbon by Oxidation. *Carbon* **31,** 721 (1993).

17. Donnet, J. B., Guilpain, G. Surface Treatments and Properties of Carbon Fibers. *Carbon* **27,** 749 (1989).

18. Kozlowski, C., Sherwood, P. M. X-Ray Photoelectron Spectroscopic Studies of Carbon Fibre Surfaces VII-Electrochemical Treatment in Ammonium Salt Electrolytes. A. *Carbon* **24,** 357 (1986).

19. Papirer, E., Bantzer, J., Sheng, L., Donnet, J. B. Surface Groups on Nitric Acid Oxidized Carbon Black Samples Determined by Chemical and Thermodesorption Analysis. *Carbon* **29,** 69 (1991).

20. Otake,Y., Jenkins, R. G. Characterization of Oxygen-Containing Surface Complexes Created on a Microporous Carbon by Air and Nitric Acid Treatment. *Carbon* **31,** 109 (1993).

21. Jagiello, J., Bandosz, T. J., Schawrz, J. A. Study of Carbon Microstructure by Using Inverse Gas Chromatography. *Carbon* **32,** 687 (1994).

22. Radovic, L. R., Monerp-Castilla, C., Rivera-Utrilla, J. In "Chemistry and Physics of Carbon," Thrower, P. A., and Radovic, L. R., Marcel Dekker, 1997, Vol. 26.

23. Rodriguez-Reinoso, F., Milano-Sabio, M., Munecas, M. A. Effect of Microporosity and Oxygen Surface Groups of Activated Carbon in the Adsorption of Molecules of Different Polarity. *J. Phys. Chem.* **96,** 2707 (1992).

24. Carrasco-Marin, F., Mueden, A., Centeno, T. A., Stoeckli, F., Moreno-Castilla, C. Water Adsorption on Activated Carbons with Different Degrees of Oxidation. *J. Chem. Soc. Faraday Trans.* **93,** 2211 (1997).

25. Maddox, M., Ulberg, D., Gubbins, K. E. Molecular Simulation of Simple Fluids and Water in Porous Carbons. *Fluid Phase Equilib.* **104,** 145 (1995). Ulgerg, D. E., Gubbins, K. E. Water Adsorption in Microporous Graphitic Carbons. *Mol. Phys.* **84,** 1139 (1995). Muller, E. A., Rull, L. F., Vega, L. F., Gubbins, K. E. Adsorption of Water on Activated Carbons: A Molecular Simulation Study. *J. Phys. Chem.* **100,** 1189 (1996).

26. Naono, H., Hakuman, M., Shimoda, M., Nakai, K., Kondo, S. Separation of Water and Ethanol by the Adsorption Technique: Selective Desorption of Water from Micropores of Active Carbon. *J. Colloid Interface Sci.* **128,** 230 (1996).

27. Foley, N. J., Thomas, K. M., Forshaw, P. L., Stanton, D., Norman, P. R. Kinetics of Water Vapor Adsorption on Activated Carbon. *Langmuir* **13,** 2083 (1997).

28. Hanzawa, K., Kaneko, K. Lack of Predominant Adsorption of Water Vapor on Carbon Mesopores. *Langmuir* **13,** 5802 (1997).

29. Iiyama, T., Nishikawa, K., Otowa, T., Kaneko, K. An Ordered Water Molecular Assembly Structure in Slit-Shaped Carbon Nanospace. *J. Phys. Chem.* **99,** 10075 (1995).

30. Bandosz, T. J., Blas, F. J., Gubbins, K. E., McCalumm, C. L., McGrother, S. C., Sowers, S. L., Vega, L. F. *Mater. Res. Soc. Symp. Proc.* **497,** 231 (1998).

31. Salame, I. I., Bandosz, T. J. Experimental Study of Water Adsorption on Activated Carbons. *Langmuir* **15,** 587 (1999).

32. Salame, I. I., Bandosz, T. J. Study of Water Adsorption on Activated Carbons with Different Degrees of Oxidation. *J. Colloid Interface Sci.* **210,** 367 (1999).

33. Bandosz, T. J., Buczek, B., Grzybek, T., Jagiello, J. The Determination of Surface Changes in Active Carbons by Potentiometric Titration and Water Vapor Adsorption. *Fuel* **76,** 1409 (1997).

34. McCallum, C. L., Bandosz, T. J., McGrother, S. C., Muller, E. A., Gubbins, K. E. A Molecular Model for Adsorption of Water on Activated Carbon: Comparison of Simulation and Experiment. *Langmuir* **15,** 533 (1999).

35. Gong, R., Keener, T. C. A Qualitative Analysis of the Effect of Water Vapor on Multi-Component Vapor-Phase Carbon Adsorption. *J. Air Waste Manage. Assoc.* **43,** 497 (1993).

36. Muller, E. A., Gubbins, K. E. Molecular Simulation Study of Hydrophilic and Hydrophobic Behavior of Activated Carbon Surfaces. *Carbon* **36,** 1433 (1999).

37. Dubinin, M. M., Serpinsky, V. V. Isotherm Equation for Water Vapor Adsorption by Microporous Carbonaceous Adsorbents. *Carbon* **19,** 402 (1981).

38. Evans, M. J. B. The Adsorption of Water by Oxidized Microporous Carbon. *Carbon* **25,** 81 (1987).

39. Bandosz, T. J., Jagiello, J., Schwarz, J. A., Krzyzanowski, A. Effect of Surface Chemistry on Sorption of Water and Methanol on Activated Carbon. *Langmuir* **12,** 6480 (1996).

40. Harding, A. W., Foley, N. J., Norman, P. R., Francis, D. C., Thomas, K. M. Diffusion Barriers in the Kinetics of Water Vapor Adsorption/Desorption on Activated Carbons. *Langmuir* **14,** 3858 (1998).

41. Barton, S. S., Evans, M. J. B., MacDonald, J. A. F. Adsorption and Immersion Enthalpies on BPL Carbon. *Carbon* **36,** 969 (1998).

42. Sun, J., Satyapal, S. *Extended Abstracts and Program of the 24th Biennal Conference on Carbon,* Charleston, SC, American Carbon Society, University Park, PA, 1999, p. 562.

43. Barrow, G. M. "Physical Chemistry," McGraw Hill, New York, 1961, p. 395.

44. Paserba, K., Shukla, N., Gellman, A. J., Marchon, B. Bonding of Ethers and Alcohols to a-CNx Films. *Langmuir* **15,** 1709 (1999).

45. Stanley, B. J., Guiochon, G. Calculation of Adsorption Energy Distributions of Silica Samples Using Nonlinear Chromatography. *Langmuir* **11,** 1735 (1995).

46. Radovic, L. R., Silva, I. F., Ume, J. I., Menendez, J. A., Leon y Leon, C. A., Scaroni, W. A. An Experimental and Theoretical Study of the Adsorption of Aromatics Possessing Electron-Withdrawing and Electron-Donating Functional Groups by Chemically Modified Activated Carbons. *Carbon* **35,** 1339 (1997).

47. Leng, C. C., Pinto, N. G. Effects of Surface Properties of Activated Carbons on Adsorption Behavior of Selected Aromatics. *Carbon* **35,** 1375 (1997).

48. Liu, X., Pinto, N. G. Ideal Adsorbed Phase Model for Adsorption of Phenolic Compounds on Activated Carbon. *Carbon* **35,** 1387 (1997).

49. Caturla, F., Martin-Martinez, M., Molina-Sabio, M., Rodriguez-Reinoso, F., Torregrosa, R. Adsorption of Substituted Phenols on Activated Carbon. *J. Colloid Interface Sci.* **124,** 528 (1988).

50. Magne, P., Walker, P. L. Jr. Phenol Adsorption on Activated Carbons: Application to Regeneration of Activated Carbons Polluted with Phenol. *Carbon* **24,** 101 (1986).

51. Vidic, R. D., Suidan, M. T. Role of Dissolved Oxygen on the Adsorptive Capacity of Activated Carbon for Synthetic Natural Organic Matter. *Environ. Sci. Technol.* **25,** 1612 (1991).

52. Mahagan, O. P., Moreno-Castilla, C., Walker, P. L. Jr. Surface-Treated Activated Carbon for Removal of Phenol from Water. *Sep. Sci. Technol.* **15,** 1733 (1980).

53. Coughlin, R. W., Ezra, F. S. Role of Surface Acidity in the Adsorption of Organic Pollutants on the Surface of Carbon. *Environ. Sci. Technol.* **2,** 291 (1968).

54. Mattson, J. S., Mark, H. B. "Activated Carbon, Surface Chemistry and Adsorption from Solution," Marcel Dekker, New York (1971).

55. Moreno-Castilla, C., Rivera-Utrilla, J. Adsorption of Some Substituted Phenols on Activated Carbons from a Bituminous Coal. *Carbon* **33,** 845 (1995).

56. Tessmer, C. H., Vidic, R. D., Uranowski, L. J. Impact of Oxygen-Containing Surface Functional Groups on Activated Carbon Adsorption of Phenol. *Environ. Sci. Technol.* **31,** 1872 (1997).

57. Grant, T. M., King, C. J. Mechanism of Irreversible Adsorption of Phenolic Compounds by Activated Carbons. *Ind. Eng. Chem. Res.* **29,** 264 (1990).

58. Salvador, F., Merchan, M. D. Study of the Desorption of Phenol and Phenolic Compounds from Activated Carbon by Liquid-Phase Temperature Programmed Desorption. *Carbon* **34,** 1543 (1996).

59. Bertoncini, C., Odetti, H., Bottani, E. J. Computer Simulation of Phenol Physisorption on Graphite. *Langmuir* **16,** 7457 (2000).

60. Barton, S. S., Evans, M. J. B., Holland, J., Koresh, J. E. Water and Cyclohexane Vapour Adsorption on Oxidized Porous Carbon. *Carbon* **22,** 265 (1984).

61. D'Arcy, R. L., Watt, I. C. Analysis of Sorption Isotherms of Nonhomogeneous Sorbents. *Trans. Farad. Soc.* **66,** 1236 (1970).

62. Kraehenbuehl, F., Quellet, C., Schmitter, B., Stoeckli, H. F. The Relationship between Immersion Calorimetry and the Parameters of Water Adsorption Isotherm on Active Carbons. *J. Chem. Soc. Faraday Trans.* **82,** 3439 (1986).

63. Lodewyckx, P., Vansant, E. F. Water Isotherms of Activated Carbons with Small Amounts of Surface Oxygen. *Carbon* **37,** 1647 (1999).

64. Do, D. D., Do, H. D. A Model for Water Adsorption in Activated Carbon. *Carbon,* **38,** 767 (2000).

65. Talu, O., Meunier, F. Adsorption of Associating Molecules in Micropores and Application to Water on Carbon. *AICHE J.* **42,** 809 (1996).

66. Stoeckli, H. F., Kraehenbuehl, F., Morel, D. The Adsorption of Water by Activated Carbons: In Relation to the Enthalpy of Immersion. *Carbon* **21,** 589 (1983).

67. Stoeckli, F., Currit, L., Laederach, A., Centeno, T. A. Water Adsorption in Carbons Described by the Dubinin-Astakhov and Dubinin-Serpenski Equations. *J. Chem. Soc. Farad. Trans.* **90,** 3689 (1994).

68. Rodriguez-Reinoso, F., Milano-Sabio, M., Gonzalez, M. T. Effect of Oxygen Surface Groups on the Immersion Enthalpy of Activated Carbons in Liquids of Different Polarity. *Langmuir* **13,** 2354 (1997).

69. Ndaji, F. E., Chagger, H. K., Sykes, M. L., Thomas, K. M. *Carbon* **33,** 1405 (1995).

70. Phillips, J., Kelly, D., Radovic, L., Xie, F. Microcalorimetric Study of the Influence of Surface Chemistry on the Adsorption of Water by High Surface Area Carbons. *J. Phys. Chem. B* **104,** 8170 (2000).

71. Aharoni, C. The Solid-Liquid Interface in Capillary Condensation Sorption of Water by Active Carbons. *Langmuir* **13,** 1270 (1997).

72. Groszek, A. J., Aharoni, C. Study of the Active Carbon-Water Interaction by Flow Adsorption Microcalorimetry. *Langmuir* **15,** 5956 (1999).

73. Segarra, E. I., Glandt, E. D. Model Microporous Carbons: Microstructure, Surface Polarity and Gas Adsorption. *Chem. Eng. Sci.* **49,** 2953 (1994).

74. Sircar, S. New Adsorption-Condensation Theory for Adsorpion of Vapors on Porous Activated Carbons. *Carbon* **25,** 39 (1987).

75. Mahle, J. J., Friday, D. K. Water Adsorption Equilibria on Microporous Carbons Correlated Using a Modification to the Sircar Isotherm. *Carbon* **27,** 835 (1989).

76. Bradley, R. H., Rand, B. A Comparison of the Adsorption Behavior of Nitrogen, Alcohols, and Water towards Active Carbons. *Carbon* **29,** 1165 (1991).

77. Gregg, S. J., Sing, K. S. W. "Adsorption, Surface Area, and Porosity," Academic Press, London, 1982.

78. Lopez-Ramon, M. V., Stoeckli, F., Moreno-Castilla, C., Carrasco-Marin, F. Specific and Nonspecific Interactions between Methanol and Ethanol and Active Carbons. *Langmuir* **16,** 5967 (2000).

79. Tamon, H., Okazaki, M. Influence of Acidic Surface Oxides of Activated Carbon on Gas Adsorption Characteristic. *Carbon* **34,** 741 (1996).

80. Wang, N., Sasaki, M., Yoshida, T., Kotanigawa, T. Flow Microcalorimetry Study of Methanol Adsorption from n-Hexanes on Coals. *Energy and Fuels* **11,** 1293 (1997).

81. Ohkubo, T., Iiyama, T., Nishikawa, K., Suzuki, T., Kaneko, K. Pore-Width-Dependent Ordering of C_2H_5OH Molecules Confined in Graphitic Slit Nanospaces. *J. Phys. Chem. B* **103,** 1859 (1999).

82. Jagtoyen, M., Derbshire, F. Some Considerations of the Origins of Porosity in Carbons from Chemically Activated Wood. *Carbon* **31,** 1185 (1993).

83. Baker, F. S. *U. S. Patent 5,710,092* (1998).

84. Bandosz, T. J., Jagiello, J., Schwarz, J. A. Comparison of Methods to Assess Surface Acidic Groups on Activated Carbons. *Anal. Chem.* **64,** 891 (1992).

85. Jagiello, J., Bandosz, T. J., Putyera, K., Schwarz, J. A. Determination of Proton Affinity Distributions for Chemical Systems in Aqueous Environments Using a Stable Numerical Solution of the Adsorption Integral Equation. *J. Colloid Interface Sci.* **172,** 341 (1995).

86. Contescu, C., Jagiello, J. Scwarz, J. A. Heterogeneity of Proton Binding Sites at the Oxide/Solution Interface. *Langmuir* **9,** 1754 (1993).

87. Stumm, W., Morgan, J. J. "Aquatic Chemsitry," Wiley, New York, 1981.

88. Jagiello, J. Stable Numerical Solution of the Adsorption Integral Equation Using Splines. *Langmuir* **10,** 2778 (1994).

89. Dubinin, M. M. In "Chemistry and Physics of Carbon," Walker, P. L. Ed., Marcel Dekker, New York, 1966, Vol. 2.

90. Olivier, J. P., Conklin, W. B. *Presented at 7th International Conference on Surface and Colloid Science,* Campiegne, France (1991). Olivier, J. P., Conklin, W. B. Determination of Pore Size Distribution from Density Functional Theoretic Models of Adsorption and Condensation within Porous Solids. *Presented at the International Symposium on the Effects of Surface Heterogeneity in Adsorption and Catalysis on Solids,* Kazimierz Dolny, Poland (1992). Olivier, J. P. The Determination of Surface Energetic Heterogeneity Using Model Isotherms Calculated by Density Functional Theory. *Presented at the Fifth International Conference on the Fundamentals of Adsorption,* Pacific Grove, California (1995).

91. Langmuir, I. Constitution and Fundamental Properties of Solids and Liquids. *J. Amer. Chem. Soc.* **38,** 2221 (1916).

92. Paryjczak, T. "Gas Chromatography in Adsorption and Catalysis," Polish Scientific Publishers, Warszawa, Poland, 1986.

93. Jagiello, J., Bandosz, T. J., Schawrz, A. J. Inverse Gas Chromatographic Study of Activated Carbons: The Effect of Controlled Oxidation on Microstructure and Surface Chemical Functionality. *J. Colloid Interface Sci.* **151,** 1026 (1992).

94. Jagiello, J., Bandosz, T. J., Schwarz, J. A. Application of Inverse Gas Chromatography at Infinite Dilution to Study the Effects of Oxidation on Activated Carbons. *Carbon* **30,** 62 (1992).

95. Ahsan, T., Colenutt, B. A., Sing, K. S. Application of Gas Chromatography for the Study of Precipitated Calcium Carbonate. *J. Chromatogr.* **464,** 416 (1989).

96. Milonjiae, S. K., Kopeeni, M. M. A Chromatographic Study of the Adsorption of Organics on Thermally Treated Silicas. *Chromatographia* **19,** 342 (1984).

97. Belyakova, L. D., Kiselev, A. V., Soloyan, G. A. Specificity of Adsorption and Chromatographic Separation of Some Cyclic Olifins and Aromatic Hydrocarbons on Barium Sulfate. *Chromatographia* **3,** 254 (1970).

98. Sidqi, M., Linger, G., Jagiello, J., Balard, H., Papirer, E. Characterization of Specific Interaction Capacity of Solid Surfaces by Adsorption of Alkanes and Alkenes, Part I. Adsorption on Open Surfaces. *Chromatographia* **28,** 588 (1989).

99. Kiselev, A. V., Yashin, Y. I. "Gas Adsorption Chromatography," Plenum, New York, 1969.

100. Conder, J. R., Young, C. L. "Physicochemical Measurements by Gas Chromatography," Wiley-inter-science, New York, 1979.

101. Habgood, H. W., Flood, E. A., Ed. "The Solid-Gas Interface," Marcel Dekker, New York, 1967.

102. Karger, B. L., Sewell, P. A., Castells, R. C., Hartkoft, A. Gas Chromatographic Study of the Adsorption of Insoluble Vapors on Water. *J. Colloid Interface Sci.* **35,** 328 (1971).

103. Hartkoft, A., Karger, B. L. Study of the Interfacial Properties of Water by Gas Chromatography. *Acc. Chem. Res.* **6,** 209 (1973).

104. Domingo-Garcia, M., Lopez-Garzon, F. J., Domingo-Garcia, R., Moreno-Castilla, C. Gas Chromatographic Determination of Adsorption Isotherms, Spreading Pressures, London Forces Interactions and Equations of State for n-Alkanes on Graphite and Carbon Blacks. *J. Chromatogr* **324,** 19 (1985).

105. Jagiello, J., Linger, G., Papirer, E. Characterization of Silicas by Gas Chromatography at Finite Concentration: Determination of the Adsorption Energy Distribution Function. *J. Colloid Interface Sci.* **137,** 128 (1990).

106. James, A. T., Martin, A. J. Gas-Liquid Partition Chromatography: the Separation and Microestimation of Volatile Fatty Acids from Formic Acid to Dodecanoic Acid. *Biochem. J.* **50,** 679 (1952).

107. Huber, J. F. K., Gerritse, R. J. Evaluation of Dynamic Gas-Chromatographic Methods for the Determination of Adsorption and Solution Isotherms. *Chromatogr* **58,** 137 (1971).

108. Littlewood, A. B. "Gas Chromatography," Academic Press, New York, 2nd Ed. 1970.

109. Freundlich, Z. F. Physik. Chemie, **57,** 385 (1907).

110. Gregg, S. J., Sing, K. S. W. "Adsorption, Surface Area, and Porosity," Academic Press, New York, 1982.

111. Matranga, K. R., Myers, A. L., Glandt, E. D. Storage of Natural Gas by Adsorption on Activated Carbon. *Chem. Eng. Sci.* **47,** 1569 (1992).

112. Bandosz, T. J., Jageillo, J., Schwarz, J. A. Effect of Chemical Groups on Energetic Heterogeneity of Activated Carbons. *Langmuir,* **9,** 2518 (1993).

113. Salame, I. I., Bandosz, T. J. Comparison of the Surface Features of Two Wood-Based Activated Carbons. *Ind. Eng. Chem. Res.* **39,** 301 (2000).

114. Kortum, G., Vogel, W., Andrussow, K. "Dissociation Constants of Organic Acids in Aqueous Solutions," Butterworth, London, 1961.

115. Simmons, W., Ed. "The Sadtler Handbook of Infrared Spectra," Sadtler Research Laboratories, Philadelphia, 1978.

116. Zawadzki, J. *Carbon* **18,** 281 (1980).

117. Zawadzki, J. IR Spectroscopy Investigation of Acidic Character of Carbonaceous Films Oxidized with HNO_3 Solution. *Carbon* **19,** 19 (1981).

118. Dandekar, A., Baker, R. T. K., Vannice, M. A. Characterization of Activated Carbon, Graphitized Carbon Fibers and Synthetic Diamond Powder Using TPD and DRIFTS. *Carbon* **36,** 1821 (1998).

119. Salame, I. I., Bandosz, T. J. Revisiting the Effect of Surface Chemistry on Adsorption of Water on Activated Carbons. *J. Phys. Chem.* **103,** 3877 (1999).

120. Adib, F., Bagreev, A., Bandosz, T. J. Analysis of the Relationship between H_2S Removal Capacity and Surface Properties of Unimpregnated Activated Carbons. *Environ. Sci. Technol.* **34,** 686 (2000).

121. March, J. "Advanced Organic Chemistry: Reactions, Mechanisms, and Structure," Wiley, New York, 1982.

122. Stock, L. M. The Mechanism of Aromatic Nitration Reaction. *Prog. Phy. Org. Chem.* **12,** 21 (1976).

123. Ridd, J. H. Diffusion Control and Preassociation in Nitrosation, Nitration and Halogenation. *Adv. Phys. Org. Chem.* **16,** 1 (1978).

124. Weast, R. C., Ed. "Handbook of Chemistry and Physics," CRC Press, 62nd edition, Boca Raton, Florida, 1981.

125. Silverstein, R. M., Bassler, G. C., Morrill, T. C. "Spectroscopic Identification of Organic Compounds," Wiley, New York, 1981.

126. Wade, L. G., Jr. "Organic Chemistry," Prentice Hall: Englewood Cliffs, NJ, 3rd edittion, 1995.

127. Kirby, A. J. "Ester Formation and Hydrolysis Related Reactions. In *Comprehensive Chemical Kinetics,*" Bamford, C. H., Tipper, C. F. H., Eds., Elsevier: Amsterdam, volume 10, 1972.

128. Czepirski, L., Jagiello, J. Virial-Type Thermal Equation of Gas-Solid Adsorption. *J. Chem. Eng. Sci.* **44,** 797 (1989).

129. Jagiello, J., Bandosz, T. J., Putyera, K., Schwarz, J. A. Adsorption Near Ambient Temperatures of Methane, Carbon Tetrafluoride and Sulfur Hexafluoride on Commercial Activated Carbons *J. Chem. Eng, Data* **40,** 1288 (1995).

130. Bandosz, T. J., Jagiello, J., Schawrz, J. A. Adsorption of Sulfur Hexafluoride and Propane at Temperatures Near Ambient on Pillared Clays *J. Chem. Eng. Data* **41,** 880 (1996).

131. Martin, B. R. "Statistics for Physicists," Academic Press: London, 1961.

132. Groszek, A. J., Aharoni, C. Proceedings of Third International Symposium on Effects of Surface Heterogeneity in Adsorption and Catalysis on Solids. Torun, Poland, 1998, pp 129-133.

133. Everett, D. H., Powl, J. C. Adsorption in Slitlike and Cylindrical Micropores in the Henry's Law Region. *J. Chem. Soc. Faraday Trans. I* **72,** 619 (1976).

134. Pan, H., Ritter, J. A., Balbuena, P. B. Isosteric Heats of Adsorption on Carbon Predicted by Density Functional Theory. *Ind. Eng. Chem. Res.* **37,** 1159 (1998).

135. Webster, C. E., Drago, R. S., Zerner, M. C. Molecular Dimensions for Adsorptives. *J. Am. Chem. Soc.* **120,** 5509 (1998).

136. Cooney, D. O., "Adsorption Design for Wastewater Treatment," Lewis Publishers: Boca Raton, Florida, 1999.